

TRANSGENIC USE OF SMAD7 TO SUPPRESS TGF $\beta$  SIGNALING  
DURING MOUSE DEVELOPMENT

Sunyong Tang

Submitted to the faculty of the University Graduate School  
in partial fulfillment of the requirements  
for the degree  
Doctor of Philosophy  
in the Department of Biochemistry and Molecular Biology  
Indiana University

August 2010

Accepted by the Faculty of Indiana University, in partial fulfillment of the requirements for the degree of Doctor of Philosophy.

---

Simon J. Conway, Ph.D., Chair

Doctoral Committee

---

Maureen A. Harrington, Ph.D.

June 24, 2010

---

David G. Skalnik, Ph.D.

---

Simon J. Rhodes, Ph.D.

This thesis is dedicated to my beloved family.

## **Acknowledgements**

I would like to thank my advisor Dr. Simon J. Conway. I have received fully support from Dr. Conway throughout my whole Ph.D. program. Without his encouragement, guidance and patience, I could not finish my thesis project and dissertation.

I sincerely appreciate the thoughtful guidance and constructive suggestions from my committee members: Dr. David G. Skalnik, Dr. Maureen A. Harrington and Dr. Simon J. Rhodes. Your expertise and dedication shaped my thesis project and helped me to grow as a scientist.

I would also like to express my appreciation to the faculty and staff of the department of Biochemistry and Molecular Biology. Thank you for all the assistance. You guys are the best. To the staff of the University Graduate School, thank you for all the assistance and guidance throughout my whole Ph.D. study.

I would like to thank my current and former colleagues in Conway lab: Dr. Jian Wang, Dr. Hongmin Zhou, Dr. Paige Snider, Mica Gosnell, Michael Olaopa, Ronda Rogers, Goldie Lin, Dr. Doug Metcalf, Olga Simmons. I have got lots of help from you and I really enjoy working with you. I also want to give my special thanks to Chao Wang and Xi Wu for their friendship and help.

Finally, I would like to acknowledge my mother, Ailin, and my sister and brother in law, Jinyan and Lingming, for their understanding, encouragement and endless love. Last but not least, I would like to thank my wife Min Zhang for her love, understanding, encouragement and support for my effort to chase my dream. Without her company, I can not imagine to complete such a long journey!

## Abstract

Sunyong Tang

### TRANSGENIC USE OF SMAD7 TO SUPPRESS TGF $\beta$ SIGNALING DURING MOUSE DEVELOPMENT

Neural crest cells (NCC) are a multipotent population of cells that form at the dorsal region of neural tube, migrate and contribute to a vast array of embryonic structures, including the majority of the head, the septum of the cardiac outflow tract (OFT), smooth muscle subpopulations, sympathetic nervous system and many other organs. Anomalous NCC morphogenesis is responsible for a wide variety of congenital defects. Importantly, several individual members of the TGF $\beta$  superfamily have been shown to play essential roles in various aspects of normal NCC development. However, it remains unclear what role Smad7, a negative regulator of TGF $\beta$  superfamily signaling, plays during development and moreover what the spatiotemporal effects are of combined suppression of TGF $\beta$  superfamily signaling during NCC formation and colonization of the developing embryo. Using a cre/loxP three-component triple transgenic system, expression of Smad7 was induced via doxycycline in the majority of pre- and post-migratory NCC lineages (via Wnt1-Cre mice). Further, expression of Smad7 was induced via doxycycline in a subset of post-migratory NCC lineages (via Periostin-Cre mice, after the NCC had reached their target organs and undergone differentiation). Induction of Smad7 within NCC significantly suppressed TGF $\beta$

superfamily signaling, as revealed via diminished phosphorylation levels of both Smad1/5/8 and Smad2/3 *in vivo*. This resulted in subsequent loss of NCC-derived craniofacial, pharyngeal and cardiac OFT cushion tissues. ROSA26r NCC lineage mapping demonstrated that cardiac NCC emigration and initial migration were unaffected, but subsequent colonization of the OFT was significantly reduced. At the cellular level, increased cell death was observed, but cell proliferation and NCC-derived smooth muscle differentiation were unaltered. Molecular analysis demonstrated that Smad7 induction resulted in selective increased phospho-p38 levels, which in turn resulted in the observed initiation of apoptosis in trigenic mutant embryos. Taken together, these data demonstrate that tightly regulated TGF $\beta$  superfamily signaling is essential for normal craniofacial and cardiac NCC colonization and cell survival *in vivo*.

Simon J. Conway, Ph.D., Chair

## Table of Contents

List of Tables .....	x
List of Figures .....	xi
List of Abbreviations .....	xiii
Chapter I: Introduction	
A. TGF $\beta$ superfamily signaling pathway .....	1
B. Neural crest development.....	2
C. Heart development.....	3
D. Congenital heart defects.....	4
E. TGF $\beta$ superfamily signaling role in neural crest development.....	5
F. TGF $\beta$ superfamily signaling role in endocardial cushion maturation and heart valve homeostasis.....	6
G. Hypothesis.....	7
Chapter II: Trigenic neural crest-restricted Smad7 over-expression results in congenital craniofacial and cardiovascular defects.....	
Abstract.....	12
Introduction .....	13
Materials & Methods .....	16
Results.....	20
Discussion .....	35



Chapter III: Regulation of TGF $\beta$ superfamily signaling is critical during sympathetic ganglia and craniofacial neural crest differentiation but is dispensable post-differentiation.....	65
Abstract.....	65
Introduction.....	66
Materials & Methods.....	69
Results.....	73
Discussion.....	84
Chapter IV: Discussion and future studies.....	107
A. The purpose of creating the inducible trigenic mouse system.....	107
B. The reasons of using Smad7 to study NCC development.....	108
C. The common results from <i>Wnt1-Cre</i> and <i>Peri-Cre</i> trigenic mouse models.....	109
D. The differences between <i>Wnt1-Cre</i> and <i>Peri-Cre</i> trigenic mouse models.....	109
E. Smad7 and its role in apoptosis.....	111
F. Future studies.....	113
References.....	115
Curriculum Vitae	

## List of Tables

Table 1. Embryos harvested at E14.5 fed regular food .....	43
--	----

## List of Figures

Figure 1. Model of TGF $\beta$ superfamily signaling pathway.....	9
Figure 2. Neural crest development.....	10
Figure 3. Heart development model .....	11
Figure 4. No mycSmad7 was detected by western blot in E14.5 embryos fed with regular food .....	44
Figure 5. Evaluation of the trigenic Cre/loxP-dependent, tetracycline inducible transgenic system.....	46
Figure 6. Western analysis of NCC-enriched craniofacial tissues .....	49
Figure 7. Early Smad7 induction within the neural crest lineage suppresses normal craniofacial and pharyngeal arch development.....	51
Figure 8. Histological examination of E13.5 Smad7 trigenic phenotypes fed doxycycline at E7.5.....	53
Figure 9. NCC develop in Smad7 trigenic mutant embryos fed doxycycline at E7.5 .....	55
Figure 10. Elevated cell death of NCC in Smad7 trigenic mutants fed doxycycline at E7.5.....	58
Figure 11. NCC-restricted Smad7 overexpression results in decreased TGF $\beta$ and BMP signaling.....	60
Figure 12. Molecular marker analysis of E10.5 trigenic mutant phenotype .....	63
Figure 13. Analysis of E14.5 Smad7 trigenic heart phenotypes fed Doxycycline at E10 .....	64

Figure 14. Peri-Cre early lineage mapping .....	88
Figure 15. Smad7 induction kinetics in doxycycline inducible <i>Peri-Cre/R26<sup>rtTA-EGFP</sup>/tetO-Smad7</i> trigenic mouse system .....	90
Figure 16. Overexpression of Smad7 in the post-migratory neural crest cells impaired normal facial and pharyngeal arch development, and resulted in mid-gestational lethality.....	92
Figure 17. Overexpression of Smad7 in post-migratory neural crest cells affected sympathetic ganglia but not dorsal root ganglia and cardiac development .....	94
Figure 18. Elevated cell death in craniofacial regions of the Smad7 trigenic mutants.....	96
Figure 19. Increased pp38 in pharyngeal arches and frontofacial tissues .....	98
Figure 20. Unaffected cardiac structure and intact blood vessels in trigenic embryos.....	100
Figure 21. Hypoplastic sympathetic ganglia and decreased TH synthesis in trigenics .....	102
Figure 22. Isoproterenol rescued trigenic embryos.....	104
Figure 23. Overexpression of Smad7 in post-differentiated sympathetic ganglia did not result in mid-gestational lethality .....	106

## List of Abbreviations

AVC	Atrioventricular Canal
BMP	Bone Morphogenetic Protein
cDNA	Complementary Deoxyribonucleic Acid
dAo	Dorsal Aorta
DNA	Deoxyribonucleic Acid
Drg	Dorsal Root Ganglia
ECM	Extracellular Matrix
EMT	Epithelial To Mesenchymal Transformation
FGF	Fibroblast Growth Factor
H&E	Haemotoxylin-Eosin Staining
mRNA	Messenger Ribonucleic Acid
NCC	Neural Crest Cells
NS $\beta$ T	Neuron Specific $\beta$ III Tubulin
Nt	Neural Tube
oft	Outflow Tract
OFT	Outflow Tract
pAkt	Phospho-Akt
PBS	Phosphate-Buffered Saline
PCR	Polymerase Chain Reaction
PECAM	Platelet-Endothelial Cell Adhesion Molecule
pp38	Phospho-p38

pSmad1/5/8	Phospho-Smad1/5/8
pSmad2	Phospho-Smad2
sg	Sympathetical Ganglia
Smad	Sma- And Mad-Related Protein
SM	Smooth Muscle
$\alpha$ SMA	$\alpha$ -Smooth Muscle Actin
TGF $\beta$	Transforming Growth Factor Beta
Trigenic	Triple Transgenic
TUNEL	Terminal Deoxynucleotidyl Transferase Mediated dUTP Nick End Labeling
VE-Cadherin	Vascular Endothelial Cadherin
WNT	Wingless-Type Mmtv Integration Site Family

## Chapter I: Introduction

### A. TGF $\beta$ superfamily signaling pathway

The Transforming Growth Factor Beta (TGF $\beta$ ) superfamily consists of more than 30 ligand proteins [1] including TGF $\beta$  isoforms, activins, Bone Morphogenetic Proteins (BMP)s and other ligands. Members of the TGF $\beta$  superfamily family represent structurally similar, but functionally diverse growth factors which play a variety of biological roles during cell proliferation, differentiation, apoptosis and many other tissue remodeling processes, including early embryogenesis and heart morphogenesis.

The signaling by TGF $\beta$  superfamily members is initiated by binding of ligands to the type II receptor (Fig. 1), which then recruits type I receptor and phosphorylates and activates it [2]. There are different type I and II receptors that can interact with a set of distinct co-receptors, adding to the signaling complexity. Activation of these serine/threonine kinase receptors leads to signal propagation by phosphorylation of Receptor- Smad- And Mad-Related Proteins (R-Smad)s, with Smad2 and 3 mediating the activities of TGF $\beta$  isoforms and activins, and Smads 1, 5, and 8, the activities of BMPs. Phosphorylated R-Smads form complexes with Smad4, which is common to both the TGF $\beta$  and BMP signaling pathways, the complexes then translocate to the nucleus to regulate gene transcription. In contrast to the R-Smads, the inhibitory I-Smads (Smad6 and 7) negatively regulate TGF $\beta$  superfamily signaling *in vitro*. While Smad6 is a

specific negative regulator of BMP signaling [3-4], Smad7 negatively regulates both TGF $\beta$  and BMP signaling [4-8]. He [9] and Kuang [10] showed that over-expression of Smad7 in the skin and pancreas, respectively, specifically disrupted TGF $\beta$  pathway signaling *in vivo*.

## **B. Neural crest development**

Neural crest cells (NCC) are a pluripotent cell population that gives rise to and influences the development of a diverse array of tissues in the developing embryo. They are a transient population of cells formed during early vertebrate embryonic development on the dorsal side of the developing neural tube, where it contacts with the surface ectoderm (Fig. 2A). NCC are highly plastic and are known to be dependent on cues from the extracellular environment, such as sonic hedgehog, Wingless-Type Mmtv Integration Site Family (WNT) members, BMPs and Fibroblast Growth Factors (FGF)s to differentiate into defined cell types [11]. After neurulation, NCCs undergo epithelial to mesenchymal transformation, delaminate and migrate (Fig. 2B) along defined pathways to colonize and contribute to the formation of a variety of target tissues and organs [12-13].

Cranial NCC, located at the anterior neural tube (Fig. 2C), migrate and populate the first, second and third pharyngeal arches and frontonasal mass. After the migration, these cells differentiate into a number of structures, including cranial neurons, glia, cartilage, bone and connective tissues of the face [14-19]. Cardiac



NCC, located at the regions from the otic vesicle to the third somite (Fig. 2C), migrate through the third, fourth and sixth pharyngeal arches to the OFT, and contribute to the formation of smooth muscle cells surrounding the pharyngeal arch arteries and aorticopulmonary septum [13, 20]. At the trunk level, NCC migrate out of neural tube (Fig. 2C) and give rise to many structures such as dorsal root ganglia, sympathetic ganglia, the adrenal medulla, and the nerve clusters surrounding the aorta [18, 20-21].

### **C. Heart development**

The heart is the first functional organ. The vertebrate heart arises from cardiac progenitors and extracardiac sources. At embryonic day 7.75 (E7.75) in mouse, cardiac progenitors form a cardiac crest at the ventral side. At E9.5, cardiac progenitors give rise to the primitive linearized heart tube (Fig. 3) composed of an outer layer of myocardium and an inner layer of endocardial cells, separated by an extensive extracellular matrix referred to as the cardiac jelly. Subsequently, the primitive heart tube generates a right-side bend and forms segments. These segments will give rise to OFT, ventricles, atrioventricular canal (AVC), atria and inflow tract, anteroposteriorly. Proper development of heart chambers and valves requires the formation of endocardial cushion tissue in the AVC and OFT segments. The endocardial cells at the OFT and AVC undergo epithelial to mesenchymal transformation (EMT) by the signals from the underlying myocardium and migrate into the acellular cardiac jelly. Locally expanded cardiac jelly and mesenchymal cells are referred to as cardiac cushions. Neural crest

cells and other extracardiac sources also contribute mesenchymal cells to the formation of endocardial cushions [22-23]. EMT occurs at around E9.5 in AVC and E10 in OFT. During EMT, endocardial cells down-regulate VE-cadherin and PECAM expression and express SM- $\alpha$ -actin [24]. Once transformed, the mesenchymal cells proliferate and invade the cardiac jelly. Cardiac cushion formation ends around E10.5 and E11 in the AVC and OFT, respectively. Heart valves and septal structures are derived from those cardiac cushions. The OFT septum between aorta and pulmonary trunk starts to form at E11.5. The extracardiac neural crest cells contribute to its formation [20, 25-26].

As development proceeds, aorticopulmonary septum, AV septum and ventricular septum come into alignment, resulting in completion of the four-chambered heart. The last major morphogenetic event is valve formation. The cardiac cushions undergo further maturation and remodeling to form mature heart valves. The aortic and pulmonary valves are derived from OFT endocardial cushion, and the mitral and tricuspid valves are from the AV endocardial cushion. Thus, along with the formation of heart conduction system, the linearized primitive tubular heart has become a dual-channel, synchronously beating four chambered heart with one-way valves.

#### **D. Congenital heart defects**

Heart defects are the leading cause of birth defect-related deaths. About 40,000 (~1%) infants are born with heart defects each year in the United States, which

makes it the number 1 birth defect in the US (AHA, 2005). Defects in cardiac valves and associated structures are the most common subtypes, accounting for 25% to 30% of all cardiovascular malformations [27]. The high prevalence of congenital heart defects demands our thorough understanding of the underlying molecular mechanisms of heart development and remodeling.

### **E. TGF $\beta$ superfamily signaling role in neural crest development**

Several of the above mentioned TGF $\beta$  signaling components have been manipulated *in vivo* in the developing neural crest. Inactivation of genes encoding TGF $\beta$ 2 and TGF $\beta$ 3 in mice resulted in severe craniofacial malformations, while BMP over-expression or blocking BMP by its inhibitor Noggin in developing chicken affected sympathetic ganglia formation [28-31]. BMP4 and BMP7 have been shown to be the growth factors produced by dorsal aorta to trigger the neural crest to undergo adrenergic differentiation normally [28].

With respect to receptors for TGF $\beta$  family factors, TGF $\beta$  type II receptor (Tgbr2) and TGF $\beta$  type I receptor (Alk5) inactivation in the neural crest caused extensive craniofacial defects, such as cleft palate, and cardiovascular malformations including aortic arch patterning deficiencies, persistent truncus arteriosus, and septal defects [30, 32-36]. Similar defects resulted from neural crest specific deletion of receptors mediating BMP responses [37-39].

In addition, ablation of Smad4 or over-expression of Smad7 in neural crest lineages leads to massive cell death and thus malformations in both craniofacial and cardiovascular neural crest derivatives [40-42] and to reduced size and altered patterning of trigeminal ganglia [41]. All these data demonstrate that TGF $\beta$  superfamily signaling plays important roles in neural crest development.

#### **F. TGF $\beta$ superfamily signaling role in endocardial cushion maturation and heart valve homeostasis**

A number of TGF $\beta$  superfamily members have been implicated in heart development. High level TGF $\beta$ 1 expression occurs in the endothelial cells of the heart valves from E8.0 until after birth [43]. At E10.5, TGF $\beta$ 2 mRNA expression in the heart is limited to the AVC and OFT myocardium/cushions; from E12.5-14.5, TGF $\beta$ 2 is no longer expressed in myocardium, but is expressed in the mesenchymal cells [44]. Cardiac TGF $\beta$ 3 is limited to mesenchymal cells at the base of the heart valves from E14.5-16.5 [44]. At E10.5, Bmp4 expression is restricted to the myocardium of OFT, but not the AVC [45]. In addition, strong Bmp4 expression is also found in OFT myocardium E12-14 [46]. At E10.5, Bmp6 is expressed in OFT myocardium [45] and at E12.5 Bmp6 is expressed in OFT cushions [47]. High level and ubiquitous Bmp7 expression is found throughout the myocardium of the heart tube from E8.5-15.5 [48].

These expression patterns of TGF $\beta$  ligands correlate with valve development. Mice lacking either TGF $\beta$ 1 or TGF $\beta$ 3, however, do not exhibit cardiac defects

[49-50]. *Bmp4* null mice die by E8.5, excluding the possibility to study heart development [51]. Mice with single mutations of either *Bmp5*, *Bmp6* or *Bmp7* did not display any heart defects [52-54]. An explanation for these unexpected phenotypes includes functional redundancy among TGF $\beta$  superfamily ligands. Indeed, double knock out of *Bmp5* and *7* in mice demonstrate delayed cardiac development and lack of cushion formation [48]. In addition, OFT cushion morphogenesis is delayed in *Bmp6* and *7* double null mice [47].

Both *Smad6* and *Smad7* are predominantly expressed in the developing OFT and AV cushion between E9.5 to E13.5 [55]. *Smad6* expression remains in cardiac valves and OFT after birth and adulthood and null mice have defects in cardiovascular system [56]. Dr. Conway's lab has shown that *Smad6* null hearts exhibit persistent truncus (PTA) defects and enlarged cushions/heart valves [57]. *Smad7* mutant mice with exon 1 deletion have altered B-cell responses but are not known to exhibit any cardiovascular defects [58]. However, one major caveat of this mouse model was deleting the exon 1 of *Smad7* gene did not completely abolish the repressing ability of *Smad7* on TGF $\beta$  signaling. Another *Smad7* null mouse model [59], by deleting the indispensable exon 2, demonstrated *Smad7* is required for normal cardiac function and OFT development.

### **G. Hypothesis**

After formed at the dorsal neural tube, NCC migrate away from neural tube and colonize their target organs, there they differentiate into a variety of specialized

cells. Many research studies have shown that TGF $\beta$  superfamily signaling is required for NCC development [28-31]. However, all these research only focused on the role of TGF $\beta$  superfamily signaling in pre-migratory NCC. The distinct developmental phases of NCC development suggest NCC may or may not require TGF $\beta$  superfamily signaling at each stage. I hypothesize that TGF $\beta$  superfamily signaling plays an essential role at pre-migratory, post-migratory, differentiating, and post-differentiation NCC development. To test this hypothesis, I used Smad7 as a tool to study the roles of TGF $\beta$  superfamily signaling at various NCC developmental phases via a doxycycline inducible tissue specific transgenic mouse system.

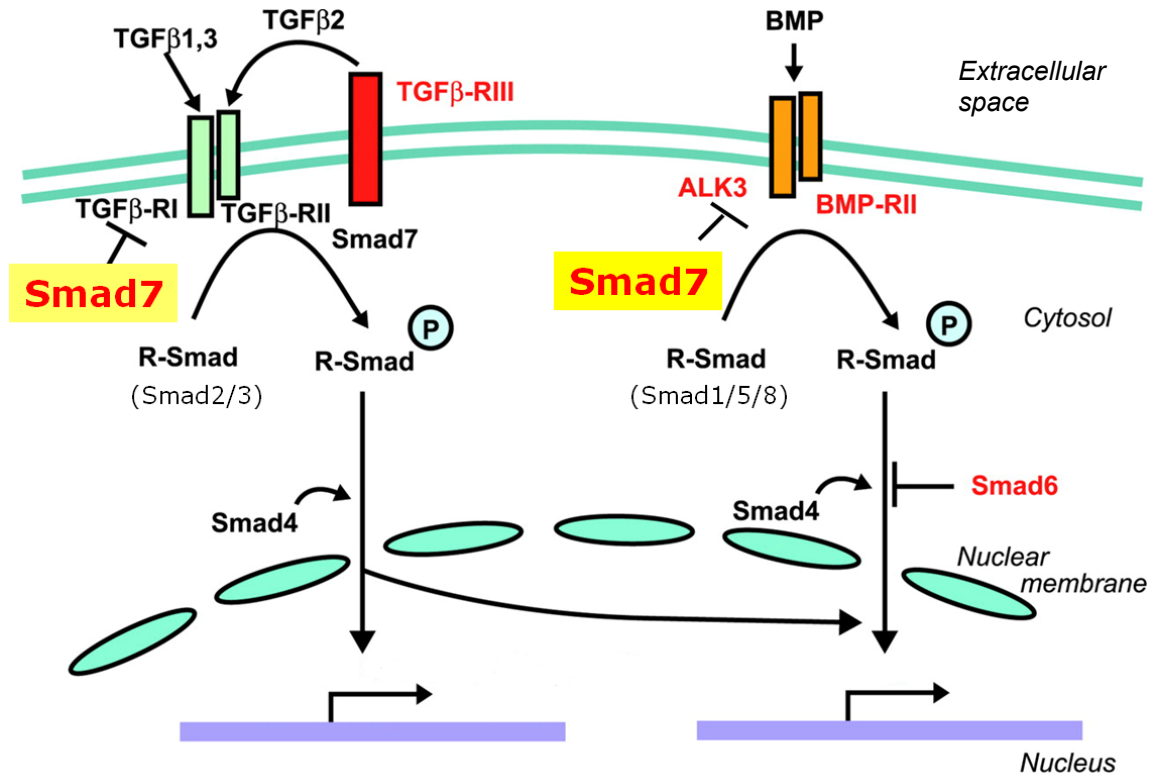


**Figure 1. Model of TGFβ superfamily signaling pathway.** (Adapted from Armstrong and Bischoff [60])

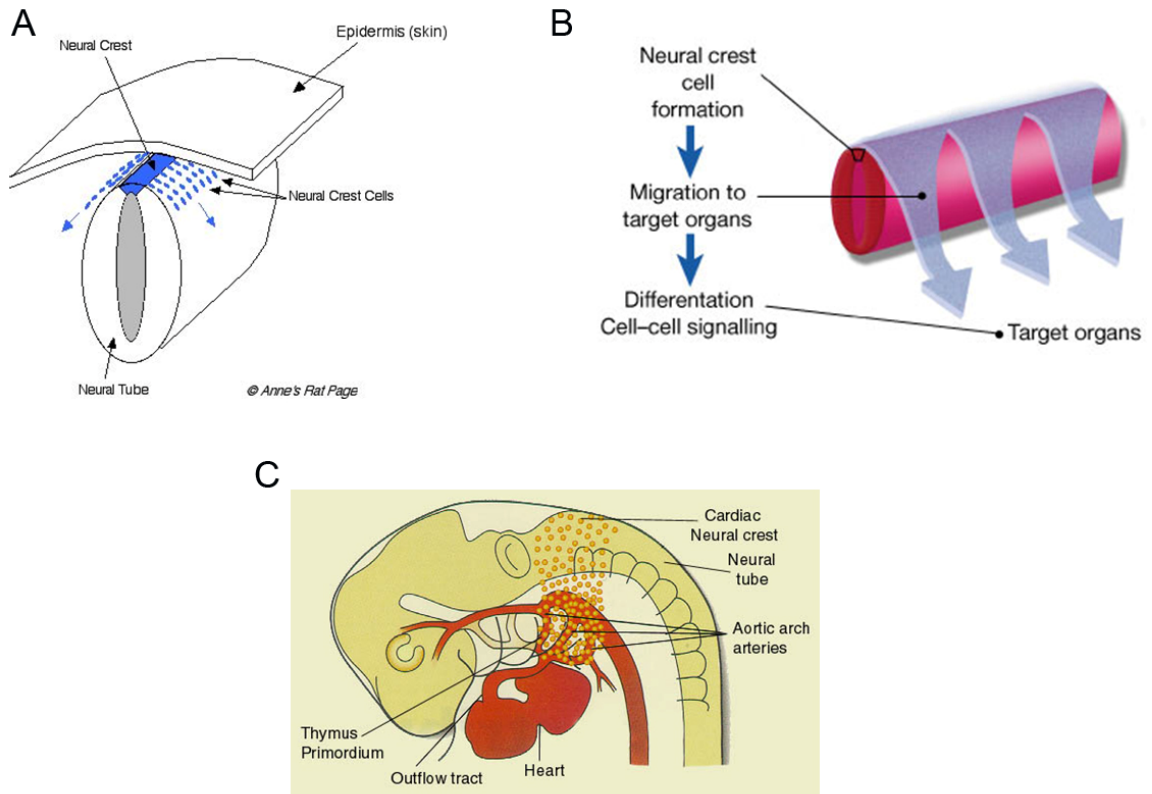


**Figure 2. Neural crest development.** (Pictures are obtained from internet <http://www.ratbehavior.org/images/NeuralCrest.jpg>, [http://www.nature.com/nature/journal/v407/n6801/fig\\_tab/407227a0\\_F1.html](http://www.nature.com/nature/journal/v407/n6801/fig_tab/407227a0_F1.html), <http://www.stonybrook.edu/biochem/BIOCHEM/facultypages/holdener/c112k.html> respectively)



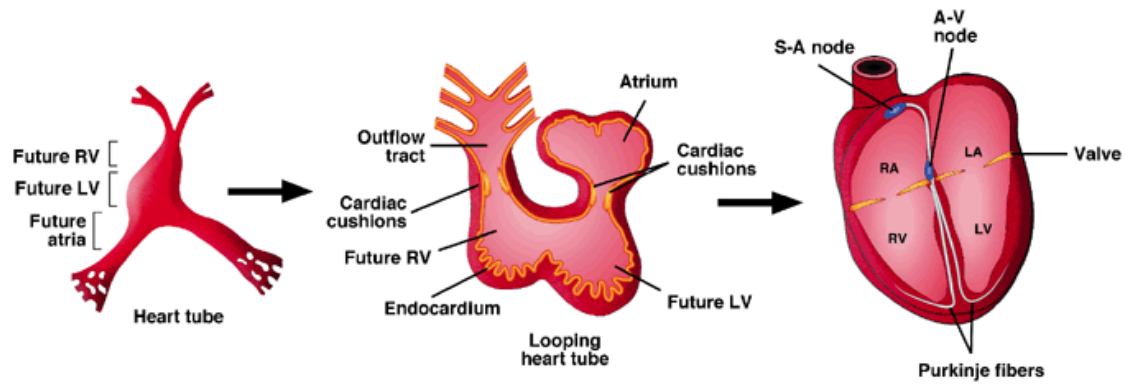


**Figure 3. Heart development model.** (Courtesy to Eric Olson [61])

## **Chapter II: Trigenic neural crest-restricted Smad7 overexpression results in congenital craniofacial and cardiovascular defects**

### **Abstract**

Smad7 is a negative regulator of TGF $\beta$  superfamily signaling. Using a three-component triple transgenic system, expression of Smad7 was induced via doxycycline within the neural crest lineages at pre- and post-migratory stages. Consistent with its role in negatively regulating both TGF $\beta$  and BMP signaling *in vitro*, induction of Smad7 within the NCC significantly suppressed phosphorylation levels of both Smad1/5/8 and Smad2/3 *in vivo*, resulting in subsequent loss of NCC-derived craniofacial, pharyngeal and cardiac OFT cushion tissues. At the cellular level, increased cell death was observed in pharyngeal arches. However, cell proliferation and NCC-derived smooth muscle differentiation were unaltered. NCC lineage mapping demonstrated that cardiac NCC emigration and initial migration were not affected, but subsequent colonization of the OFT was significantly reduced. Induction of Smad7 in post-migratory NCC resulted in cardiac OFT anomalies and interventricular septal chamber septation defects, suggesting that TGF $\beta$  superfamily signaling is also essential for cardiac NCC to govern normal cardiac development at post-migratory stage. Taken together, the data show that tightly regulated TGF $\beta$  superfamily signaling plays an essential role during craniofacial and cardiac NCC colonization and cell survival *in vivo*.

## Introduction

Neural crest cells (NCC) are a transient population of cells created during higher vertebrate early embryonic development. During neurulation, NCC undergo successive epithelial-to-mesenchymal transformation along the cranial-caudal embryonic axis [62], delaminate and migrate along defined pathways to contribute to the formation of a wide variety target tissues, including neurons and glia of the peripheral nervous system, melanocytes, smooth muscle cells and most craniofacial cartilages and bones [12, 14, 63]. NCC also contribute crucial cell populations to several thoracic tissues, including the developing aortic arch arteries (AAA) and OFT of the heart [13, 20, 64-65]. Despite the diversity of NCC fates, they are divided broadly into cranial, cardiac and trunk NCC populations based on their site of origin and ability to colonize target tissues and organs [12-13, 15-16, 19].

TGF $\beta$  superfamily members are obligatory growth factors for early embryogenesis and heart morphogenesis, and play diverse biological roles during cell proliferation, differentiation, apoptosis and many other tissue remodeling processes. There are over 30 members in TGF $\beta$  superfamily in mammals, including BMPs, TGF $\beta$ s, activins and other cytokines [1]. Signaling via the TGF $\beta$  superfamily initiates by binding of ligands to the membrane bound type II receptor, which then recruits and activates the type I receptor. Activated type I receptor then phosphorylates regulatory (R)-Smads (Smad1, 2, 3, 5 or 8), which subsequently form a complex with the co-Smad, Smad4. The complex then

translocates into nucleus to regulate gene transcription [66-68]. In contrast to the R-Smads, the inhibitory (I)-Smads (Smad6 and 7) negatively regulate TGF $\beta$  superfamily signaling *in vitro*. While Smad6 negatively regulates BMP signaling [3-4], Smad7 negatively regulates both TGF $\beta$  and BMP signaling [4-8]. BMP signaling (particularly via BMP2/BMP4 ligands and their receptors Alk2, Alk3, Alk4) has been implicated in promoting NCC induction, maintenance, migration and differentiation in several different model organisms [21, 37-39, 69-71]. Similarly, there is accumulating evidence that TGF $\beta$  signaling in NCC is critical, as NCC-restricted deletion of type I (Alk5) and type II receptors results in a spectrum of defects in the craniofacial, pharyngeal and cardiac regions [30, 32, 34, 36]. In addition, previous studies have shown that *Wnt1-Cre* mediated conditional knockout of *Smad4* within the NCC results in craniofacial, pharyngeal and cardiac malformations [40-41, 72-73], demonstrating that NCC-specific Smad4-mediated TGF $\beta$ /BMP signal transduction is required for NCC normal development. Overall, TGF $\beta$  superfamily signaling has been strongly implicated in NCC development, but its detailed *in utero* molecular mechanisms are still poorly understood due to the large number of family members with wide range of overlapping functions, and complex receptor-ligand associations. Due to Smad7's unique role in repressing both BMP and TGF $\beta$  signaling and its contrasting role to that of Smad4 within TGF $\beta$  superfamily signaling, we hypothesized that *Wnt1-Cre* mediated Smad7 overexpression would phenocopy *Wnt1-Cre* mediated loss of Smad4 function.

To test this hypothesis and examine further the spatiotemporal role of TGF $\beta$  superfamily signaling during NCC morphogenesis and the temporal consequence of TGF $\beta$  superfamily inhibition during development, we generated a three-component triple transgenic *Smad7* expression mouse model (herein termed trigenic) based on Cre/loxP recombination (to induce spatially-restricted *Smad7* expression) and doxycycline-inducible control elements (to temporally regulate *Smad7* expression). As *Smad7* has already been demonstrated to negatively regulate both TGF $\beta$  and BMP signaling *in vivo* in mammalian adult tissues, B cells, retinal pigment epithelium and *Xenopus* explant assays [4-8], we are using spatiotemporally-regulated *Smad7* induction as a tool to attenuate TGF $\beta$  superfamily signaling *in utero* within restricted cell lineages and defined developmental temporal windows. Results reported here demonstrate that pre-migratory *Smad7* induction attenuates both TGF $\beta$  and BMP signaling by suppressing R-Smad phosphorylation, resulting in elevated NCC death, diminished NCC colonization of craniofacial, pharyngeal, cardiac tissues, dysregulated epithelial-mesenchymal interactions and *in utero* lethality. Additionally, *Smad7* induction in post-migratory cardiac NCC results in isolated intraventricular septal defects and neonatal lethality. This work demonstrates that tightly regulated TGF $\beta$  superfamily signaling plays an essential role during both craniofacial and cardiac NCC colonization and cell survival *in vivo*.

## Materials & Methods

### Conditional neural crest-specific trigenic mice:

In the construct used to generate (tetO)-*Smad7* transgenic mice, myc-tagged *Smad7* cDNA [10] was inserted between a (tetO)<sub>7</sub>CMV minimal promoter and the bovine growth factor polyadenylation signal sequence (bGHpA) within the pUHD10-3 vector (generously provided by Dr. Andras Nagy, Samuel Lunenfeld Research Institute [74]). Following diagnostic restriction digest verification and sequencing, the linearized construct was given to the IU Transgenic Core Facility for microinjection into inbred C3HeB/FeJ zygotes to obtain transgenic founders as described [75]. Forward primer 5'- ATCCACGCTGTTTTGACCTC-3' and reverse primer 5'- GAGCGCAGATCGTTTGGT-3' were used for genotyping tetO-*Smad7* transgenic offspring via PCR using mouse genomic DNA from tail using established protocols [76]. Three independent lines were generated and all three were viable up to two years of age. In order to generate triple transgenic doxycycline-inducible mice, *tetO-Smad7* mice were intercrossed with both the reverse tetracycline transactivator *Rosa26<sup>tTA-EGFP</sup>* (*R26<sup>tTA-EGFP</sup>*) (JaxLab stock #005670) and *Wnt1-Cre* [20] mice. For the lineage mapping studies, *Rosa26 reporter* (*R26r*) mice (JaxLab stock #003474) were intercrossed with the trigemics. Genotyping was carried out using PCR primers specific for each transgene (<http://www.jax.org>; [20]). All mice were maintained on mixed genetic backgrounds and age-matched littermates were used as appropriate controls. To induce *Smad7* transgene expression in trigenic embryos, pregnant females were given doxycycline administered in green dyed food pellets at a concentration of

200mg/kg (Bio-Serv) for specified time periods. Mice were maintained under specific-pathogen-free conditions with a 12 hours light/dark cycle. The animal use protocols were approved by the Institutional Animal Care and Use Committee at IUPUI (study #3301).

### **RNA and Protein Analysis:**

In order to verify *Smad7* cDNA induction by RT-PCR, cDNA was synthesized from RNA isolated from individual control (trigenic mice without doxycycline food) and mutant (trigenic mice fed doxycycline food) embryonic day 10.5 (E10.5) whole embryos (n = 4 embryos of each treatment) using a Superscript-II kit (Invitrogen) with 5µg RNA and oligo(dT) primer. cDNAs were amplified with specific *Smad7* primers (30 cycles; forward primer 5'-GCATTCCTCGGAAGTCAAGA-3' and reverse primer 5'-TTGTTGTCCGAATTGAGCTG-3') and normalized with *GAPDH* (16 cycles; Glyceraldehyde-3-phosphate dehydrogenase) as described previously [77]. In order to verify myc-tagged Smad7 protein induction and suppressive effects upon TGFβ superfamily signaling via western blotting, doxycycline-fed E10.5 embryos were homogenized on ice in RIPA buffer with 1% phosphatase inhibitor mixture (Sigma). Proteins were blotted onto PVDF membrane and the following antibodies used: Smad1 (1:2000, Santa Cruz Biotech, sc-81378), phospho-Smad1/5/8 (1:1000, Cell signaling, 9511), Smad2/3 (1:2,000, Santa Cruz Biotech, sc-8332), phospho-Smad2 (1:1000, Cell signaling, 3101), Myc (1:5000, Santa Cruz Biotech, A-14), αTubulin (1:10000, Sigma, T-5168). Primary antibody

binding as visualized by HRP-conjugated secondary antibodies and enhanced chemiluminescence (Amersham, GE Healthcare Biosciences). Densitometry was quantified from at least 3 samples and the combined data graphically displayed.

### **Histological Analysis, X-Gal Staining and Immunohistochemistry:**

Tissue isolation, 4% paraformaldehyde fixation, processing, paraffin embedding, H&E staining, and whole mount detection of R26r indicator  $\beta$ -galactosidase activity were performed as described [75-77]. Following whole mount lacZ staining, embryos were dehydrated through alcohol and embedded in paraffin. Sections (n= 3 individual embryos of each genotype) were cut at 10 $\mu$ m thickness and counterstained with Eosin. As our mice lines are not isogenic, doxycycline-fed single and double transgenic age-matched littermates were used as negative controls. Immunostaining was carried out using ABC kit (Vectorstain) with DAB and hydrogen peroxide chromogens as described previously [78]. The following primary antibodies were used to assess neural crest differentiation and TGF $\beta$  superfamily signaling:  $\alpha$ -smooth muscle actin (1:5000,  $\alpha$ SMA, Sigma), phospho-Smad1/5/8 (1:750, Cell Signaling, 9511), phospho-Smad2 (1:1500, Cell Signaling, 3101). Negative controls were obtained by substituting the primary antibody with serum at 1:150 dilution and positive staining within serial sections was examined using at least three individual embryos of each genotype at each developmental stage.



**Apoptosis and cell proliferation:**

Apoptotic cells were detected in paraffinembedded tissue sections using TdT-FragEL™ DNA Fragmentation Detection Kit (Calbiochem). Cell proliferation was immunodetected using the Ki67 antibody (1:25, DakoCytomation). Both assays were performed on paraffin serial sections (n=4). The total cell number and positively stained cell number were counted manually in defined areas of tissues under 40X magnification. Statistical analysis of cell counts in serial sections and comparison of mutant specimens with controls was performed using one-tailed Student's t test (P values were assigned, with 0.05 being significant).

***In Situ* Hybridization:**

Radioactive *in situ* hybridization for *Ap2α*, *Crabp1*, and *Fgf8* expression was performed as described [75, 79-80]. Both sense and antisense <sup>35</sup>S-UTP-labeled probes were used, and specific signal was observed only with hybridization of the antisense probe, in serial sections within at least three independent embryos of each genotype. In order to quantitate expression differences, silver grains were counted/cell on serial sections.

## Results

### Generation of neural crest-restricted inducible *Smad7* over-expressor mouse line

In order to spatially restrict *Smad7* overexpression to the neural crest lineages, we used the *Wnt1-Cre* transgenic driver line (Fig. 5A) [14, 20, 39, 64, 81]. Temporal regulation of the onset of *Smad7* expression within the neural crest was achieved with the inducible reverse tetracycline transactivator (rtTA). The *Rosa26R*<sup>rtTA-EGFP</sup> mice contain the rtTA with a nuclear localization signal targeted into the *Rosa26* locus, and a downstream EGFP separated by an IRES sequence to ensure efficient EGFP translation (Fig. 5A). The ROSA locus has been shown to be expressed in all cell types at all developmental and postnatal stages, and its expression is not subject to genetic or environmental changes [82]. In the absence of its inducer doxycycline (a derivative of tetracycline), rtTA does not recognize its DNA binding sequence, *tetO*. On the other hand, addition of doxycycline allows rtTA to bind the *tetO* minimal promoter resulting in transcription of the *myc-Smad7* transgene (Fig. 5A). Furthermore, as the rtTA expression module is preceded by a floxed STOP expression cassette, rtTA expression is dependent upon Cre/loxP recombinase to remove the loxP-flanked STOP expression cassette from within the *R26* locus. The *R26*<sup>rtTA-EGFP</sup> mice have previously been shown to drive robust expression of doxycycline-inducible *tet-O* controlled transgenes [74]. *TetO-Smad7* transgenic mice (three separate lines) were generated by placing full length *Smad7* cDNA under the control of heptamerized *tetO* promoter (Fig. 5A). As there are no commercially-available

specific Smad7 antibodies and in order to unequivocally detect transgenic Smad7 protein *in vivo*, we used a *myc*-tagged *Smad7*, which has already been demonstrated to block TGF $\beta$  signaling *in vivo* in adult transgenic mice [10]. Utilizing our *Wnt1-Cre/R26<sup>rtTA-EGFP</sup>/tetO-Smad7* trigenic mice, we can control temporal induction of *in utero* NCC-restricted *myc-Smad7* by feeding doxycycline-containing food to the pregnant mother (Fig. 5A).

### **Inducible overexpression of Smad7 *in vivo***

In order to verify the “silent but inducible” feature of our trigenic system, we placed each of the three individual *TetO-Smad7* target mouse lines onto *R26<sup>rtTA-EGFP</sup>/Wnt1-Cre* genetic background to generate *Wnt1-Cre/R26<sup>rtTA-EGFP</sup>/tetO-Smad7* trigenic mice. Male trigenic offspring were then crossed to homozygous female *R26<sup>rtTA-EGFP</sup>* mice (fed regular chow) and resultant trigenic embryos examined for *myc-Smad7* protein and *Smad7* mRNA overexpression. To simultaneously detect both endogenous and transgenic *Smad7* mRNA, forward and reverse primers were designed to locate within the *Smad7* cDNA transcript. For simplicity, the embryos containing all three transgenes (*Wnt1-Cre/R26<sup>rtTA-EGFP</sup>/tetO-Smad7*) are referred to as trigenic embryos, and all littermates with other genotypes (*Wnt1-Cre*, *R26<sup>rtTA-EGFP</sup>*, *tetO-Smad7*, *Wnt1-Cre/R26<sup>rtTA-EGFP</sup>*, *Wnt1-Cre/tetO-Smad7*, *R26<sup>rtTA-EGFP</sup>/tetO-Smad7*) are referred to as control embryos. As expected, normal litter sizes ( $n=8\pm 2$  embryos/litter from 10 litters) and trigenic offspring were recovered at expected Mendelian ratios (23.75%) when harvested at E14.5 (Table 1). Additionally, western analysis did not detect

myc-Smad7 protein expression in normal fed trigenic embryos (Fig. 4). Without doxycycline administration to the mother, these embryos develop normally and reach adulthood.

When the food was switched from regular to doxycycline-containing food, both myc-Smad7 protein induction and elevated *Smad7* mRNA expression were observed only in trigenic embryos (Fig. 5B, C). Specifically, feeding pregnant females doxycycline at E10.5 resulted in both *Smad7* mRNA upregulation (8x fold) and myc-Smad7 induction in E11.5 trigenic whole embryos but not within control (remaining allelic single and double transgenic combinations) littermates (Fig. 5B). This rapid induction is consistent with other studies that have shown rtTA-driven transgene expression is detectable with adult lungs 6-12 hours after doxycycline [83]. Additionally, the relative level of myc-Smad7 induction is comparable to the 3x fold elevation in aged skin and 4x fold elevation in some tumors [84]. Similarly, mycSmad7 is detected within trigenic E10.5 mutants only after being fed doxycycline (Fig. 5C). As similar levels of myc-Smad7 induction were observed using all three independent trigenic lines, results from just one line are presented to simplify data. Since *Smad7* has been shown to negatively regulate both TGF $\beta$  and BMP signaling *in vitro* [6], we examined whether myc-Smad7 induction attenuated both phosphorylated *Smad1/5/8* (pSmad1/5/8) and phosphorylated *Smad2/3* (pSmad2/3) levels *in vivo*. Western analysis reveals that pSmad1/5/8 levels were reduced by 55.5% ( $P < 0.037$ ) and pSmad2 levels were reduced by 58.3% ( $P < 0.021$ ) in doxycycline-fed trigenic whole embryos at

E10.5 (Fig. 5C, D). Similarly, when just NCC-enriched craniofacial and 1st pharyngeal arch tissues were used (Fig. 6), the presence of myc-Smad7 suppressed both pSmad1/5/8 (by ~72%) and pSmad2 (by ~85%) levels when compared to age-matched control tissues. Combined, these data demonstrate that transgenic Smad7 expression is tightly controlled in this three-component genetic system, and that myc-Smad7 expression is induced rapidly in NCC-derived tissues by application of doxycycline to the system and the induced myc-Smad7 represses both TGF $\beta$  and BMP signaling *in vivo*. In addition, when doxycycline was administered to wild type pregnant females throughout gestation starting at E6, normal litter sizes (n=8 embryos/litter from 6 litters) were recovered postnatally, demonstrating that sustained doxycycline does not adversely affect *in utero* morphogenesis.

### **Overexpression of Smad7 in the neural crest impairs normal craniofacial and pharyngeal arches development**

During craniofacial development, cranial NCC migrate ventrolaterally as they populate the craniofacial region. The proliferative activity of cranial NCC produces the frontonasal process and the discrete swellings that demarcate each branchial arch [14]. NCC lineage tracing experiments by crossing *Wnt1-Cre* with *Rosa26* reporter [85] mice show *Wnt-Cre* mediated *lacZ* gene expression starts in the rostral hindbrain around the four somite (E8.0) stage and extends to the midbrain, forebrain and caudal hindbrain, and progresses to increasingly caudal cardiac and trunk levels by eight somite (E8.5) stage [39]. Thus, *Wnt1-Cre* allows

recombination of floxed STOP  $R26^{rtTA-EGFP}$  rtTA expression within the NCC from very early stages of its development.

To examine the effects of Smad7 overexpression and to directly test the *in vivo* requirement of regulated TGF $\beta$  superfamily signaling during early NCC morphogenesis *in utero*, we fed pregnant trigenic females doxycycline from E7.5, a stage that is prior to the onset of *Wnt1-Cre* expression [39] and NCC emigration from the neural tube [12-13, 62-64]. Resultant embryos were harvested at E9 to birth. Initially, E9 trigenic embryos are indistinguishable from control littermates, but by E10 the trigenics are slightly smaller and exhibit subtle craniofacial and pharyngeal arch dysplasia defects (Fig. 7A-C). Specifically, the 1<sup>st</sup> pharyngeal arch is hypoplastic and the face/forebrain region is undersized. This is more evident at E11.5, as all the trigenic embryos have significantly smaller craniofacial regions (n=7/7 trigenics exhibit craniofacial defects) and greatly reduced 1<sup>st</sup>, 2<sup>nd</sup> and 3<sup>rd</sup> pharyngeal arches (Fig. 7D-F). By E13.5, the trigenic embryos grossly lack identifiable upper and lower jaws (Fig. 7G-I) but are otherwise viable. In addition, none of the doxycycline-fed trigenic offspring were recovered at birth (n=7 litters). The non-trigenic littermates with remaining allelic combinations were phenotypically normal and serve as genetic background, age-matched and doxycycline-exposure controls ( $R26^{rtTA-EGFP}/Wnt1-Cre$ ;  $R26^{rtTA-EGFP}/tetO-Smad7$ ;  $R26^{rtTA-EGFP}/R26^{rtTA-EGFP}$ ). Histology revealed that the upper and lower jaws were indeed hypoplastic and that the tongue was reduced in size, but that Meckel's cartilage, which forms a template for mandible formation and is

derived from the cranial NCC [14], is still present (Fig. 8B). This data is consistent with the underdevelopment of medial nasal prominences and incomplete tongue formation observed in *Wnt1-Cre;Smad4<sup>loxp/loxp</sup>* embryos [40-41]. Histology also revealed that 100% of E13.5 trigenic mutants (n=5) lack the choroid plexus that extends into the fourth ventricle, even though the choroid plexus extending into the lateral ventricle is present (Fig. 8B). X-Gal staining of *Wnt1-Cre;R26r* brains has shown that recombination of the *R26r* allele is confined to the CNS midbrain, hindbrain and cerebellum & choroid plexus in 4<sup>th</sup> vent /hindbrain [86] and robust TGFβ signaling has been shown to be present within the migrating cranial NCC, meninges, and choroid plexus [87]. The observed selective loss of the choroid plexus that extends into the fourth ventricle is likely due to the restricted *Smad7* overexpression within the NCC that contribute to this particular choroid plexus.

### **Induced *Smad7* overexpression impairs normal cardiac development**

As trigenic mutants fed doxycycline from E7.5 onwards were not recovered at birth and *Wnt1-Cre;R26r* marked NCC have been shown to be essential for heart morphogenesis [13, 64], we examined the effects of overexpression of *Smad7* within NCC lineages in cardiovascular system. Cardiac NCC migrate along the 3<sup>rd</sup>, 4<sup>th</sup>, and 6<sup>th</sup> pharyngeal arches to colonize the OFT cushions, where they are required for septation of the truncus arteriosus into the aorta and pulmonary artery [13]. Histology revealed that all trigenic mutants exhibit OFT defects (n=11/11 trigemics fed doxycycline at E7.5), specifically a single outlet forming

persistent truncus arteriosus (PTA). Besides a failure of OFT separation, the ascending aorta in trigenic embryos was retroesophageally located (Fig. 8D) and the outlet valve leaflets were abnormally thickened (Fig. 8F) when compared to those seen in the control embryos (Fig. 8C, E). Additionally, trigenic embryos present accompanying membranous intraventricular septal defects (VSD) (Fig. 8H). However, trigenic dorsal root ganglia and thymus appeared grossly unaffected relative to the overall embryo size (Fig. 8J, L), notwithstanding having a NCC contribution [20]. Furthermore, trigenic dorsal root ganglia were normally colonized via NCC lineage (Fig. 9).

### **Neural crest lineage mapping reveals regional deficiencies**

To verify *Wnt1-Cre* recombination efficiency in trigenics and to determine the origin of defects found in craniofacial structures, pharyngeal arches, and the heart, trigenic mice NCC were lineage mapped. Earlier studies have shown that elements of TGF $\beta$  superfamily signaling are required for normal craniofacial and cardiac NCC migration. For example, *Wnt1-Cre* conditional deletion of *Smad4* [40-41, 72-73] and transgenic overexpression of the BMP-antagonist Noggin [15] can result in NCC deficiency. Analysis of *lacZ* stained trigenic mutant embryos carrying the *R26r* reporter showed normal NCC migration and contribution to the craniofacial region and dorsal root ganglia, but reduced NCC colonization to the OFT. From E10.5-11.5, robust *lacZ* staining was evident in the frontonasal prominence, trigeminal nerve ganglia, 1<sup>st</sup>, 2<sup>nd</sup> pharyngeal arches along with facial nerve ganglia, and primordium of the 3<sup>rd</sup> pharyngeal arch in trigenic embryos



(Fig. 9A, C, D), similar to that observed in controls (Fig. 9A, B, D). Intriguingly, this assay revealed that whereas the NCC populate the craniofacial and pharyngeal regions, the 1<sup>st</sup>, 2<sup>nd</sup> and facial regions failed to form normally and were hypoplastic in trigenics (Fig. 7). However, in E13.5 trigenic embryos there were subsequent *lacZ*-negative areas of frontonasal mesenchyme, suggesting that there was a subsequent loss of *lacZ*-positive cells (Fig. 9N). Similar to the cranial NCC, migration of the *lacZ*-marked cardiac NCC was largely unaffected in E10.5 trigenic embryos (Fig. 9A-C), and trunk NCC contribution to the trigenic dorsal root ganglia was unchanged when compared to littermate controls (Fig. 9A, D). However, further analysis of cardiac NCC colonization of the heart shows that although a significant number of NCC have populated the pharyngeal arches and aortic sac, only a few trigenic NCC colonized the truncal region and there was a complete lack of colonization of the more proximal conal cushion region of the trigenic truncus arteriosus (Fig. 9G, H, L) when compared to control littermates (Fig. 9E, F, K). The foremost difference of cardiac NCC contribution to the trigenic OFT embryos could also be seen at later stages (Fig. 9P). The difference between the presence of fully penetrant OFT defects and dramatically reduced cardiac NCC colonization and unaffected NCC contribution to the dorsal root ganglia and normal cranial NCC migration patterns suggests that the cardiac NCC population and morphogenesis of the OFT are especially sensitive to suppression of TGF $\beta$  superfamily signaling. Furthermore, lineage mapping established that Smad7-mediated suppression of TGF $\beta$  superfamily signaling

principally inhibits later cardiac NCC colonization of the OFT rather than early NCC emigration and migration from the neural tube.

### **Trigenic mutants exhibit normal proliferation but increased cell death**

Such dramatic changes in the morphology of the frontonasal and OFT tissues could be accomplished via a change in the amount of cell death and/or cell proliferation. Cell proliferation assays, using Ki67 to mark cells in all active phases of the cell cycle (G1, S, G2, and mitosis) in sectioned E10.5 trigenic embryos fed doxycycline from E7.5 onwards, did not detect any decrease in facial, 1<sup>st</sup> pharyngeal arch mesenchyme or OFT cushion cell proliferation index (Fig. 10A-C). Total E10.5 1<sup>st</sup> pharyngeal arch proliferation in trigenic mutants was reduced (~675 Ki67 positive cells/arch/10 $\mu$ m section) when compared to age-matched control embryos (~1,003 Ki67 positive cells/arch/10 $\mu$ m section), due to the hypoplastic trigenic phenotype. This was specifically apparent at the base of the 1<sup>st</sup> trigenic arch (Fig. 10B), where the mesenchyme was sparse compared to control littermates. However, when proliferating cells were tallied (as a percentage of total cells in the 1<sup>st</sup> pharyngeal arch) to calculate a mitotic index, there was no significant difference by this measure (90.9% in controls versus 91.2% in trigenics). Thus, the defects in mutant embryos were unlikely to be caused by reduced NCC proliferation.

In contrast, using the TUNEL assay to mark apoptotic cells, dramatic increases in cell death in the E10.5 trigenic facial and pharyngeal arch mesenchyme and

within migratory NCC lineages were observed (Fig. 10D-F). Considerable and aberrant cell death was localized to the facial primordia and 1<sup>st</sup> (Fig. 10E), 2<sup>nd</sup> and 3<sup>rd</sup> pharyngeal arches of trigenic embryos, but not within the OFT cushions (Fig. 10M) nor the cardiomyocytes of the heart (Fig. 10M). The sparse mesenchyme at the base of the 1<sup>st</sup> trigenic arch still contained several apoptotic cells, but is adjacent to a region of very robust apoptosis (Fig. 10E). When TUNEL positive cells were tallied as a percentage of total cells in the 1<sup>st</sup> arch to calculate a cell death index, there was a significant increase in cell death (1.55% in controls versus 16.52% in trigenics,  $P < 0.001$ ). To test if these apoptotic cells were limited to NCC, we performed X-gal staining on E11.0 trigenic; *R26r* embryos to label NCC and their derivatives followed by TUNEL assay (Fig. 10G). As expected, many NCC were positively stained with the TUNEL signal. These data are consistent with the dramatic increases in cell death observed in *Wnt1-Cre;Smad4<sup>loxp/loxp</sup>* [40-41, 72-73] and *Wnt1-Cre;Alk5<sup>loxp/loxp</sup>* embryos [36], as both *Smad4* and *Alk5* are required for survival of cardiac NCC. Similarly, *Wnt1-Cre;Alk3<sup>loxp/loxp</sup>* embryos exhibit normal NCC migration, but NCC subpopulations die immediately after colonization of their target tissues [21]. Intriguingly, loss of BMP antagonists (Noggin and Chordin) result in excessive NCC emigration from the neural tube that results in elevated NCC-restricted apoptosis [88]. Combined, these data reveal that tightly regulated TGF $\beta$  superfamily signaling within early NCC is required for normal survival of migratory NCC-derived mesenchyme, either block of individual TGF $\beta$  or BMP pathway effectors or increased BMP signaling can both likewise distress NCC survival *in vivo*.

### **Aortic arch artery remodeling is unaffected**

Given the frequent association of anomalous pharyngeal aortic arch artery (AAA) remodeling and pathogenesis of OFT defects [13, 80, 89-90] we used histology and  $\alpha$ -smooth muscle actin ( $\alpha$ SMA) immunohistochemistry to determine whether AAAs were properly patterned in trigenic mutants fed doxycycline from E7.5 onwards (Fig. 10H-K). This analysis revealed that the trigenic AAAs were well formed by E10.5, suggesting that induction of Smad7 in NCC does not disrupt initial arch artery formation. However,  $\alpha$ SMA staining of the OFT cushions was reduced in E10.5 mutants, and as colonizing cardiac NCC express  $\alpha$ SMA [91], these results confirm the reduced *Wnt1-Cre; R26r* lineage mapping data in trigenic OFT cushions (Fig. 9). We further examined whether AAAs were correctly remodeled E11.5-13.5 and whether  $\alpha$ SMA positive NCC-derived cells ensheath the remodeled trigenic AAAs (Fig. 10J, K). Both the control and trigenic 4<sup>th</sup> and 6<sup>th</sup> AAAs were intact and exhibit similar intact  $\alpha$ SMA expression patterns. Despite suppression of TGF $\beta$  signaling within NCC lineage, we did not observe abnormal regression of AAAs, a defect which was reported in *Wnt1-Cre;Alk2<sup>loxp/loxp</sup>* and *Wnt1-Cre;Alk5<sup>loxp/loxp</sup>* embryos [36, 38].

### **Localized attenuated TGF $\beta$ and BMP signaling**

To further resolve the molecular defects in trigenic mutants caused by NCC-restricted induction of Smad7, we examined the spatial expression of both pSmad1/5/8 and pSmad2 in trigenic and control embryos fed doxycycline from E7.5 onwards. Consistent with western data (see Fig. 5C, D and Fig. 6),

pSmad1/5/8 and pSmad2 expression was reduced in E10.5 trigenic embryo NCC lineages compared to control littermates (Fig. 11). Significantly reduced numbers of pSmad1/5/8-positive and pSmad2-positive cells were detected in the mesenchyme and ectoderm-derived epithelium of the trigenic frontal facial region (Fig. 11B, J) and pharyngeal arches (Fig. 11D, L), and within the aortic sac mesenchyme (Fig. 11F, N), but not in the trigenic ventricular myocardium/epicardium/endothelium (Fig. 11H, P). Each of the mesenchymal sites of reduced pSmad1/5/8 and pSmad2 expression correlate with *Wnt1-Cre;R26r* lineage mapped NCC (Fig. 9) [14, 20], indicating that both TGF $\beta$  and BMP signaling were significantly attenuated within NCC *in vivo* by overexpression of myc-Smad7. These immunohistochemical data are consistent with the significantly reduced pSmad levels detected via whole body (Fig. 5) and NCC-enriched western blotting (Fig. 6).

### **Altered gene expression in pharyngeal arches in trigenic embryos**

To investigate the signaling mechanism of Smad7 overexpression in regulating epithelial-mesenchymal interactions, we examined expression patterns of genes that express in the early neural tube and migratory NCC and genes that are critical during early mandible development. We examined expression of the *Crabp1* and *Ap2 $\alpha$*  NCC markers, as well as *Fgf8* expression in E10.5-13.5 trigenic and control embryos fed doxycycline from E7.5 onwards (Fig. 12). Both *Crabp1* and *Ap2 $\alpha$*  transcription factors are retinoic acid responsive genes that are expressed in migrating NCC [79-80]. In developmentally older embryos, *Ap2 $\alpha$*  is

still expressed within migratory NCC but is also expressed robustly within the ectoderm [92]. *Fgf8* encodes a signaling growth factor molecule expressed in the epithelia of pharyngeal arches, and is required for normal growth of pharyngeal arches and remodeling of OFT [93]. Significantly, expression of *Crabp1* (Fig. 12B) and *Ap2α* were visibly reduced (but not eliminated) from their expression domains within E10.5 trigenic migratory cardiac NCC, whereas expression of *Crabp1* was not noticeably affected within non-NCC derived body wall. *Ap2α* was also reduced within trigenic facial mesenchyme, but that most likely reflected apoptotic loss of cranial NCC. Intriguingly, while ectodermal *Ap2α* expression appeared comparable between control and trigenic littermates, trigenic 1<sup>st</sup> arch mesenchyme *Ap2α* expression was increased compared to control mesenchyme (Fig. 12C, D). Correspondingly, *Fgf8* was specifically elevated within the trigenic 1<sup>st</sup> pharyngeal arch and facial ectodermal lineages (Fig. 12F). Counting of silver grains/cell revealed a ~4x increase in *Fgf8* expression in trigenic (87 +/-11 grains/cell; n=3 embryos, five 10μm sections/embryo) vs. control (22 +/-8 grains/cell; n=3 embryos, five 10μm sections/embryo) 1<sup>st</sup> arch ectoderm. Collectively, these results indicate that suppression of TGFβ superfamily signaling within the cranial and cardiac NCC disrupted not only gene expression in distinct NCC populations but also normal developmental processes in neighboring cell populations. Thus, bystander effects upon neighboring epithelial TGFβ superfamily signaling may augment the subsequent hypoplasia of these structures and contribute to the overall pathogenesis of the severe malformations in trigenic mutant embryos.

## **Overexpression of Smad7 in the neural crest following OFT colonization also results in abnormal heart development**

To examine the effects of Smad7 overexpression within post-migratory NCC following colonization of their target tissues, we fed pregnant trigenic females doxycycline from E10 onwards. Our initial characterization of the trigenic system revealed that feeding pregnant females doxycycline at E10.5 resulted in both *Smad7* mRNA upregulation and myc-Smad7 induction by E11.5 in only trigenic but not control littermates (see Fig. 5). Grossly, E14.5 trigenic fetuses were indistinguishable from control littermates, but histology revealed that 100% of the E14.5 trigenic mutants exhibit membranous VSD (n=7/7 trigenics exhibit heart defects; Fig. 13D) that persisted until birth (n=3/3 trigenics). Additionally, although the trigenic OFT was divided and separate aorta and pulmonary arteries exit their respective right and left ventricles, there was a significantly dilated outflow lumen and possibly reduced endocardial cushion cells (Fig. 13B). Further examination of the dorsal root ganglia, thymus and craniofacial regions did not reveal any other histological defects (not shown). *Wnt1-Cre;R26r* lineage mapping revealed that regular numbers of NCC colonize the trigenic OFT and aorticopulmonary septum at the appropriate developmental stage, and that they survive until at least E13.5 (Fig. 13F) following post-migratory Smad7 overexpression. Additionally, histology revealed that the OFT was fully divided and that the trigenic valves were normal (Fig. 13F). Significantly, myocardialization of the cushions occurs (Fig. 13G, H) and there are similar levels of apoptosis (Fig. 13I, J) in both trigenic and control littermates. This is

significant as it has been proposed that the relatively small population of cardiac NCC cells that migrate into the proximal cushions are required to die to promote myocardialization [94].



## Discussion

The physiological consequences of postnatal Smad7 dysregulation is demonstrated by the finding that SMAD7 is upregulated in a number of pathological conditions in patients, including development of malignancy [95-96], scleroderma [97], and chronic inflammatory bowel diseases [98]. *Smad7* has also recently been shown to be required for embryogenesis as the majority of *Smad7* knockout mouse embryos die *in utero* due to multiple defects in cardiovascular development, including VSD and OFT malformations [99]. Indeed, endogenous *Smad7* mRNA is transiently activated pre-implantation, then is re-expressed widely post-gastrulation [100]. In E10 and E12.5 embryos, *Smad7* mRNA is widespread outside the developing central nervous system, including the NCC-derived mandibular and medial nasal processes, developing pharyngeal arches, OFT cushions of the heart, adrenal primordium and trigeminal ganglion [55, 100]. Transgenic reporter and Cre/loxP lineage mapping using a partial *Smad7* promoter have also confirmed the robust expression of *Smad7* mRNA within the craniofacial, pharyngeal arch and cardiovascular system [75, 101]. However, the role of *Smad7* within the NCC lineage and specifically the effects of misregulation of Smad7 and overexpression *in utero* remain unknown.

We hypothesized that *in vivo* misexpression of a potent TGF $\beta$  signaling inhibitor like Smad7 would generate severe NCC cell hypoplasia and resultant neurocrestopathies. Our data provide compelling genetic evidence demonstrating that forced expression of Smad7 within NCC is detrimental to development of

NCC and their derivatives. Moreover, we showed that levels of both TGF $\beta$  and BMP phosphorylated R-Smads were reduced in the NCC expressing myc-Smad7. Since TGF $\beta$  superfamily signaling is known to increase production of phosphorylated forms of R-Smad proteins, our data provide good evidence that TGF $\beta$  signaling *in vivo* is impaired by myc-Smad7 induction in NCC. The spectrum of trigenic phenotypes fit well with previous studies reporting craniofacial, pharyngeal, cardiac defects and *in utero* lethality within NCC restricted Wnt1-Cre;Smad4<sup>loxp/loxp</sup> embryo mutants [40-41, 72-73]. Thus, combined these data strongly suggest that altered NCC TGF $\beta$  superfamily signaling, either via targeted deletion of Smad4 or upregulation of Smad7 can both play pathogenic roles that result in neurocrestopathies.

Although members of the WNT family have been shown to specify NCC from early dorsal neuroepithelial cells [102-103] and Wnt/ $\beta$ -Catenin signal activation plays an instructive role in specification of NCC sensory fate [104], the molecular mechanisms underlying the determination, pathway-dependent control and morphogenesis of the diversity of NCC fates remains far from clear. Some alternative NCC fates have been shown to be instructively promoted by TGF $\beta$  superfamily members [102, 105]. For example, Bmp2 causes cloned NCC to form autonomic neurons and can also induce some smooth muscle differentiation, while TGF $\beta$ 1 exclusively promotes smooth muscle differentiation [105]. Surprisingly, although our lineage analysis and immunohistochemical assays revealed robust NCC death within trigenic embryos fed doxycycline from

E7.5 onwards, subsequent NCC colonization of the trigenic dorsal root ganglia, trigeminal ganglion, thymus and  $\alpha$ SMA-positive NCC-derived subpopulation that ensheath the remodeling trigenic AAA which give rise to the great vessels exiting the heart were all unaffected (Fig. 9, 10). Thus, Smad7 induction appears to aberrantly affect specific subpopulations of NCC, independent of where they originate from, when they initiate migration or even how far they are required to migrate prior to target tissue colonization. Indeed, forced expression of Smad7 within pancreatic beta cells [106] and human umbilical cord blood cells [107] has similarly been shown to inhibit differentiated cell formation and suppression of TGF $\beta$  signaling alters cell fate decisions.

Craniofacial and cardiac defects thought to arise principally from perturbation of NCC morphogenesis are prominent features of DiGeorge syndrome (DGS)/velocardiofacial syndrome (VCFS), as well as Noonan syndrome (NS) [108-109]. While NS is caused by a gain-of-function mutation in SHP2 [109], DGS/VCFS is the result of a recurrent deletion in chromosome 22q11 [110]. DGS/VCFS is the most common micro-deletion syndrome in patients [108], but not all DGS/VCFS patients have the 22q11 deletion [111-112]. Additionally, several modifiers of the DGS/VCFS have been identified in patients and modeled using mouse transgenics, including VEGF [90], FGF8 [108] and CHD7 [113]. Although the microdeletion of 22q11 encompasses ~30 genes, including Arc105, Tbx1 and Crk1, it does not include any of the TGF $\beta$  superfamily receptors or ligands. Thus, gene products eliminated by 22q11 deletions may functionally

interact with TGF $\beta$  signaling within the NCC lineage. For instance, Arc105 has been shown to modulate TGF $\beta$  signaling within embryos [114], and both Tbx1 [113] and Crkl [30] can directly regulate TGF $\beta$  signaling within murine NCC via modulating R-Smad phosphorylation and altering the ability of R-Smads to bind Smad4 [115]. These findings imply that the common developmental abnormalities observed in DGS/VCFS and NS patients may arise from perturbation of the same pathway. Although the reduced expression levels of *Ap2 $\alpha$*  and *Crabp1* mRNA are to be expected (Fig. 12) given the observed elevation of NCC death (Fig. 10), our molecular marker analysis did reveal an unexpected finding. One particularly significant discovery is that *Fgf8* levels are elevated within the epithelia of the trigenic pharyngeal arches, as FGF8 is a known modifier of DGS/VCFS and FGF8 signaling is mediated by Crkl [108]. Functions of these genes have been implicated in mediating interactions between NCC and their neighboring cells in facial primordia and pharyngeal arches, and subsequent organogenesis [116]. Combined, these data indicate that suppression of TGF $\beta$  signaling within the cranial and cardiac NCC disrupts not only distinct NCC gene expression, but also normal developmental processes in neighboring cell populations. In order to find the common downstream effectors, detailed analysis of the resultant gene expression profile changes within isolated trigenic NCC subpopulations will be required to identify which NCC-restricted gene pathways are altered in response to suppressed TGF $\beta$  signaling.

The spectrum of cardiac defects caused by Smad7 induction in early NCC resembles those associated with cardiac NCC ablation in avian embryos, in which both anomalous AAA remodeling and lack of OFT septation with concomitant VSDs are observed [117]. Cardiac NCC normally migrate to the OFT region via the 3<sup>rd</sup>, 4<sup>th</sup> and 6<sup>th</sup> pharyngeal arches to form the two-pronged cushions in the truncal region of the OFT where they contribute to the septation of aorta and pulmonary outlets [65]. However, not all cardiac NCC colonize the OFT cushions, as a subpopulation remains in the caudal pharyngeal arches and differentiates in a smooth muscle layer enveloping the 4<sup>th</sup> and 6<sup>th</sup> arch arteries [20, 118]. Surprisingly, despite extensive NCC death and reduced Wnt1-Cre;R26r reporter expression within trigenic mutants that exhibit severe OFT septation and VSD defects, both smooth muscle actin expression and normal AAA remodeling were observed (Fig. 9, 10). This is consistent with the phenotypes reported in *Wnt1-Cre;Smad4<sup>loxp/loxp</sup>* and *Wnt1-Cre;Tgfb2<sup>loxp/loxp</sup>* mutants [34, 40-41, 72-73]. Thus, OFT septation defects appear to be a common feature of all mouse models in which TGF $\beta$  signaling is impaired in NCC, indicating a central role for TGF $\beta$  superfamily signaling within NCC during cardiac development. Although it is possible for embryos to exhibit OFT septation defects without AAA abnormalities and it is possible to have AAA defects without OFT septation defects [118], it remains unclear why suppression of TGF $\beta$  signaling within the cardiac NCC subpopulation predominantly results in only OFT septation defects. It has been proposed that TGF $\beta$  signaling may not be required for specification of a smooth muscle fate because this is the default

pathway or that TGF $\beta$  signaling within cardiac NCC acts as a local morphogenic factor rather than as an instructural cue for cell lineage specification or smooth muscle differentiation [34]. Our trigenic data would support these conclusions and additionally infer that TGF $\beta$  signaling in cardiac NCC within the pharyngeal arches is required to provide the stimulus for subsequent NCC colonization of the OFT itself and for survival of this colonizing OFT subpopulation. This conclusion is further supported by our significant finding that later induction of Smad7 in NCC that have already reached the pharyngeal arches and OFT also results in OFT anomalies and VSD (Fig. 13). Since Smad7 blocks multiple receptor-activated TGF $\beta$  signaling pathways, our work has not yet revealed roles of individual receptor-mediated TGF $\beta$  pathways that are responsible for maintaining this colonizing OFT NCC subpopulation.

Elucidating the molecular pathways and mechanisms regulating the fate of the cranial and cardiac NCC subpopulations is fundamental to our understanding of the pathogenesis of numerous congenital syndromes. In addition to stimulatory factors, migrating NCC encounter environments rich in inhibitors that may counteract signaling molecules such as WNTs, BMPs and TGF $\beta$ . Our Smad7 inhibitory NCC-restricted studies reinforce the notion that TGF $\beta$  signaling is dispensable for NCC formation and emigration but plays a critical role during craniofacial and cardiac NCC morphogenesis and colonization of target tissues. We observed a severe reduction of NCC pSmad2 and pSmad1/5/8 expression, resulting in suppression of the temporal and spatial specification of TGF $\beta$

signaling and subsequent loss of craniofacial and OFT cushion NCC in trigenic Smad7 embryos. Moreover, Smad7 overexpression within post-migratory cardiac NCC also resulted in cardiac defects, suggested that TGF $\beta$  signaling plays multiple roles at multiple times, even in the same NCC subpopulation. Although there is a paucity of data regarding the function of post-migratory NCC within the heart itself, it has been shown that NCC-specific N-cadherin, RhoA and Cx43 expression are each required for normal OFT morphogenesis, cell shape, alignment and cell-cell communication. *Wnt1-Cre;N-cadherin* mutant NCC are unable to elongate and align properly along the midline and remained rounded with limited contact with their neighbors within mutant OFTs [119]. Activation of RhoA is required for NCC contact inhibition of locomotion *in vivo* to control NCC directional migration [120]. Cx43 mediates modulation of polarized cell movement and the directional migration of cardiac NCC [121]. Significantly, N-cadherin, RhoA and Cx43 are all known to be responsive to TGF $\beta$ -signaling [2], thus these data suggest that further studies are required to understand the link between lineage commitment and the many changes in cushion cell shape, cell-matrix adhesion, and cell-cell adhesion that occur within the OFT itself and during interventricular septal morphogenesis, and how suppression of TGF $\beta$  superfamily signaling may aberrantly affect one or more of these processes. Perhaps inhibitors of TGF $\beta$  inhibitors are required to titrate or delay responses as NCC differentiate along particular pathways, and that Smad7 overexpression prevents endocardial cushion differentiation resulting in defective septation. Taken together, these results demonstrate that fine-tuning of TGF $\beta$  signaling via

proteins including Smad7 is crucial for normal development. We speculate that this method for conditional myc-Smad7 expression may be useful for elucidating further TGF $\beta$  roles in other organs and tissues and addressing the biological significance of the concerted action between growth and transcription factors in regulating normal development and disease.



Litters	Embryos from each litter	Trigenic embryos
1	7	3
2	5	2
3	10	1
4	10	2
5	7	2
6	9	2
7	7	1
8	6	1
9	11	3
10	8	1
	Total: 80	Total: 19 (23.75%)

**Table 1. Embryos harvested at E14.5 fed regular food.**

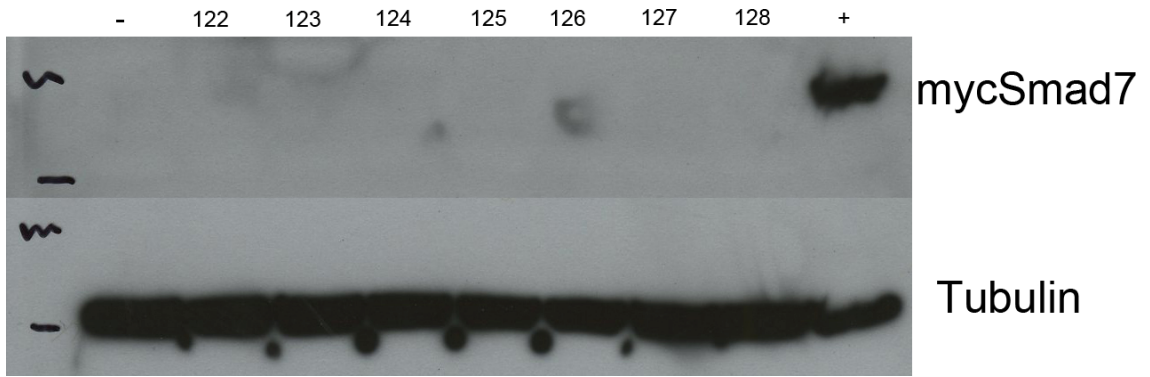


**Figure 4. No mycSmad7 was detected by western blot in E14.5 embryos fed with regular food.** -, mycSmad7 negative sample; +, mycSmad7 positive sample; 122, 123, 125 are trigenic embryos based on PCR; 124, 126, 127, 128 are control embryos based on PCR.

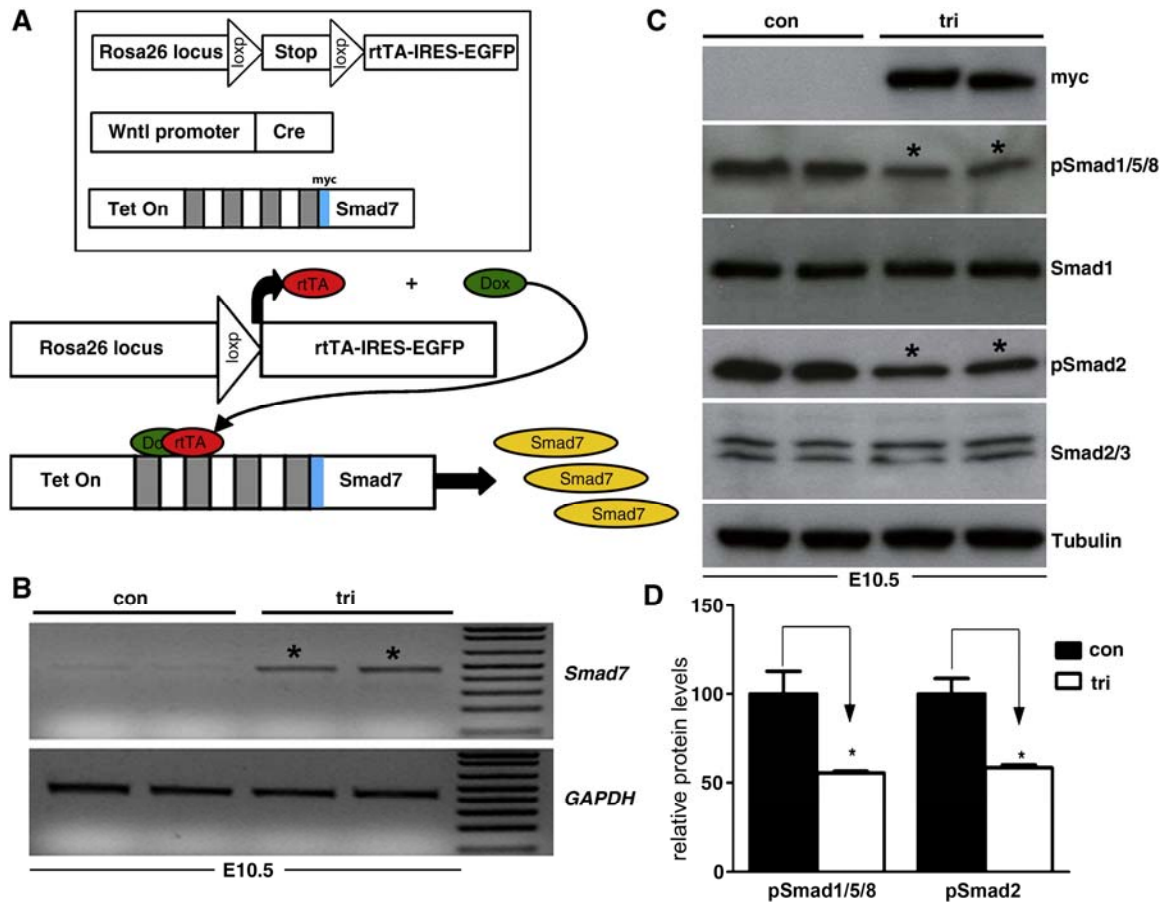


**Figure 5. Evaluation of the trigenic Cre/loxP-dependent, tetracycline inducible transgenic system. (A)** Schematic illustrating operation of the trigenic system. The  $R26^{rtTA-EGFP}$  knockin mice will only express the rtTA from the *Rosa26* locus upon Cre-mediated recombination [74]. *Wnt1-Cre* transgenic mice have been shown to label almost all NCC, including the cardiac and craniofacial NCC lineages [14, 20]. In the *tetO-Smad7* transgenic mice, myc-Smad7 full length cDNA (myc tag is blue box 5' of *Smad7* cDNA) is under the control of heptamerized tetOn promoter, but Smad7 is not expressed until both the transactivator (rtTA) and inducer (doxycycline) are present within the same cell. Although all three transgenes are individually silent within the compound trigenic mice, myc-tagged Smad7 can be specifically induced within Cre-positive neural crest lineages upon doxycycline feeding. Thus, the spatiotemporal timing of myc-tagged Smad7 expression is determined by the timing of doxycycline addition and positionally by the expression of Cre recombinase. **(B)** RT-PCR analysis reveals that *Smad7* mRNA expression is upregulated ~10 fold in trigenic E10.5 embryos fed doxycycline at E7.5 compared to control embryo expression of endogenous *Smad7* (n= 4 embryos of each genotype). Loading was normalized using GAPDH housekeeping control. **(C, D)** Western analysis verifies that myc-Smad7 is only expressed within trigenic E10.5 embryos fed doxycycline at E7.5, and is absent from littermate control embryos (n=3). The presence of myc-Smad7 suppressed both pSmad1/5/8 and pSmad2 levels relative to total Smad1 and pSmad2/3 levels when compared to age-matched control littermates, indicating overexpression of Smad7 attenuates both BMP and TGF $\beta$  signaling

by ~55% (D). Loading was normalized using tubulin housekeeping control.  
Abbreviations: tri, trigenic *Wnt1-Cre/Rosa<sup>rtTA-EGFP</sup>/tetO-Smad7* embryos; con, control embryos; \*, significant change.

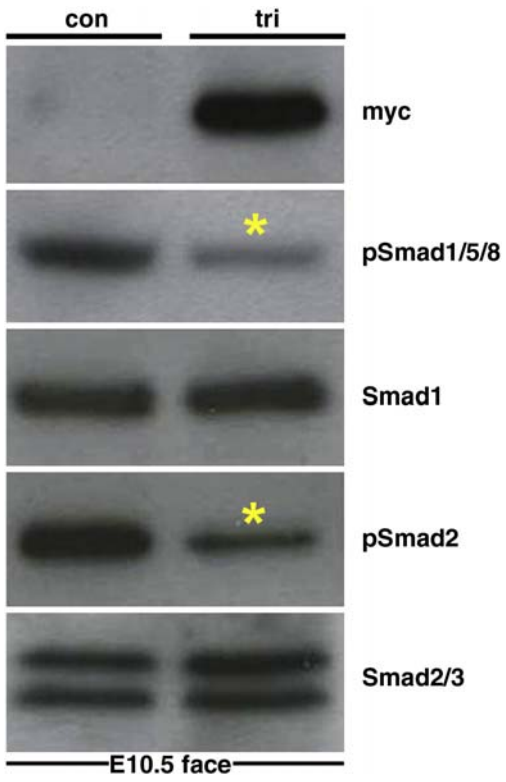


**Figure 6. Western analysis of NCC-enriched craniofacial tissues.** Both E10.5 control (con) and Smad7 trigenic (tri) microdissected frontonasal regions (including 1st pharyngeal arch) fed doxycycline at E7.5, were examined via Western analysis. Note that myc-Smad7 is only expressed within pooled (n=4) doxycycline-fed trigenic E10.5 tissues, but is absent from pooled control (n=4) samples. Moreover, in tissues known to be mostly populated by NCC, densitometry revealed that the presence of myc-Smad7 suppressed both pSmad1/5/8 (by ~72%) and pSmad2 (by ~85%) levels relative to total Smad1 and pSmad2/3 levels when compared to age-matched controls. Abbreviations: tri, trigenic *Wnt1-Cre/Rosa<sup>rtTA-EGFP</sup>/tetO-Smad7* embryos; con, control embryos; \*, significant change.

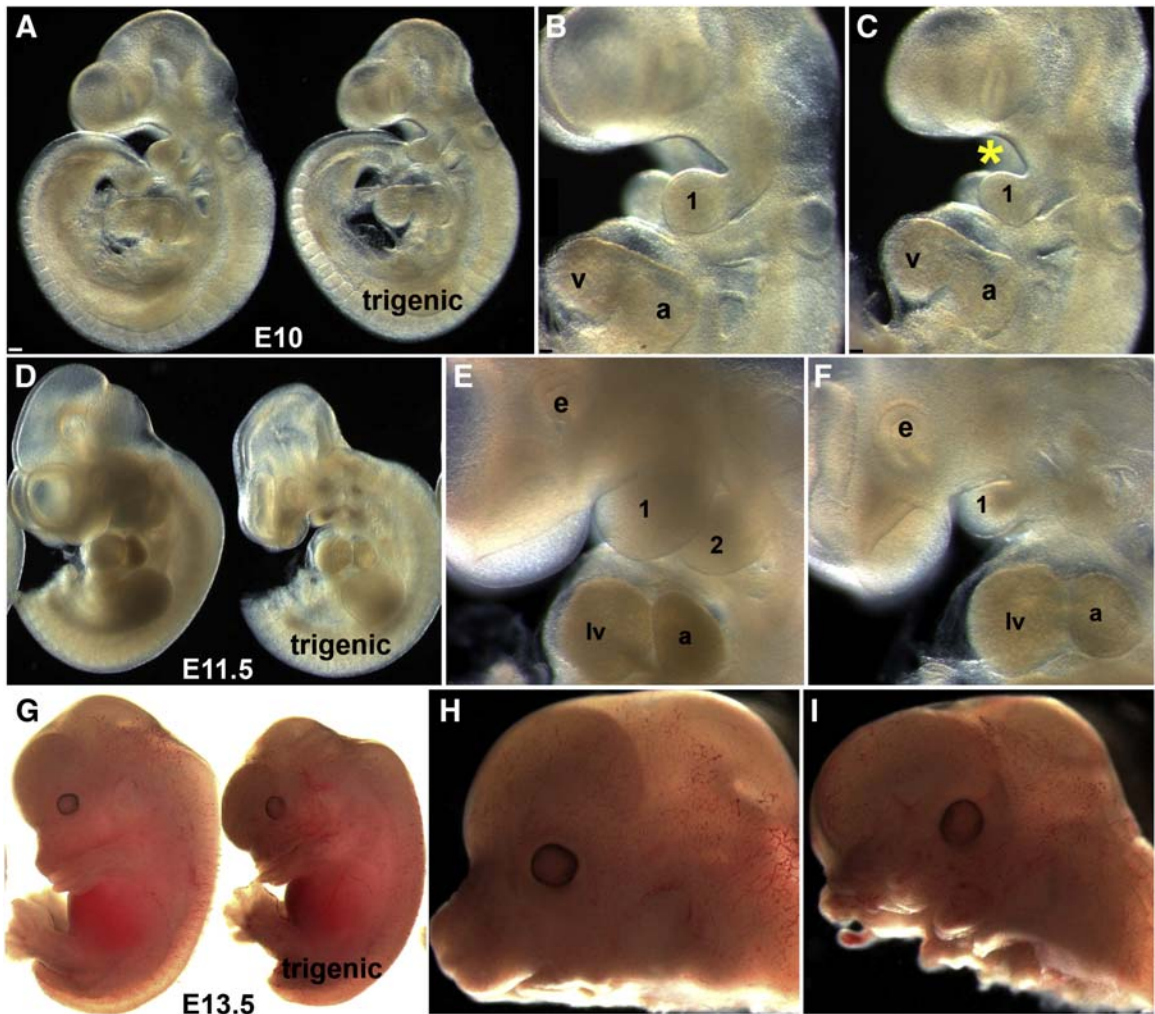




**Figure 7. Early Smad7 induction within the neural crest lineage suppresses normal craniofacial and pharyngeal arch development. (A-C)** E10.0 control and trigenic (right embryo in A) whole embryos fed doxycycline at E7.5 appear grossly similar except smaller facial processes, but higher magnification reveals that the mandibular component of the E10.0 trigenic mutant 1<sup>st</sup> pharyngeal arch is undersized and the oropharyngeal region below the nasal process is enlarged (indicated by \* in C) when compared to age-matched control (B). **(D-F)** E11.5 control and trigenic (right embryo in D) whole embryos. Note trigenic 1<sup>st</sup> and 2<sup>nd</sup> arches are dramatically underdeveloped and the facial processes are hypoplastic (F) when compared to controls (E), but the size of the trigenic heart appears unaffected. **(G-I)** E13.5 control and trigenic (right embryo) whole embryos fed doxycycline at E7.5. Note in isolated heads (severed immediately below lower jaw) both the upper and lower jaws of the trigenic mutant are severely hypoplastic and largely absent (I) when compared to control littermates (H). Abbreviations: 1, first pharyngeal arch; 2, second pharyngeal arch; a, atrium; v, ventricle; lv, left ventricle; e, eye. Bar in A=0.1mm; B, C=0.05mm. [Paige L. Snider contributed to this figure].

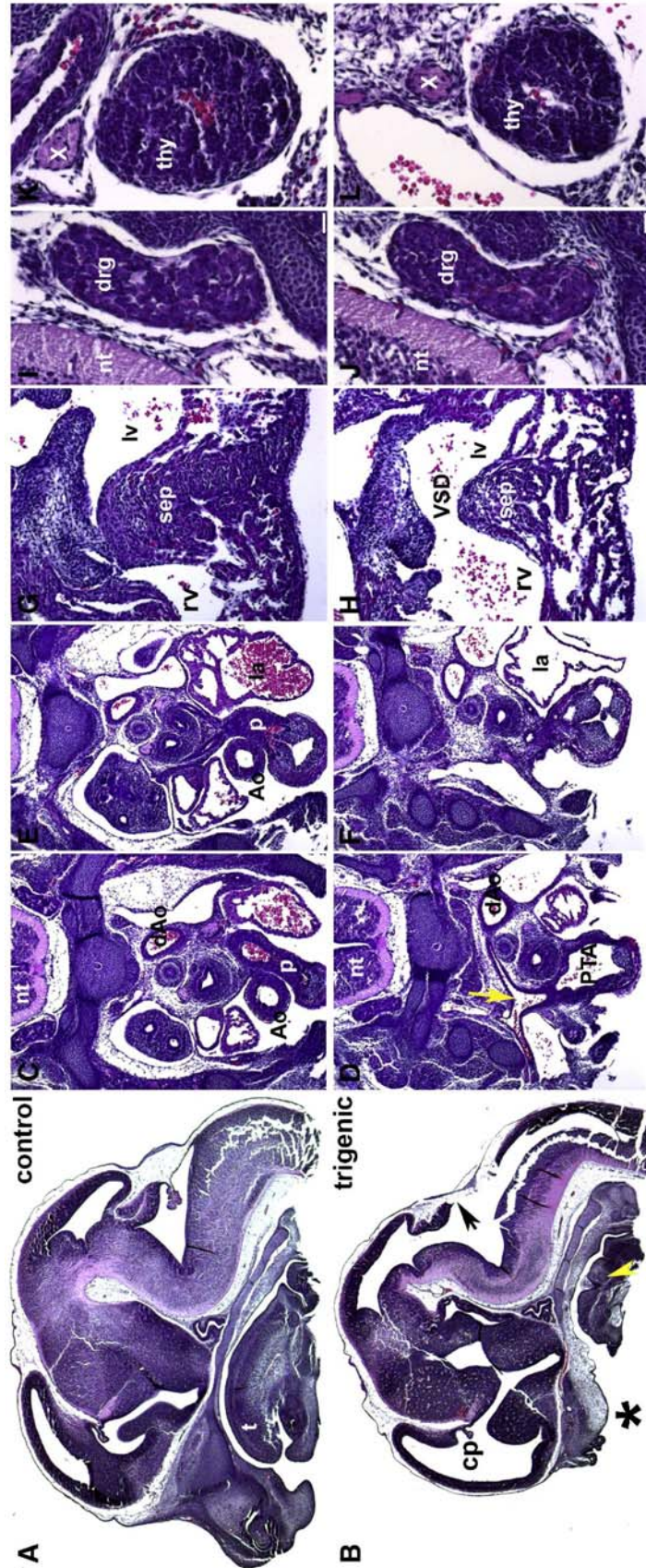


**Figure 8. Histological examination of E13.5 Smad7 trigenic phenotypes fed doxycycline at E7.5. (A, B)** Control and trigenic littermate cranial regions sectioned sagittally and stained with H&E. Note the absent ventral extremity of the lower jaw and lip, hypoplastic tongue, absent primary palate, and absent upper jaw and lip in trigenic mutant (\* in B). However, Meckel's cartilage is still present in the mutant (yellow arrowhead). While the choroid plexus (cp) extending into the trigenic lateral ventricle is present, the choroid plexus differentiating from the roof of the fourth ventricle is absent (arrow in B). **(C-H)** Low power images of serial sagittal sections through control (C, E, G) and trigenic (D, F, H) cardiothoracic regions at the level of the OFT and high power images of the interventricular septum (G, H). While the control has separate ascending aorta and pulmonary trunk vessels (C, E), the trigenic mutant outflow tract has failed to separate and remains as a single outlet (PTA; E) and the single OFT is retroesophageally located in the trigenic embryo (arrow in D). Additionally, the trigenic embryo exhibits accompanying interventricular septal defects (H). **(I-L)** Higher power images of transverse sections reveal that both the trigenic dorsal root ganglia (J) and thymus (L) are histologically normal when compared to control littermates (I, K). Abbreviations: t, tongue; nt, neural tube; PTA, Persistent Truncus Arteriosus; VSD, Ventricular Septum Defect; sep, septum; rv, right ventricle; lv, left ventricle; la, left ventricle; Ao, aortic trunk; dAo, descending aorta; p, pulmonary trunk; drg, dorsal root ganglia; thy, thymus; X, vagal X trunk. Bars in I, J=10µm. [Paige L. Snider and Mica Gosnell contributed to this figure].

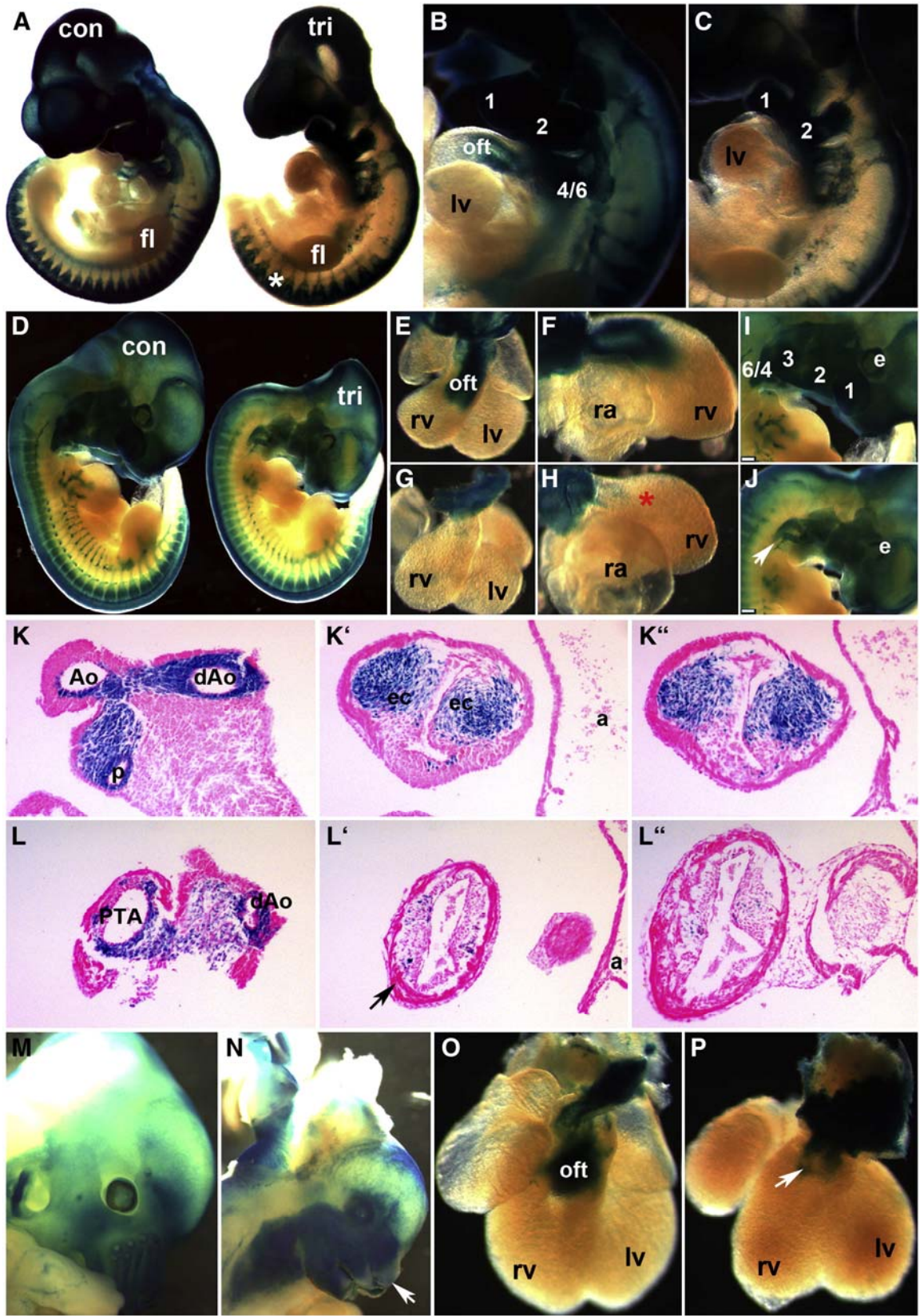


**Figure 9. NCC develop in *Smad7* trigenic mutant embryos fed doxycycline at E7.5.** To lineage map both the trigenic and control NCC populations, *R26<sup>lacZ</sup>* reporter mice were crossed with *Smad7* trigenic to enable us to visualize NCC migration and colonization of the craniofacial and OFT regions. **(A-C)** E10 whole mount lacZ staining of trigenic and control littermates revealed that initial NCC migration was largely unaffected within the trigenic (right embryo in A) cranial, cardiac and trunk regions when compared to control littermates. Robust lacZ expression is evident in trigenic frontonasal prominence, trigeminal nerve ganglia, hypoplastic 1<sup>st</sup>, 2<sup>nd</sup> and 3<sup>rd</sup> arches and within the facial nerve ganglia, and primordium of the 3<sup>rd</sup> pharyngeal arch. Similarly, lacZ-marked NCC are present within the cardiac 4/6<sup>th</sup> arch region and the DRGs (\*) in trigenic mutants. **(D-J)** LacZ stained E11.5 trigenic and control littermate whole embryos (D); isolated control (E, F) and trigenic (G, H) hearts viewed frontally (E, G) and from the right (F, H); and higher power views of control (I) and trigenic (J) craniofacial regions. Note there is a deficiency of NCC-derived Schwann cells within SNS of trigenic forelimb, but trunk NCC migration is unaltered. **(E-H)** Higher power views of isolated hearts clearly show that *Smad7* trigenic NCC reach the pharyngeal arches and aortic sac region, that a few mutant NCC can enter the OFT truncal region but that there are no lacZ stained NCC within the trigenic OFT conal region (\* in H) when compared to controls (E, F). Similarly, although trigenic NCC do colonize the hypoplastic craniofacial regions, there are reduced numbers of lacZ positive cells, particularly evident within the frontal nasal process and 3<sup>rd</sup>, 4<sup>th</sup> and 6<sup>th</sup> pharyngeal arches (arrow in J). **(K, L)** Sections through OFT from distal

to proximal in E11.5 control (K, K', K'') and trigenic embryos (L, L', L''). Histology confirms a lack of trigenic NCC colonizing the OFT, that there are fewer cells within the conal cushions and that the mutant NCC are not found in ectopic locations within the adjacent myocardial cuff (arrow in L') or overlying endothelium. **(M-P)** *LacZ* stained E13.5 control (M, O) and trigenic littermate whole embryos and isolated hearts viewed frontally. Note the absent *lacZ* NCC within the trigenic upper and lower craniofacial regions (arrow in N) and the absence of *lacZ* positive NCC within the trigenic OFT (arrow in P). Abbreviations: fl, forelimb; lv, left ventricle; a, atria; oft, outflow tract; ec, endocardial cushions; rv, right ventricle; ra, right atria; e, eye. Bars in I, J=0.2mm. [Paige L. Snider, Sunyong Tang and Mica Gosnell contributed to this figure].

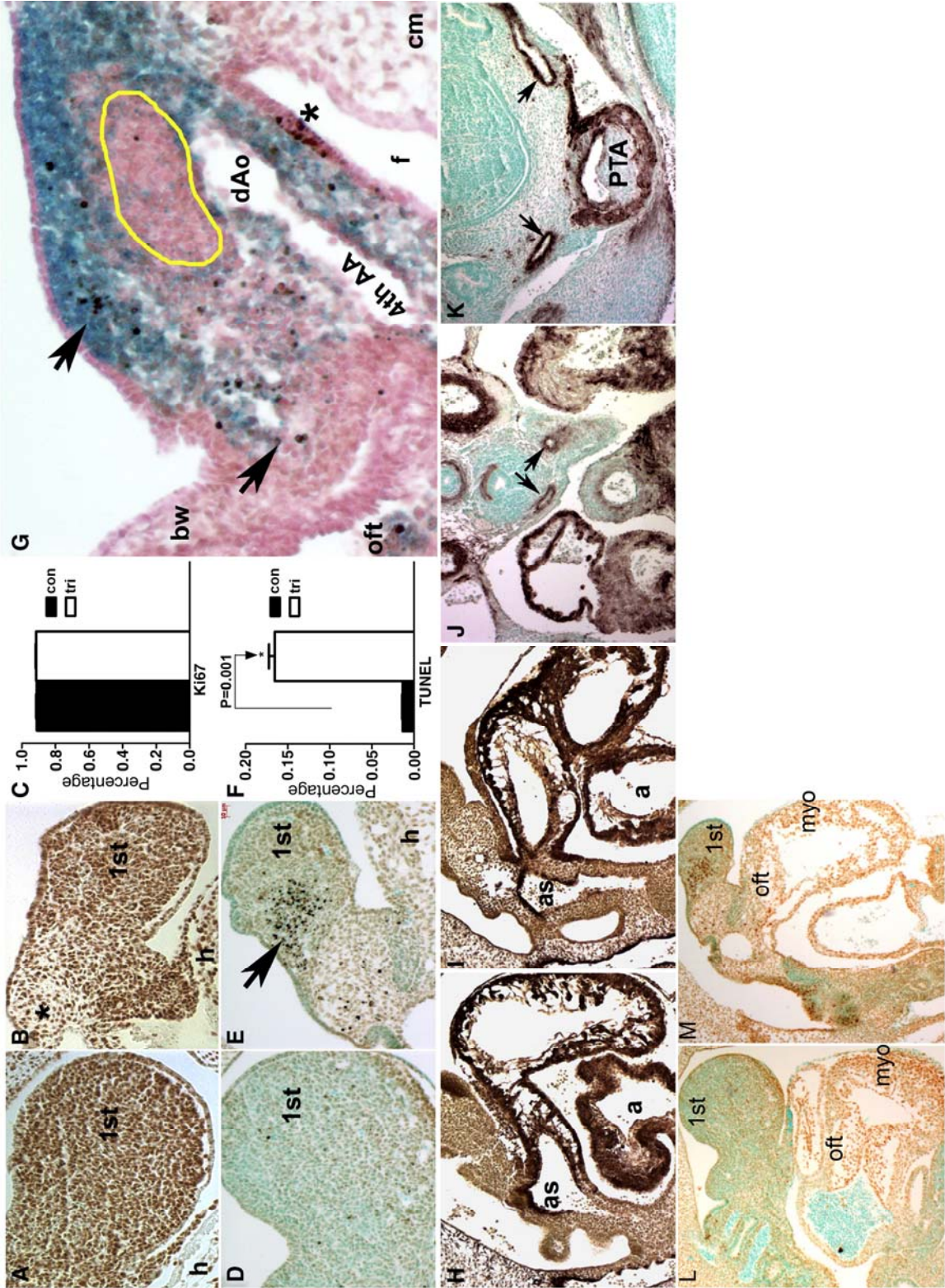


**Figure 10. Elevated cell death of NCC in Smad7 trigenic mutants fed doxycycline at E7.5. (A-C)** Ki67 staining at E10.5 on sagittal sections reveals equivalent levels of cell proliferation (n=4) within the trigenic 1<sup>st</sup> (B) and 2<sup>nd</sup> (not shown) pharyngeal arches when compared to controls (A). **(D-F, L, M)** In contrast, TUNEL staining at E10.5 (n=4) demonstrates a notable increase in cell death in trigenic mutants within the mandibular component of the 1<sup>st</sup> arch (arrow in E) compared to controls (D), but not in the OFT cushions (M) nor in the myocardium (M). **(G)** TUNEL staining (brown) of lacZ-stained E11 R26r trigenic embryo (transverse section of right pharyngeal/OFT region lying on left hand side) demonstrates that apoptotic cells (arrows) are of NCC (blue) origin. Note that trigenic non-NCC derived core arch mesenchyme (indicated by yellow line), cephalic mesenchyme (cm) and body wall (bw) are largely devoid of apoptotic cells. However, as expected the pharyngeal pouch endoderm exhibits robust apoptosis (\*). **(H-K)**  $\alpha$ -SMA staining showed that NCC differentiation into smooth muscle within the E10.5 trigenic (I) aortic sac was comparable to controls (H), that  $\alpha$ -SMA staining (brown) within the trigenic OFT cushions was reduced (\*) and that transient cardiomyocyte expression of  $\alpha$ -SMA was unaffected in both control and trigenic mutant hearts. Similarly, NCC-derived smooth muscle colonization of the control (J) and trigenic (K) 6<sup>th</sup> aortic arch arteries (arrows) was comparable at E13.5. Abbreviations: as, aortic sac; a, atria; h, heart; myo, myocardium; oft, outflow tract; PTA, Persistent Truncus Arteriosus.



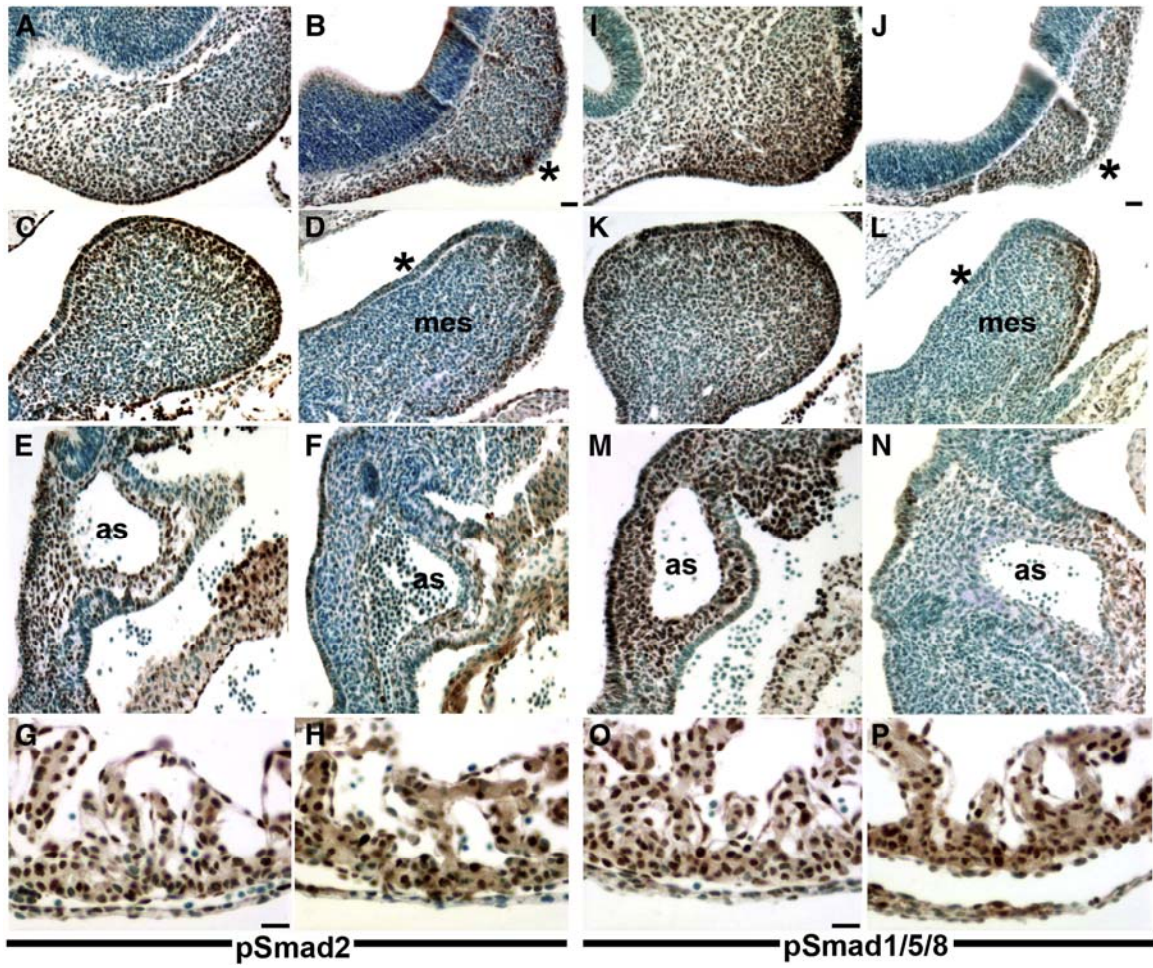


**Figure 11. NCC-restricted Smad7 overexpression results in decreased TGF $\beta$  and BMP signaling. (A-H)** pSmad2 immunohistochemistry on E10.5 sagittal sections demonstrated that TGF $\beta$  signaling is reduced in both craniofacial and cardiovascular tissues colonized by NCC within trigenic (B,D,F) embryos fed doxycycline at E7.5 when compared to control littermates (A,C,E) but that pSmad2 expression is unaffected within control (G) and trigenic (H) ventricles. Note that pSmad2-positive cells (brown staining) are significantly reduced within the trigenic mesenchymal nasal process and the overlying epithelium (\* in B), as well as within the 1<sup>st</sup> pharyngeal arch mesenchyme and overlying epithelium (\* in D). Similarly, there is almost a complete absence of pSmad2-positive NCC around the trigenic aortic sac and within the truncal region of the OFT (F). **(I-P)** pSmad1/5/8 immunohistochemistry on E10.5 sagittal sections similarly demonstrated that Bmp signaling is attenuated in both craniofacial and cardiovascular tissues colonized by NCC within trigenic (J, L, N) embryos fed doxycycline at E7.5, when compared to control littermates (I, K, M) but that pSmad1 expression (brown staining) is unaffected within control (O) and trigenic (P) ventricles to which NCC do not contribute. Sections were counterstained with 0.05% toluidine blue. Abbreviations: mes, mesenchyme of 1<sup>st</sup> arch; as, aortic sac. Bars in B, G, J, O=10 $\mu$ m. [Mica Gosnell contributed to this figure].

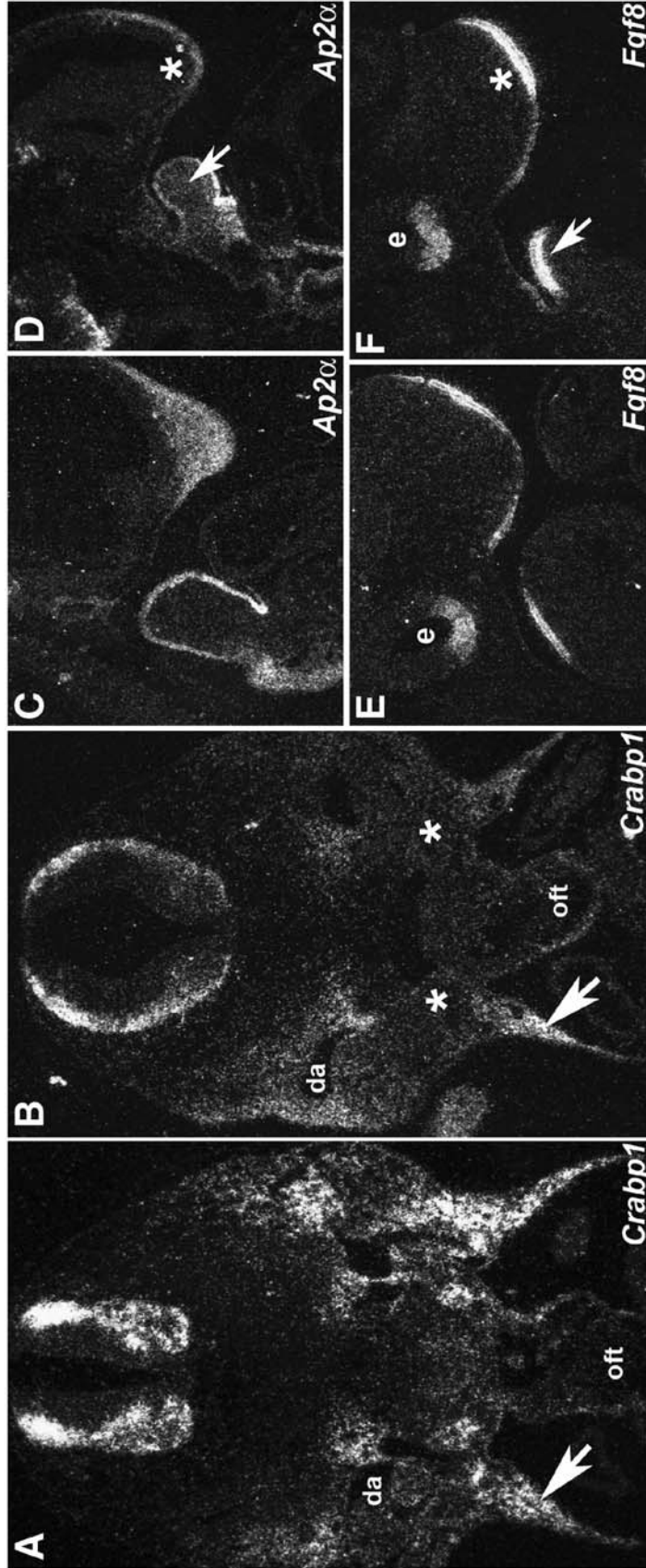


**Figure 12. Molecular marker analysis of E10.5 trigenic mutant phenotype.**

Radioactive *in situ* hybridization detection of *Crabp1* (A, B), *Ap2 $\alpha$*  (C, D) and *Fgf8* (E, F) mRNA in control (A, C, E) and trigenic mutants (B, D, F) fed doxycycline at E7.5. **(A, B)** Transverse sections through the OFT region of trigenic mutants reveal that *Crabp1* expression is reduced within the pharyngeal arch region around the foregut (indicated by \* in B) and along the NCC migration routes around the dorsal aorta, but not within the thoracic body wall (arrows). **(C, D)** Sagittal sections of trigenic mutants indicate that *Ap2 $\alpha$*  expression is reduced in the trigenic nasal process (\* in D) and that *Ap2 $\alpha$*  is ectopically expressed within the mesenchyme of 1<sup>st</sup> arch (arrow) when compared to control littermate (C). **(E, F)** Sagittal sections of trigenic mutants also reveal that *Fgf8* expression is upregulated within the epithelium overlying the nasal process (\* in F) and 1<sup>st</sup> arch mesenchyme (arrow in F) but that trigenic *Fgf8* expression within the neural epithelial layer of the optic cup is comparable with control expression levels. Abbreviations: da, dorsal aorta; oft, outflow tract; e, eye. [Jian Wang contributed to this figure].

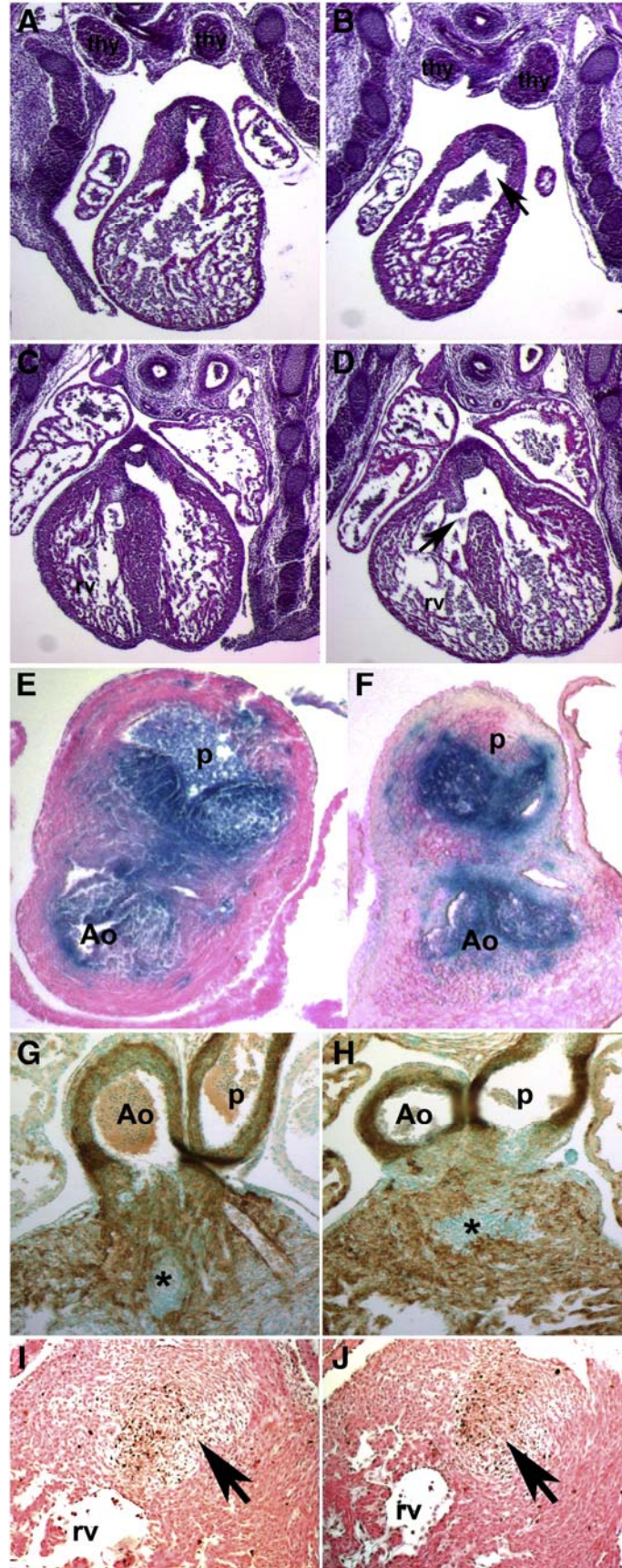


**Figure 13. Analysis of E14.5 Smad7 trigenic heart phenotypes fed doxycycline at E10. (A, B)** Control and trigenic littermate OFT regions sectioned transversely and stained with H&E. Note both the control (A) and trigenic (B) left and right lobes of the thymic rudiment are normally situated and unaffected by myc-Smad7 induction (n=4 trigenic and 5 control fetuses). However, the trigenic OFT truncal endocardial cushions are smaller and the lumen of the outlet of the right ventricle is abnormally dilated (arrow in B). **(C, D)** Additionally, the trigenic embryo exhibits an isolated VSD (arrow in D) but the control heart is separated normally (C). **(E, F)** To lineage map both the trigenic and control post-migratory NCC populations, R26r lacZ reporter mice were crossed with Smad7 trigenic mice. Transverse sections through the E13.5 OFT revealed similar patterns of cardiac NCC (blue) within the aorticopulmonary septum (not shown) and valves in both control (E) and trigenic (F) littermates. Note that trigenic cardiac NCC are still present and that the valves are normal. **(G, H)**  $\alpha$ -SMA staining showed that myocardialization occurs normally in both E13.5 control (G) and trigenic (H) hearts. Note active myocardialization of endocardial cushions at base of the OFTs (indicated by \*). **(I, J)** TUNEL staining (brown) revealed that both the patterns and level of apoptosis (indicated by arrows) are grossly similar in E13.5 control (I) and trigenic (J) OFTs. Abbreviations: thy, thymic lobes; rv, right ventricle. [Paige L. Snider, Sunyong Tang and Mica Gosnell contributed to this figure].

**Chapter III: Regulation of TGF $\beta$  superfamily signaling is critical during sympathetic ganglia and craniofacial neural crest differentiation but is dispensable post-differentiation**

**Abstract**

TGF $\beta$  superfamily signaling plays an essential role in neural crest cell (NCC) development. We are using a doxycycline inducible 3.9 kb *Periostin-Cre* (*Peri-Cre*) driven trigenic system to express Smad7, an inhibitor of TGF $\beta$  superfamily signaling, to study the role of TGF $\beta$  superfamily signaling in post-migratory NCC. Overexpression of Smad7 in post-migratory NCC marked by *Peri-Cre* resulted in hypoplastic 1<sup>st</sup> and 2<sup>nd</sup> pharyngeal arches, loss of frontofacial tissues, blood pooling in the blood vessels, and mid-gestational lethality. Cellular analysis demonstrated that the hypoplastic tissues were due to dramatically increased apoptosis in the 1<sup>st</sup> and 2<sup>nd</sup> pharyngeal arches and frontofacial region. Molecular analysis showed that overexpression of Smad7 suppressed both BMP and TGF $\beta$  signaling, and resulted in increased phospho-p38 levels in frontofacial tissues, which might be the cause of elevated apoptosis observed in these regions. The sympathetic ganglia were also hypoplastic, and they produced significantly less tyrosine hydroxylase, which resulted in the mid-gestational lethality. Overexpression of Smad7 in sympathetic ganglia after they have differentiated, however, did not result in embryonic lethality. Taken together, our data demonstrated that TGF $\beta$  superfamily signaling in the sympathetic ganglia is critical for normal differentiation but dispensable for their survival.

## Introduction

Neural crest cells (NCC) are a transient population of cells formed during early vertebrate embryonic development. After neurulation, NCC undergo epithelial to mesenchymal transformation, delaminate and migrate along defined pathways to contribute to the formation of a variety target tissues and organs [12-13]. NCC are multipotent and are known to be dependent on cues from the extracellular environment, such as sonic hedgehog, WNTs, BMPs and TGF $\beta$ s to differentiate to defined cell types [11].

TGF $\beta$  superfamily consists of more than 30 ligand proteins [1] including TGF $\beta$  isoforms, activins, BMPs and other ligands. Members of this family represent structurally similar, but functionally diverse growth factors which play diverse biological roles during cell proliferation, differentiation, apoptosis and many other tissue remodeling processes, including early embryogenesis and heart morphogenesis. The signaling of TGF $\beta$  superfamily initiates by binding of ligands to the type II receptor, which then recruits type I receptor and activates it [2]. Activated type I receptor then phosphorylates regulatory (R)-Smads (Smad1, 2, 3, 5 or 8), which subsequently form a complex with the co-Smad, Smad4. The complex then translocates into nucleus to regulate gene transcription [66-68]. In contrast to the R-Smads, the inhibitory (I)-Smads (Smad6 and 7) negatively regulate TGF $\beta$  superfamily signaling *in vitro*. While Smad6 negatively regulates BMP signaling [3-4], Smad7 negatively regulates both TGF $\beta$  and BMP signaling [4-8].



Many TGF $\beta$  superfamily signaling components have been manipulated *in vivo* in the developing neural crest. Inactivation of genes encoding TGF $\beta$ 2 and TGF $\beta$ 3 in mice resulted in severe craniofacial malformations, while BMP overexpression or blocking BMP by its inhibitor Noggin in developing chicken affected sympathetic ganglia formation [28-31]. With respect to receptors for TGF $\beta$  family factors, TGF $\beta$  type II receptor (Tgbr2) and TGF $\beta$  type I receptor (Alk5) inactivation in the neural crest caused extensive craniofacial defects, such as cleft palate, and cardiovascular malformations including aortic arch patterning deficiencies, persistent truncus arteriosus, and septal defects [30, 32-36]. Similar defects resulted from neural crest specific deletion of receptors mediating BMP responses [37-39]. In addition, ablation of Smad4 or overexpression of Smad7 in neural crest lineages led to massive cell death and thus malformations in both craniofacial and cardiovascular neural crest derivatives [40-42] as well as reduced size and altered patterning of trigeminal ganglia [41].

However, all of the above investigations were manipulating TGF $\beta$  superfamily signaling in pre-migratory NCC. Almost nothing is known about the role of TGF $\beta$  signaling in post-migratory NCC after they have reached their target tissues and organs. In this research, we crossed *Peri-Cre* transgenic mouse with our doxycycline induced overexpression of Smad7 mouse model [42] to over-express Smad7 in a subpopulation of post-migratory NCC only after they have reached their target tissues and organs.

The results presented here showed that overexpression of Smad7 in early stage post-migratory NCC marked by *Peri-Cre* resulted in hypoplastic 1<sup>st</sup> and 2<sup>nd</sup> pharyngeal arches, loss of frontofacial tissues, blood pooling in the blood vessels, and mid-gestational lethality. The hypoplastic tissues were due to dramatically increased apoptosis in the 1<sup>st</sup> and 2<sup>nd</sup> pharyngeal arches and frontofacial region. Molecular analysis showed that overexpression of Smad7 suppressed both BMP and TGF $\beta$  signaling, and resulted in increased phospho-p38 levels in frontofacial tissues. The sympathetic ganglia were also hypoplastic, and they produced significantly less tyrosine hydroxylase, which resulted in the mid-gestational lethality. Overexpression of Smad7 in later stage sympathetic ganglia after they have undergone differentiation, however, did not result in embryonic lethality and diminished tyrosine hydroxylase, demonstrating that TGF $\beta$  superfamily signaling in the sympathetic ganglia is critical for their differentiation but dispensable for their survival and homeostasis.

## Materials & Methods

### Genotyping by PCR:

Forward primer was designed within the *myc* tag sequence as followed: 5'-ATCCACGCTGTTTTGACCTC-3'; reverse primer was designed locating downstream of *Smad7* start codon ATG, as followed: 5'-GAGCGCAGATCGTTTGGT-3'. This primer pair is used for genotyping *tetOn-Smad7* transgenic mice by PCR using mouse genomic DNA from tail with previously established protocols [76].

### Mice maintenance:

Rosa26R (R26r) Cre-reporter mice were purchased from the Jackson Labs (for detailed PCR-genotyping, see <http://www.jax.org>); the animals were maintained on a light-dark cycle with light from 06:00 to 18:00 hours. Embryonic age was determined by the vaginal plug, the noon of the day plug observed defined as E0.5. All mice were maintained on mixed genetic backgrounds. All studies were carried out at the Animal Care Facility of the Indiana University in accordance with national and institutional guidelines.

### X-Gal Staining:

Whole embryos were stained for  $\beta$ -galactosidase activity based on established protocols. Briefly, embryos were fixed for 1 to 2 hours at room temperature in 4% paraformaldehyde. Fixed embryos were washed in PBS twice then incubated in  $\beta$ -galactosidase buffer (0.058 M  $\text{Na}_2\text{HPO}_4$ , 0.042 M  $\text{NaH}_2\text{PO}_4$ , 0.001 M  $\text{MgCl}_2$ ,

0.01% NP40) overnight. Next day, buffer was removed and substrate (0.1% X-gal, 0.005 M  $K_3Fe_4(CN)_6$ , 0.005 M  $K_4Fe_3(CN)_6$ , 0.001 M EGTA) added to cover the embryos. The embryos were wrapped in aluminum foil and left in the dark at 37°C overnight. They are rinsed twice in PBS and post-fixed in 4% paraformaldehyde. The embryos were dehydrated through alcohol and embedded in paraffin. Sections were cut at 10  $\mu$ m thickness and counterstained with Eosin.

#### **Apoptosis assay:**

Apoptotic cells were detected in paraffin-embedded tissue sections using TdT-FragEL™ DNA Fragmentation Detection Kit (Calbiochem). Assays were performed on 10  $\mu$ m paraffin sections. The total cells and positively stained cells were counted manually in defined areas of tissues under 40X magnification. Statistical analysis of cell counts in serial sections and comparison of trigenic specimens to controls was performed using one-tailed t-test.

#### **Western blot analyses:**

Tissues from embryos were homogenized in lysing buffer (0.02M Tris, 0.01M EDTA, 0.1M NaCl, 1% SDS) and analyzed using western blotting. Proteins were blotted onto PVDF membrane; Myc (Santa Cruz Biotech, A-14), Smad1 (Santa Cruz Biotech, sc-81378), phospho-Smad1/5/8 (cell signaling, 9511), Smad2/3 (Santa Cruz Biotech, sc-8332), phospho-Smad2 (cell signaling, 3101), phospho-p38 (cell signaling, 9211), p38 (cell signaling, 9212), phospho-Akt (cell signaling,

9271), Akt (cell signaling, 9272), tyrosine hydroxylase (Millipore, ab152), tubulin (Sigma, T-5168) antibodies were used.

### **Immunohistochemistry Analysis:**

Immunohistochemistry was carried out using ABC kit (Vectorstain) with DAB and hydrogen peroxide as chromogens as previously described [78]. The dilution of primary antibody was 1:5000 for  $\alpha$ -smooth muscle actin ( $\alpha$ SMA; Sigma), 1:750 for phospho-Smad1/5/8 (cell signaling, 9511), 1:1500 for phospho-Smad2 (cell signaling, 3101), 1:5000 for neuron specific beta III tubulin (NS $\beta$ T; Abcam, ab18207), 1:10000 for tyrosine hydroxylase (Millipore, ab152).

### **Implantation of isoproterenol osmotic minipump:**

Pregnant females (at various stages of gestation) were anesthetized in a chamber with isoflurane (2%)-oxygen (98%) mixture. Once anesthesia was achieved, the incision site was shaved with a 40-tooth blade, and loose hair blown off with compressed air or removed with tape, and cleaned twice with warm Betadine. A sterile osmotic minipump (Alzet Osmotic Pump model #2001 3cm x 0.7cm, flow rate of 1 $\mu$ l/hr) filled with 0.014g/ml isoproterenol (dissolved in saline) was then implanted through a small longitudinal incision (1/2") between the scapulae. The mini osmotic pumps deliver drug subcutaneously from the pump; no catheters are involved. The wound was sutured closed and the mice housed 1 per cage to prevent fighting and wound reopening. The procedure, from anesthesia to final closure, takes about 5 minutes. Mice are kept in surgery

room until recovered (typically only 15-30 minutes), and then transferred to main mouse room prior to harvesting 1 week later. Animals were checked for redness, swelling and/or infection two days following implantation, and animals with signs of infection would be euthanized. Only one surgical procedure was performed per animal and the pregnant dams harvested at E14 and E18 stages of gestation, and the resultant embryos/fetuses hearts analyzed.

## Results

### Generation of *Peri-Cre/R26<sup>rtTA-EGFP</sup>/tetO-Smad7* trigenic mice and examination of the kinetics of Smad7 induction *in vivo*

In order to study the role of TGF $\beta$  family signaling in post-migratory NCC after they have reached their target tissues and organs, we used *Peri-Cre* transgenic mice, which has been shown to only mark a subpopulation of NCC undergoing differentiation ([122] and Conway lab unpublished data), to drive *myc-Smad7* expression. To visualize Cre activity in *Peri-Cre* marked post-migratory NCC, *Peri-Cre* mice were crossed to a Cre recombination reporter line, *R26r* [85]. Because the recombination mediated by Cre recombinase at R26R locus is irreversible, embryos carrying *Peri-Cre; R26r* express *lacZ* in all cells that express active Cre recombinase and their daughter cells. *Peri-Cre; R26r* E11.5 embryos were whole mount stained with *lacZ* substrate for analysis. Whole mount staining showed robust *lacZ* expression in the frontonasal prominence, especially in the upper (maxillary) and lower jaw (mandible) (Fig. 14A, B), and in the peripheral nervous system, including the dorsal root ganglia (Fig. 14C). Sections through the cardiac OFT region showed robust *lacZ* expression in the endocardial cushions in the oft (Fig. 14D). *LacZ* also stained the dorsal root ganglia (drg) and sympathetic ganglia (sg) adjacent to the aorta (Fig. 14E, F), the derivatives from NCC.

We crossed three individual transgenic mice, *Peri-Cre* (Conway lab), *R26<sup>rtTA-EGFP</sup>* (Jax lab) and *tetO-Smad7* mice [42] to generate *Peri-Cre/R26<sup>rtTA-EGFP</sup>/tetO-*

*Smad7* trigenic mice (Fig. 15A). Male trigenic offspring were then crossed to homozygous female *R26<sup>rtTA-EGFP</sup>* mice and the resultant embryos were used for further investigation. As we reported in our *Wnt1-Cre/R26<sup>rtTA-EGFP</sup>/tetO-Smad7* trigenic study [42], the location and cell types that mycSmad7 will be induced is determined by *Peri-Cre* lineages; and the time of mycSmad7 induction is determined by when we apply doxycycline to the trigenic system. For simplicity, the embryos containing all three transgenes are referred to as trigenic embryos, and all other littermates are referred to as control embryos. As expected, when pregnant females were fed with normal chow, normal litter sizes (n=8 embryos/litter from 4 litters) and trigenic offspring were recovered at expected Mendelian ratios when harvested at E13.5 (25.8%). Additionally, western analysis detected no myc-Smad7 protein expression in normal fed trigenic embryos (Fig. 15B). Without doxycycline feeding, these embryos develop normally, and they reach adulthood and can breed.

When the food for pregnant females was switched from regular chow to doxycycline-containing food at E9.5 (prior to first appearance of *Peri-Cre*, unpublished data), the induction of myc-Smad7 protein was first detected after 5 hours and myc-Smad7 induction reached its maximum level after 24 hours in trigenic embryos, and myc-Smad7 protein induction was observed only in trigenic embryos (Fig. 15B). This rapid induction is consistent with other studies that have shown rtTA-driven transgene expression is detectable 6 hours after onset of doxycycline treatment [83, 123].



Combined, these data demonstrate that transgenic myc-Smad7 expression is tightly controlled in *Peri-Cre/R26<sup>rtTA-EGFP</sup>/tetO-Smad7* trigenic system, and that myc-Smad7 expression is induced rapidly in trigenic embryos by application of doxycycline to the system.

### **Overexpression of Smad7 in the post-migratory neural crest cells impaired normal facial and pharyngeal arch development, and resulted in mid-gestational lethality**

After confirm the inducibility of Smad7 in the *Peri-Cre/R26<sup>rtTA-EGFP</sup>/tetO-Smad7* trigenic system, we used this system to examine the roles of regulated TGF $\beta$  superfamily signaling in post-migratory neural crest cell development. Specifically, we bred *Peri-Cre/TetO-Smad7/ROSA26R<sup>rtTA-EGFP</sup>* male trigenic mice with female homozygous *ROSA26R<sup>rtTA-EGFP</sup>* mice to generate trigenic and control embryos. *Peri-Cre* activity can be detected as early as E9.5, so we switched the pregnant mice from the regular food to doxycycline containing food at E9.5; then we harvested embryos after 6, 24, 48, 60 hours (corresponding to E9.5, E10.5, E11.5 and E12.5, respectively). At E9.5 (5 hours), the trigenic embryos (Fig. 16B, n=4) displayed no morphological differences to the controls (Fig. 16A). At E10.5 (24 hours), trigenic embryos showed hypoplastic 1<sup>st</sup> and 2<sup>nd</sup> pharyngeal arches (arrows in Fig. 16D, n=11) and smaller upper jaws (arrows in Fig. 16F, n=20), and a ventral view of those embryos demonstrated smaller maxillary component of first pharyngeal arch and un-fused mandibular component of the first pharyngeal arch (arrow in Fig. 16H) compared to littermate control embryos (Fig.

16G). At E11.5, the trigenic embryos had severe blood pooling throughout the body, and were missing face and jaw structures (arrow in Fig. 16J, n=22). At E12.5, in addition to missing face and jaw and blood pooling, there was lack of blood in the yolk sac blood vessels in trigenic embryos (arrow in Fig. 16N, n=13), suggesting a dysfunctional circulation system in the trigenic embryos. No trigenic embryos could survive beyond E12.5. Thus, overexpression of Smad7 in the post-migratory neural crest cells results in abnormal facial and pharyngeal arch development, and mid-gestational lethality.

#### **Overexpression of Smad7 in post-migratory neural crest cells affected sympathetic ganglia but not dorsal root ganglia and cardiac development**

After migrating out of the neural tube, NCC reach the dorsal aorta by E9.5, and those cells begin to aggregate in the adjacent area around the dorsal aorta and differentiate and form compact sympathetic ganglia (sg) by E10.5 (Fig. 17A, C). In trigenic embryos, the sympathetic ganglia were still formed but in diminished size (Fig. 17B, D), indicating overexpression of Smad7 in post-migratory NCC affected the normal development of these sympathetic ganglia. Located next to the neural tube, dorsal root ganglia (drg) are also differentiated from post-migratory NCC. Consistent with previous reports [21, 39, 42], the size and shape of DRG in trigenic embryos (Fig. 5B) were comparable to those in the control embryos (Fig. 17A). The sympathetic ganglia adjacent to the dorsal aorta are responsible for the production of epinephrine and norepinephrine at this embryonic stage, while dorsal root ganglia are the sensory division of the

peripheral nervous system, the above data suggest that overexpression of Smad7 in post-migratory NCC affects the noradrenergic sympathetic ganglia, not sensory ganglia at this stage.

NCC migrate to the cardiac OFT region and differentiate into specific cell types to separate the single OFT into ascending aorta and pulmonary artery. To further examine the effects of overexpression of Smad7 in those post-migratory NCC in the OFT, control and trigenic embryos (Fig. 17E, F) were transversely sectioned and H&E stained. At E10.5, the endocardial cushions were formed normally in the trigenic embryos (Fig. 17F) when compared to control littermates (Fig. 17E), indicating that OFT endocardial cushions are not affected by overexpression of Smad7 in post-migratory NCC at this stage.

### **Increased cell death caused hypoplastic pharyngeal arches and frontofacial tissue phenotypes**

Given the observed facial and pharyngeal arch hypoplasia, TUNEL assays were used to examine apoptosis within control (Fig. 18A, C) and trigenic (Fig. 18B, D) embryos. Significantly elevated levels of apoptotic positive cells (brown) were present within the first and second pharyngeal arches in the trigenic embryo (Fig. 18B, D). When TUNEL positive cells were tallied as a percentage of total cells to calculate a cell death index, there was a significant increase in cell death in trigenic embryos (4.1% in controls versus 31.6% in trigenics,  $P < 0.001$ , Fig. 18E). Since the upper and lower jaws are derived from first pharyngeal arches, the

TUNEL data demonstrated that the observed hypoplastic facial and pharyngeal arches in trigenic embryos resulted from elevated apoptosis. However, there was only a few apoptotic cells presence in the OFT cushions in both control (Fig. 18F, H) and trigenic embryos (Fig. 18G, I) and there was no statistical difference in terms of TUNEL staining between control and trigenic embryos (Fig. 18J). This data explained why we did not see abnormal OFT cushions in the trigenic embryos.

### **Increased phospho-p38 in pharyngeal arches and frontofacial tissues**

Given the observed difference in apoptosis between pharyngeal arches and frontofacial tissues and hearts, E10.5 hearts and frontofacial tissues (including upper and lower jaws, 1<sup>st</sup> and 2nd pharyngeal arches) were microdissected. Tissues from 3 embryos were pooled to gain enough protein for western blotting analysis. Note that myc-Smad7 is only expressed within pooled (n=3) trigenic E10.5 hearts and frontofacial tissues, not in pooled control (n=3) samples (Fig. 19A). In the heart samples, myc-Smad7 suppressed pSmad1/5/8 by ~70%, pSmad2 by ~60% (Fig. 19A, B) when normalized to their respective total proteins compared to their controls. In the frontofacial sample, myc-Smad7 suppressed pSmad1/5/8 by ~90%, pSmad2 by ~87% (Fig. 19A, B). These data showed that overexpression of mycSmad7 suppressed both BMP and TGF $\beta$  signaling in both heart and frontofacial tissues.

Although Smad7 was originally identified as an inhibitory Smad of TGF $\beta$ , there are several reports suggesting that inhibitory Smads may have other cellular functions. In one report, overexpression of Smad7 by adenoviral infection induced DNA fragmentation and significant increases in cell death in rat mesangial cells [124]. In another report, Smad7 has been shown to be involved in TGF $\beta$ -induced apoptosis of prostate cancer cells by activating p38 [125]. To address these reports and further probe the mechanism underlying our observed defects, we measured p38 levels in samples from both heart and frontofacial regions. Indeed, the phospho-p38 levels were increased ~ 5.6 fold in frontofacial tissues, while its levels were unchanged in the heart (Fig. 19A, B). It has also been shown that Smad7 overexpression might antagonize pro-survival signals, such as Akt. However, our western blotting data revealed phospho-Akt levels were down in both the heart (11%) and frontofacial tissues (10%). Taken together, these data demonstrate that increased phospho-p38 may be primarily responsible for the increased apoptosis observed in Smad7 overexpressing post-migratory neural crest observed in frontofacial regions of trigenic embryos.

### **Trigenic heart and blood vessels were unaffected**

Since we observed blood pooling in E11.5 trigenic embryos, which could indicate a malfunctional circulatory system, we hypothesized that the heart might be primarily affected. We examined myocardial development in both control and trigenic embryos using  $\alpha$ -smooth muscle actin ( $\alpha$ SMA) immunohistochemistry assay since  $\alpha$ SMA stains both smooth muscle cells and the cardiomyocytes in

embryonic stages. The  $\alpha$ SMA staining revealed that the myocardium of the trigenic embryos was unaffected (Fig. 20B) when compared to control littermates (Fig. 20A). The other major component of circulation system is the blood vessels. NCC contribute to the supportive smooth muscle layer surrounding peripheral vasculature of the great vessels that exit the heart [126-128]. However,  $\alpha$ SMA immunohistochemistry on cross section of E11.5 blood pooling trigenic embryos displayed no evidence of leaky hemorrhagic blood vessels in either pharyngeal arch arteries (not shown) or dorsal aorta (Fig. 20D, F). The  $\alpha$ SMA immunohistochemistry staining detected no differences between control (Fig. 20C, E) and trigenic embryos (Fig. 20D, F) before the onset of lethality and embryonic necrosis. Therefore, our data demonstrated that the circulation problem in trigenic embryos was not caused by either abnormal formation of myocardium or blood vessels.

**Dramatically decreased Tyrosine Hydroxylase (TH) was the underlying cause of trigenic mid-gestational lethality**

Although the observed blood pooling could indicate a potential circulation problem in the trigenic embryos, our analysis demonstrated that the OFT cushions, myocardium and blood vessels were normal in trigenic embryos (Fig. 17F, Fig. 20B, and Fig. 20D, F). This discrepancy prompted us to examine other aspects of the circulation system and cardiac function. Since neural crest cells initiate adrenergic differentiation in the vicinity of dorsal aorta to form the primary sympathetic strands and *Peri-Cre* is known to drive gene expression in the

peripheral nervous system [122], we performed Neuron Specific  $\beta$  III Tubulin (NS $\beta$ T) immunohistochemistry, which labels all neurons in central nervous system and peripheral nervous system, on cross sectioned control and trigenic embryos at E10.5. NS $\beta$ T staining revealed that the sympathetic ganglia were much smaller in trigenics (Fig. 21B, D) than in the controls (Fig. 21A, C) but were present. Sympathetic ganglia in embryos are responsible for synthesis and transport of neurotransmitters, such as epinephrine and norepinephrine. Tyrosine hydroxylase, the rate-limiting enzyme in catecholamine synthesis, is a marker when NCC take the catecholaminergic phenotype [28], so we examined its expression. TH immunostaining showed significantly reduced TH expression within the trigenic sympathetic ganglia (Fig. 21F, H). This data suggested that there might be less epinephrine and norepinephrine in the circulating blood in trigenic embryos, which in turn decreased the heart beat and eventually results in *in utero* cardiac failure and hemodynamic overload. This would then result in the observed blood pooling in blood vessels (Fig. 16J). To test this hypothesis, we used isoproterenol, an epinephrine homolog, to artificially increase the catecholamine levels in trigenic embryos. An isoproterenol mini-osmotic pump was implanted into the pregnant females at E8.5 when they were on regular chow. The pregnant females were then switched to doxycycline food at E9.5, and the embryos were then harvested at E14.5. The embryos still demonstrated hypoplastic facial and other abnormalities (Fig. 22B), but significantly, they were still alive. Thus, these data was consistent with our hypothesis that dramatically decreased TH expression and reduced circulatory norepinephrine levels in

trigenics was the underlying cause of the observed mid-gestational lethality, as isoproterenol could fully rescue the non-viable embryos until birth (Fig. 22B, n=2).

### **Overexpression of Smad7 in post-differentiated sympathetic ganglia did not result in mid-gestational lethality**

NCC reach the dorsal aorta by E9.5, and differentiate and form compact sympathetic ganglia (sg) by E10.5 (Fig. 17A, C). To bypass the early lethality observed in trigenic embryos and take advantage of our inducible system, we induced mycSmad7 expression starting from E12.5. We crossed *Peri-Cre/TetO-Smad7/ROSA26R<sup>rtTA-EGFP</sup>* male trigenic mice with female homozygous *ROSA26R<sup>rtTA-EGFP</sup>* mice and fed the pregnant females doxycycline containing food at E12.5, and then harvested embryos at E14.5. Significantly, all trigenic embryos (Fig. 23B, n=8) harvested were alive and grossly normal when compared to littermate controls (Fig. 23A). TH immunohistochemistry assays on crossed sectioned embryos revealed normal and abundant TH staining within sympathetic ganglia adjacent to the dorsal aorta in both control (Fig. 23C, E) and trigenic embryos (Fig. 23D, F). The size and shape of the sympathetic ganglia also appeared normal in trigenic embryos (Fig. 23D, F). Western blotting showed that overexpression of mycSmad7 still suppressed both BMP and TGF $\beta$  signaling, demonstrated by decreased pSmad1/5/8 and pSmad2 levels, respectively (Fig. 23G), but the TH expression levels in trigenic embryos are comparable to those in control embryos (Fig. 23G). These data demonstrated



that TGF $\beta$  superfamily signaling in the sympathetic ganglia is critical for their normal differentiation but dispensable for their survival.

## Discussion

This project used the *Peri-Cre* line in our trigenic system to drive *Smad7* overexpression. It was a similar yet different system from our previous *Wnt1-Cre/R26<sup>rtTA-EGFP</sup>/tetO-Smad7* analysis [42]. Principally, as *Wnt1-Cre* is known to be expressed prior to NCC emigration out of neural tube, it not only marks significantly more NCC subpopulations, it is also expressed in undifferentiated NCC lineages [14, 20]. However, *Peri-Cre* marks specifically the peripheral nervous system and the endocardial cushions within the OFT, only a subpopulation of post-migratory NCC when they are undergoing the critical steps of differentiation and cell fate specialization (Conway lab). Thus, via use of overexpression of *Smad7* in *Wnt1-Cre* trigenic system, we were able to investigate the role and effects upon TGF $\beta$  superfamily signaling role in pre-migratory NCC. Overexpression of *Smad7* in *Peri-Cre* trigenic system, we were able to investigate the effects of TGF $\beta$  superfamily signaling suppression in only a subpopulation of post-migratory NCC.

Similar to the *Wnt1-Cre* trigenic system, the data from *Peri-Cre* trigenic system demonstrated that forced expression of *Smad7* within a subpopulation of post-migratory NCC was detrimental to development of NCC and their derivatives, resulted in hypoplastic frontofacial tissues, and reduced 1<sup>st</sup> and 2<sup>nd</sup> pharyngeal arches. Moreover, we showed that levels of both TGF $\beta$  and BMP phosphorylated R-Smads were reduced in the NCC lineages expressing myc-*Smad7*, providing additional confirmatory evidence that TGF $\beta$  superfamily signaling is impaired *in*

*vivo* by myc-Smad7 induction in NCC. In addition, we demonstrated that the hypoplastic or missing tissues observed in *Peri-Cre* trigenic mouse model were caused by elevated apoptosis in Smad7 overexpressing cells and their neighboring cells, indicating Smad7 mediated TGF $\beta$  superfamily signaling or Smad7 itself or both were probably important for NCC differentiation, specialized cell maintenance and survival.

Since *Wnt1-Cre* is thought to label all NCC lineages but *Peri-Cre* only marks a subpopulation of post-migratory NCC, we expected overexpression of Smad7 in *Wnt1-Cre* lineages would have resulted in more severe phenotypes than that in *Peri-Cre* lineages. However, we observed the opposite: there was embryonic lethality at E12.5 in *Peri-Cre/R26<sup>rtTA-EGFP</sup>/tetO-Smad7* trigenic mouse model, much earlier than the observed lethality at birth in our *Wnt1-Cre/R26<sup>rtTA-EGFP</sup>/tetO-Smad7* trigenic mouse [42]. One probable explanation is the difference between *Wnt1-Cre* and *Peri-Cre* expression patterns. *Peri-Cre* is robustly expressed in all sympathetic ganglia along all axial levels (unpublished data, Conway lab), so that Smad7 overexpression in *Peri-Cre* lineages likely affects all sympathetic ganglia differentiation, thus resulting in less epinephrine and norepinephrine in the circulating blood in trigenic embryos, which in turn decreased the heart beat and eventually results in *in utero* cardiac failure and mid-gestational lethality. However, *Wnt1-Cre* seems to not mark all the sympathetic ganglia along all axial levels. *Wnt1-Cre* lineage tracing experiments by crossing with *Rosa26* reporter [85] mice show *Wnt-Cre* mediated *lacZ* gene

expression starts in the rostral hindbrain around the four somite (E8.0) stage and extends anterior to the midbrain, forebrain, and posterior to the caudal hindbrain, cardiac and trunk levels by eight somite (E8.5) stage [39]. However, once NCC have formed, they migrate out of the neural tube at all axis levels simultaneously. So it could be that some more posterior NCC could have already migrated out of the neural tube prior to *Wnt1-Cre* expression at those axial levels. Those posterior migrated NCC may be differentiated normally into sympathetic ganglia, which then produce enough epinephrine and norepinephrine for the trigenic survival. Indeed, in support of this hypothesis, when diphtheria toxin A fragment (DTA), a fatal toxin that kills cells autonomously, was expressed in *Wnt1-Cre* lineages, *Wnt1-Cre;DTA* embryos survive to birth and developed normal adrenal glands even though the medullar portion of the adrenal gland is derived from NCC (unpublished data, Conway lab). Another possible explanation could be from the different developmental stages that the Cre mouse lines express. *Wnt1-Cre* expresses before NCC migrate out the neural tube, and *Peri-Cre* expresses in post-migratory NCC when they are undergoing differentiation. So it could be that TGF $\beta$  superfamily signaling or Smad7 itself or both play a more important role in NCC differentiation stage than they do in the stages before NCC migration. The third explanation could be as simple as these two Cre mouse lines drive gene expression in some common but not completely overlapping cell populations, thus we observed different results in those two trigenic Smad7 overexpression mouse models.

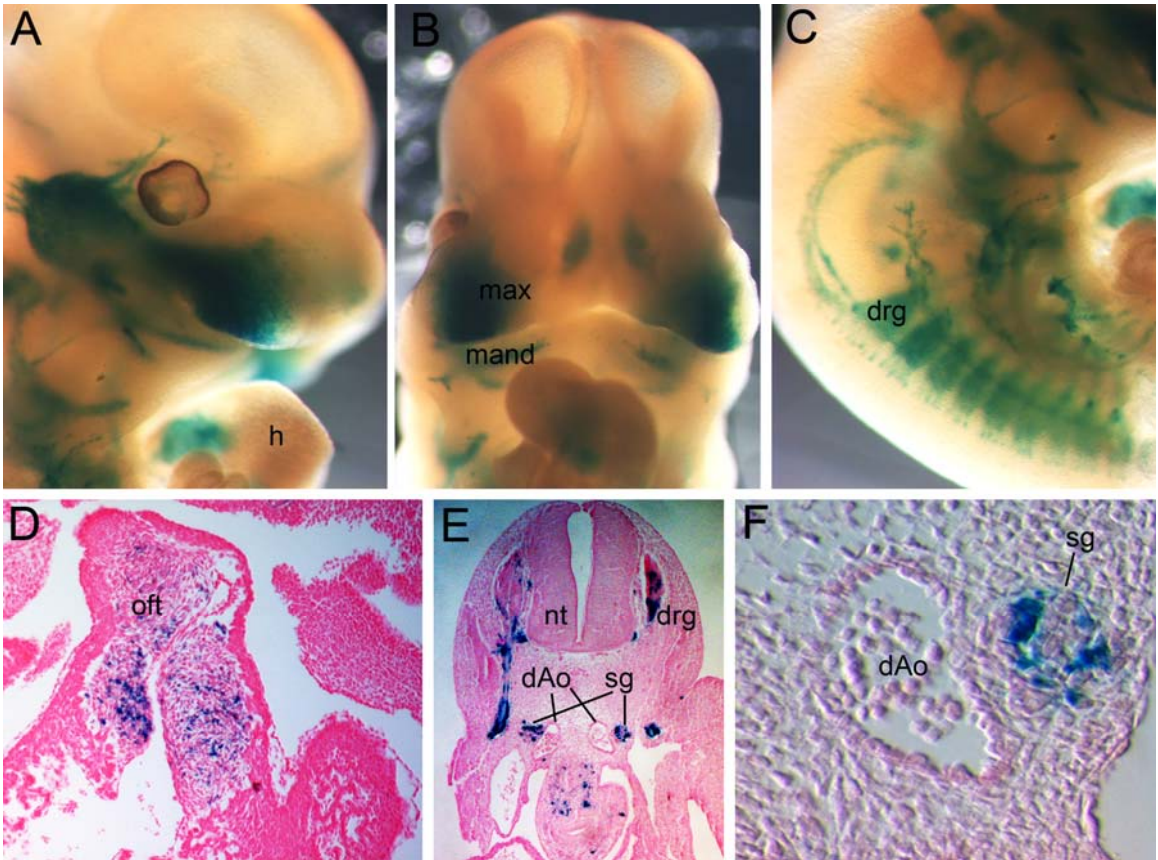


**Figure 14. *Peri-Cre* early lineage mapping.** To lineage map *Peri-Cre* populations, *Peri-Cre* transgenic mice were crossed with *R26r lacZ* reporter mice, *Peri-Cre; R26r/+* E11.5 embryos were then whole mount stained with lacZ substrate. **(A-C)** Whole mount lacZ staining showed robust lacZ expression in frontonasal prominence, especially in the upper (maxillary) and lower jaw (mandible) (A, B), and peripheral nervous system (C). **(D)** Sections through the cardiac (oft) region showed robust lacZ expression in the endocardial cushions in the oft. **(E)** LacZ stained the dorsal root ganglia (drg) and sympathetic ganglia (sg) adjacent to the aorta. **(F)** Higher magnification showing lacZ positive cells in the sympathetic ganglia (sg) adjacent to the aorta. Abbreviations: dAo, dorsal aorta; drg, dorsal root ganglia; h, heart; mand, mandible; max, maxillary; nt, neural tube; oft, outflow tract; sg, sympathetical ganglia.

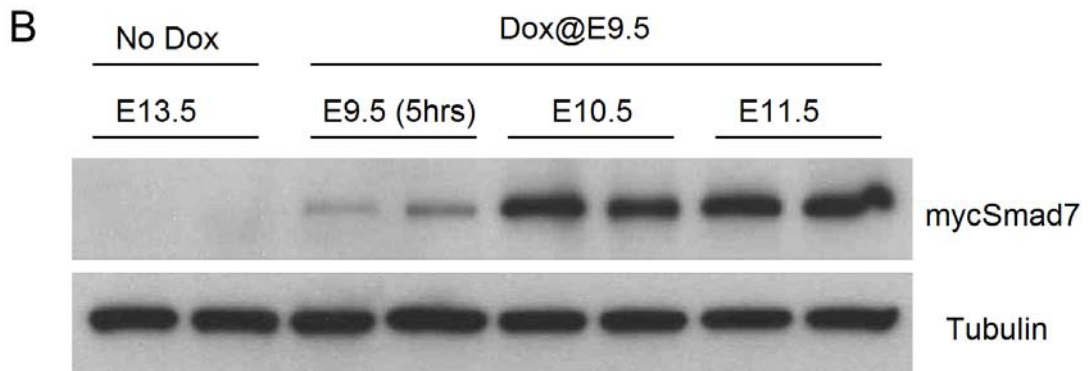
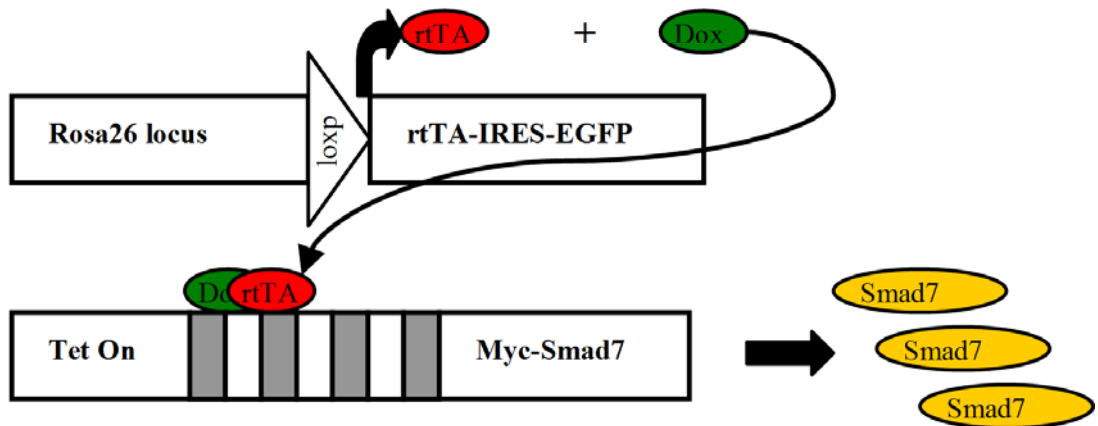
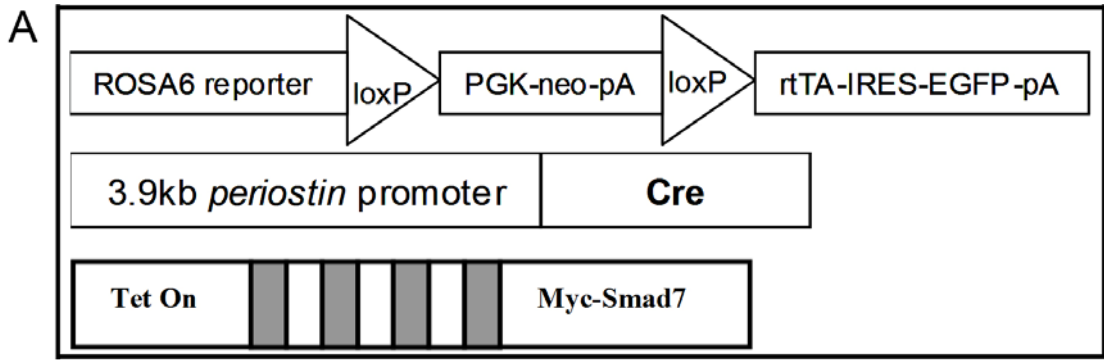


**Figure 15. Smad7 induction kinetics in doxycycline inducible *Peri-Cre/R26<sup>rtTA-EGFP</sup>/tetO-Smad7* trigenic mouse system. (A)** Schematic illustrating operation of the trigenic system. The *R26<sup>rtTA-EGFP</sup>* knockin mice will only express the rtTA from the *Rosa26* locus upon Cre-mediated recombination [74]. *Peri-Cre* transgenic mice have been shown to label peripheral nervous system [122]. In the *tetO-Smad7* transgenic mice, myc-Smad7 full length cDNA is under the control of heptamerized tetOn promoter, but Smad7 is not expressed until both the transactivator (rtTA) and inducer (doxycycline) are present within the same cell. Although all three transgenes are individually silent within the compound trigenic mice, myc-tagged Smad7 can be specifically induced within Cre-positive lineages upon doxycycline feeding. Thus, the spatiotemporal timing of myc-tagged Smad7 expression is determined by the timing of doxycycline addition and positionally by the expression of Cre recombinase. **(B)** Western blotting showed no myc-Smad7 expression in E13.5 embryos fed with normal chow. However, when the pregnant mothers were fed doxycycline (Dox) containing food at E9.5 myc-Smad7 could be detected after 5 hours, indicating quick induction of this system. Myc-Smad induction reached maximum levels after 24 hours as indicated by comparable myc-Smad7 levels in E10.5 and E11.5 embryos.



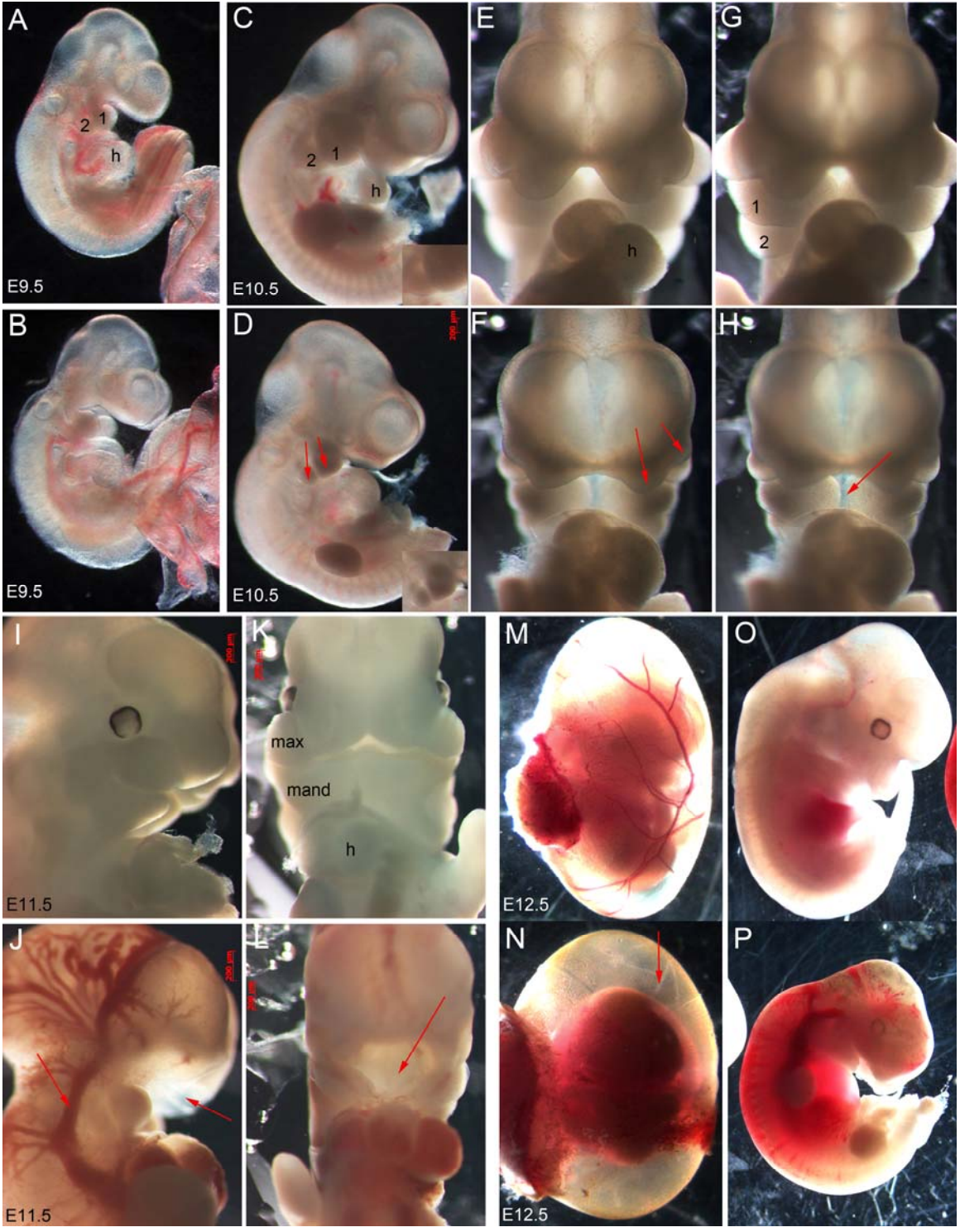


**Figure 16. Overexpression of Smad7 in the post-migratory neural crest cells impaired normal facial and pharyngeal arch development, and resulted in mid-gestational lethality.** All embryos were fed Dox food at E9.5 **(A, B)** Trigenic embryos (B) were grossly normal compared to littermate control embryos (A) after being fed with Dox for 5 hours. **(C-H)** E10.5 control (C, E, G) and trigenic (D, F, H) whole embryos. Trigenic embryos were largely comparable to the control embryos at this stage except for hypoplastic 1<sup>st</sup> and 2<sup>nd</sup> pharyngeal arches (PA) (insert in D), and less outgrowth of the frontofacial process (arrows in F). Besides, the mandibular component of the 1<sup>st</sup> PA was starting to fuse in the control littermates (G), while that fusion did not occur in the trigenic embryos (arrow in H). **(I-L)** E11.5 control (I, K) and trigenic (J, L) whole embryos. Trigenic embryos showed blood pooling in the blood vessels (arrow in J) and the heart and missing frontofacial tissues (arrow in L). Ventral view showed missing maxillary and mandible in the trigenic embryos (L). **(M-P)** E11.5 control (M, O) and trigenic (N, P) whole embryos. There was lack of blood in the yolk sac blood vessels in the trigenic embryos (arrow in N); trigenic embryos die by E12.5 (P). Abbreviations: 1, first pharyngeal arch; 2, second pharyngeal arch; h, heart; mand, mandible; max, maxillary.

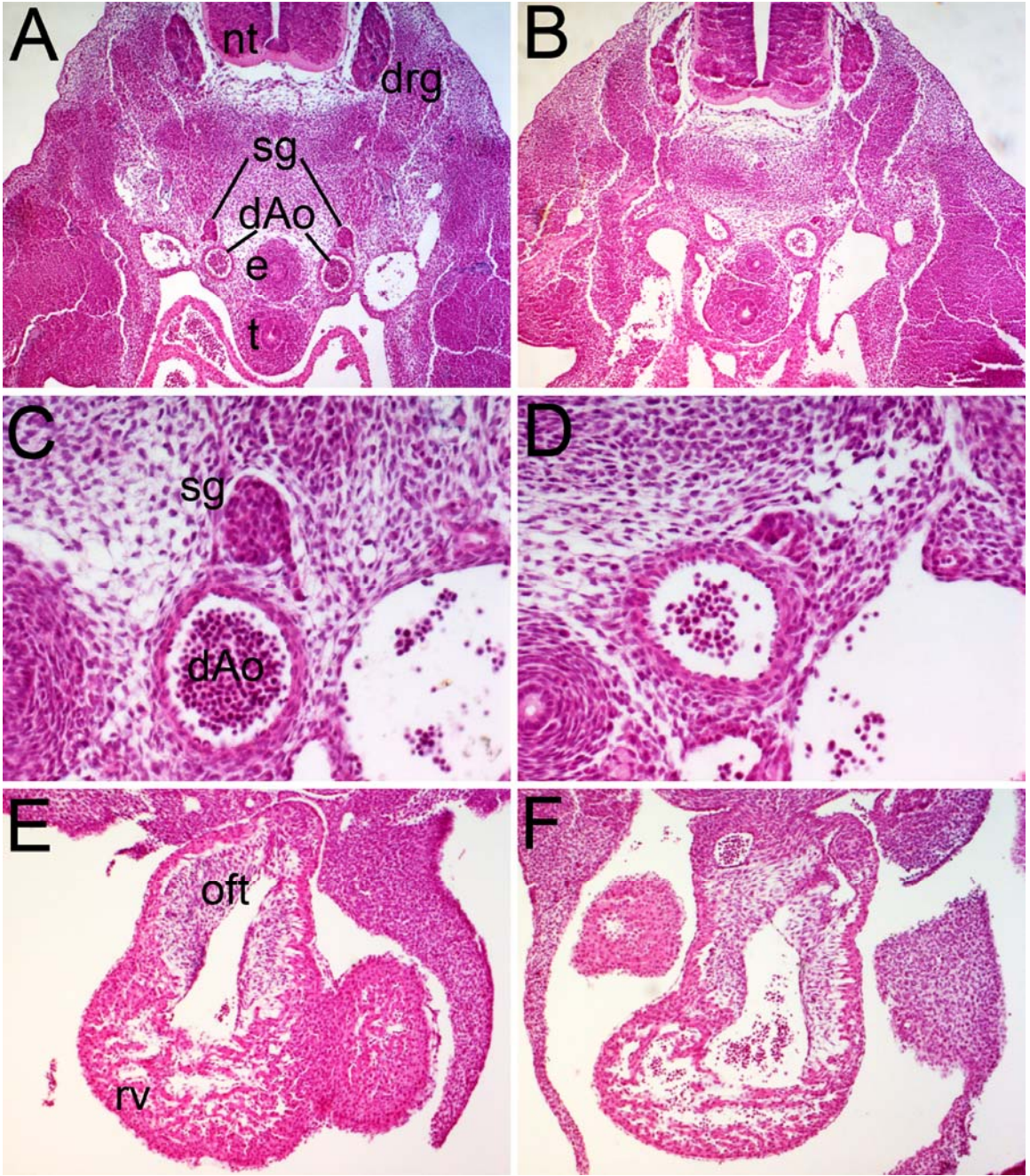


**Figure 17. Overexpression of *Smad7* in post-migratory neural crest cells affected sympathetic ganglia but not dorsal root ganglia and cardiac development.** Littermate control and trigenic embryos were cross sectioned and stained with H&E. **(A, B)** The size and shape of dorsal root ganglia were comparable in both trigenic (B) and control (A) embryos. **(C, D)** However, the catecholaminergic sympathetic ganglia adjacent to the dorsal aorta were much smaller in the trigenic embryos. **(E, F)** The size of the endocardial cushions in the OFT were similar to that of the controls. Abbreviations: dAo, dorsal aorta; drg, dorsal root ganglia; e, esophagus; nt, neural tube; oft, outflow tract; rv, right ventricle; sg, sympathetical ganglia; t, trachea.

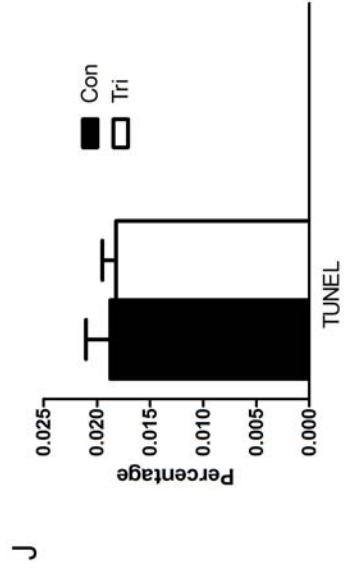
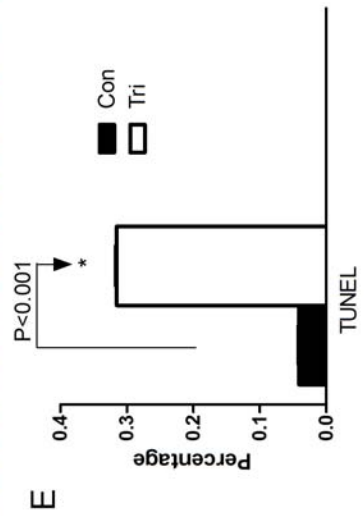
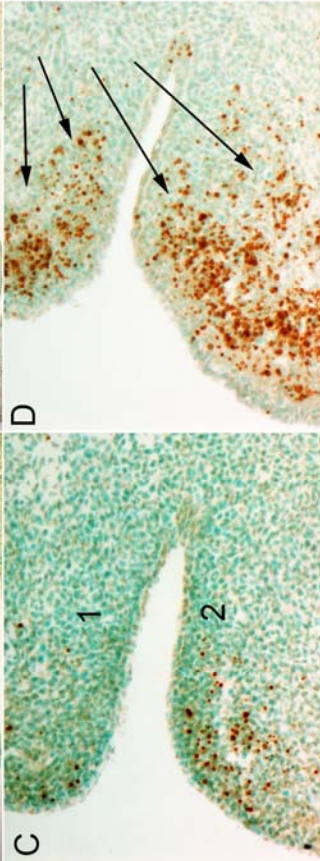
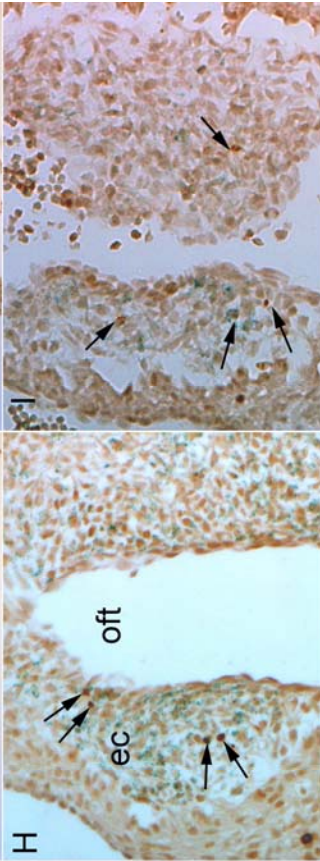
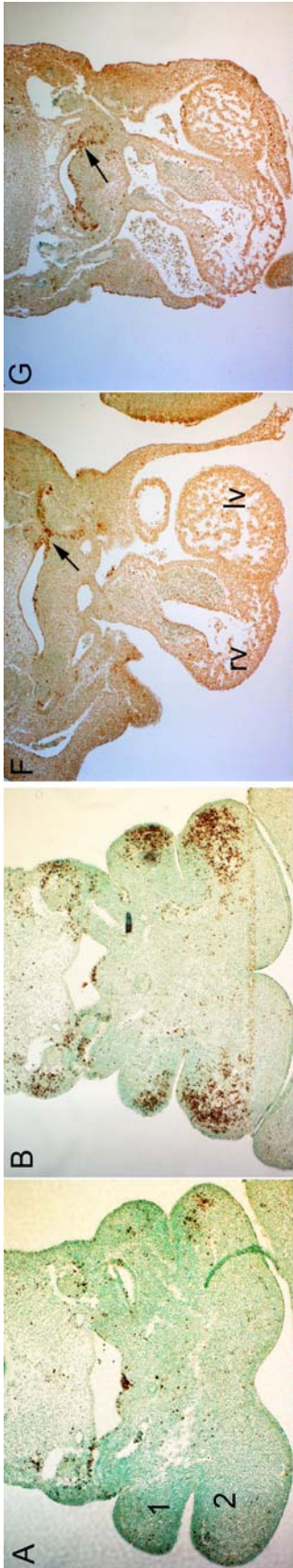


**Figure 18. Elevated cell death in craniofacial regions of the Smad7 trigenic mutants. (A-E)** TUNEL staining on cross sections through the pharyngeal arches of the control (A, C) and trigenic embryos (B, D) at E10.5 (n=4) demonstrated a notable increase in cell death in trigenic mutants (B, D) within the mandibular component of the 1<sup>st</sup> and 2<sup>nd</sup> pharyngeal arches (arrows in D) compared to controls (C). The apoptotic cell index was statistically significant higher in the trigenics (31.57%, E) than that of controls (4.12%, E). **(F-J)** TUNEL staining on cross sections through the outflow tract of the control (A, C) and trigenic embryos (B, D) at E10.5 (n=4). Note that positive TUNEL signals were evident in both control (arrow, F) and trigenic (arrow, G) foregut regions, which have been known to have high endogenous apoptosis activity. However, there were only few sporadic distributed apoptotic cells in both control (arrows in H) and trigenic (arrows in I) embryo OFT regions. There was no notable difference in terms of apoptotic cell rate in the OFT cushions between the control (1.87%) and trigenic (1.82%) embryos (J). Abbreviations: 1, first pharyngeal arch; 2, second pharyngeal arch; ec, endocardial cushions; lv, left ventricle; oft, outflow tract; rv, right ventricle.

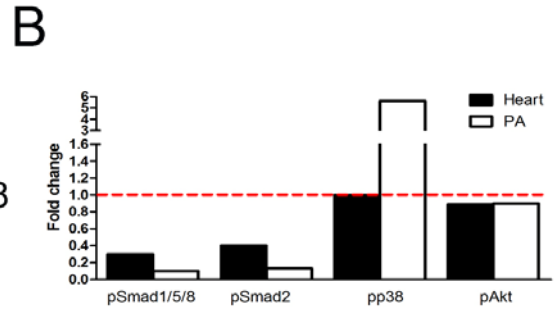
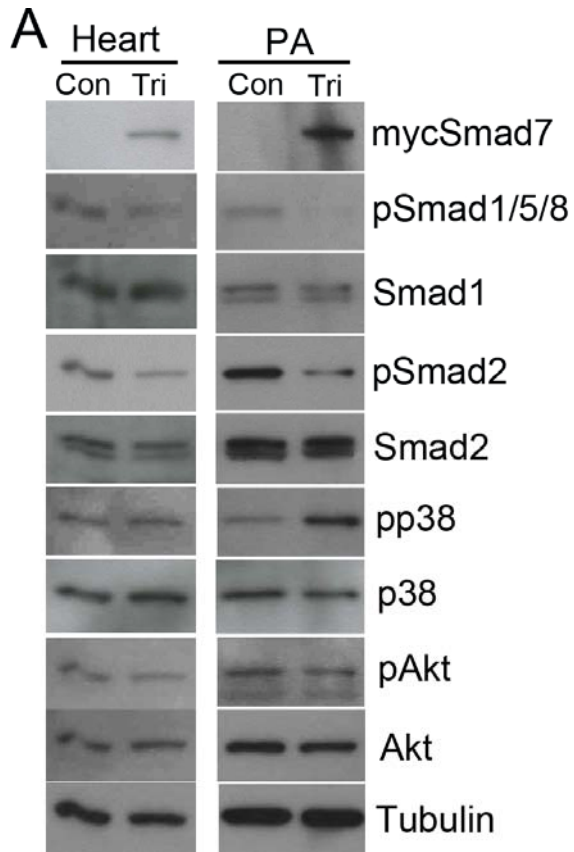


**Figure 19. Increased pp38 in pharyngeal arches and frontofacial tissues.**

**(A)** E10.5 hearts and frontofacial tissues (including upper and lower jaws, 1<sup>st</sup> and 2<sup>nd</sup> pharyngeal arches) were microdissected and examined by western analysis. Note that myc-Smad7 is only expressed within pooled (n=3) trigenic E10.5 hearts and frontofacial tissues, not in pooled control (n=3) samples. In the heart sample, myc-Smad7 suppressed pSmad1/5/8 by ~70%, pSmad2 ~60%, pp38 unchanged, and pAkt ~11% (A, B) when normalized to their respective total proteins compared to littermate controls. In frontofacial sample, where the tissues are known to be mostly populated by *Peri-Cre* lineages, presence of myc-Smad7 suppressed pSmad1/5/8 by ~90%, pSmad2 ~87%, pAkt ~10%, but pp38 levels were increased by 5.6 fold (A, B). Abbreviations: con, control embryos; tri, trigenic *Wnt1-Cre/Rosa<sup>rtTA-EGFP</sup>/tetO-Smad7* embryos; heart, pooled heart tissues; PA, pooled frontofacial tissues (including upper and lower jaws, 1<sup>st</sup> and 2<sup>nd</sup> pharyngeal arches); pp38, phospho-p38; pAkt, phospho-Akt; pSmad1/5/8, phospho-Smad1/5/8; pSmad2, phospho-Smad2.



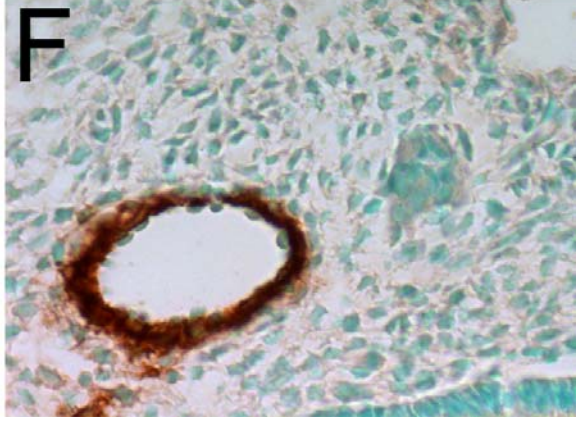
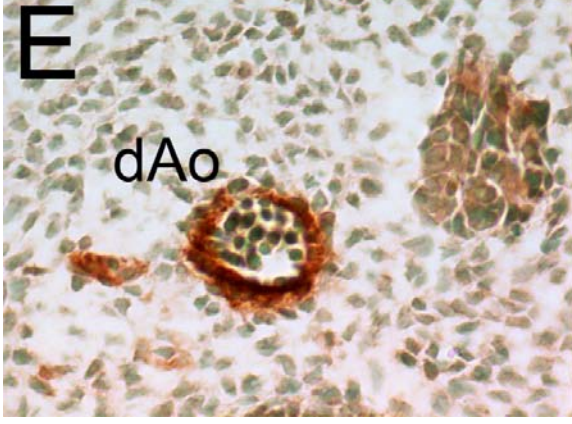
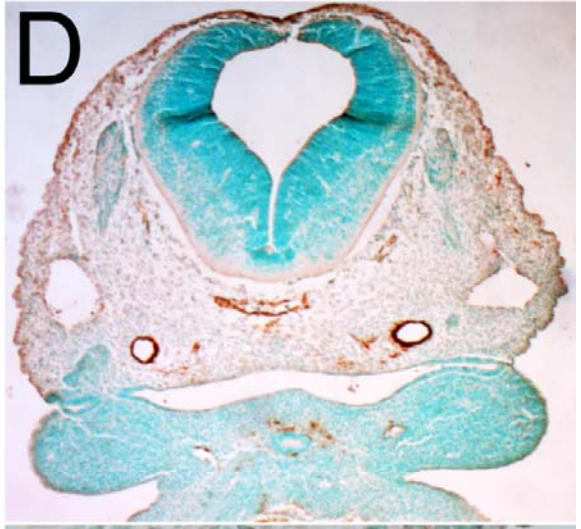
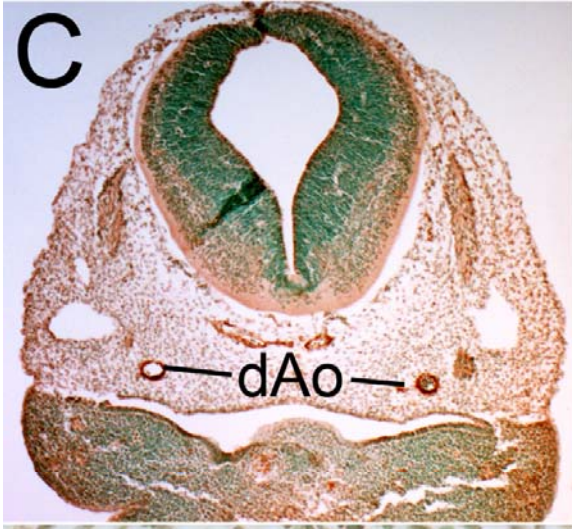
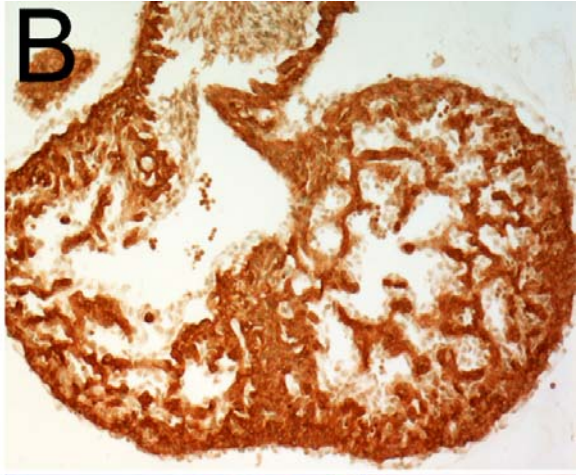
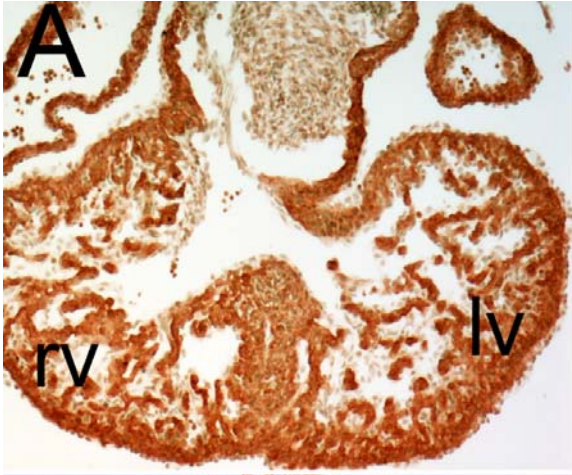


**Figure 20. Unaffected cardiac structure and intact blood vessels in trigenic embryos.** (A, B)  $\alpha$ SM-actin staining showed normal developed myocardium in trigenic embryos (B) compared to the controls (A). (C-F)  $\alpha$ SM-actin staining showed normal smooth muscle layers surrounding the dorsal aorta in the trigenic embryos (D, F) compared to controls (C, E). Abbreviations: dAo, dorsal aorta; lv, left ventricle; rv, right ventricle.

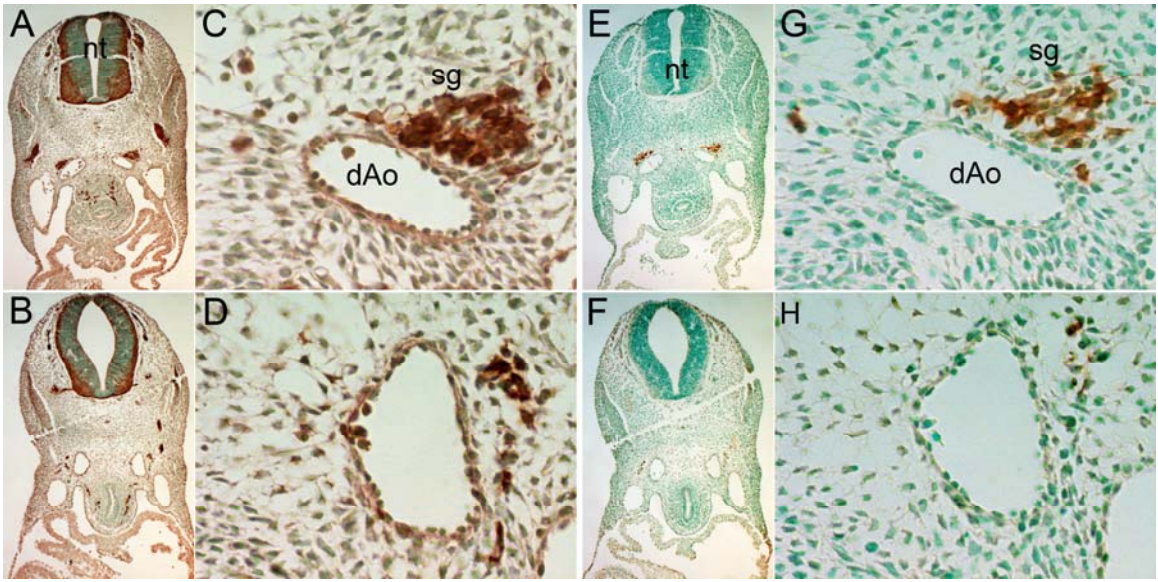


**Figure 21. Hypoplastic sympathetic ganglia and decreased TH synthesis in trigenics.** (A-D) NS $\beta$ T staining showed that the trigenic (B, D) para-aorta sympathetic ganglia were smaller than that of controls (A, C). (E-H) TH staining demonstrated that there was much lower TH expression in the trigenic sympathetic ganglia (F, H) compared to controls (E, G). Abbreviations: dAo, dorsal aorta; sg, sympathetical ganglia.

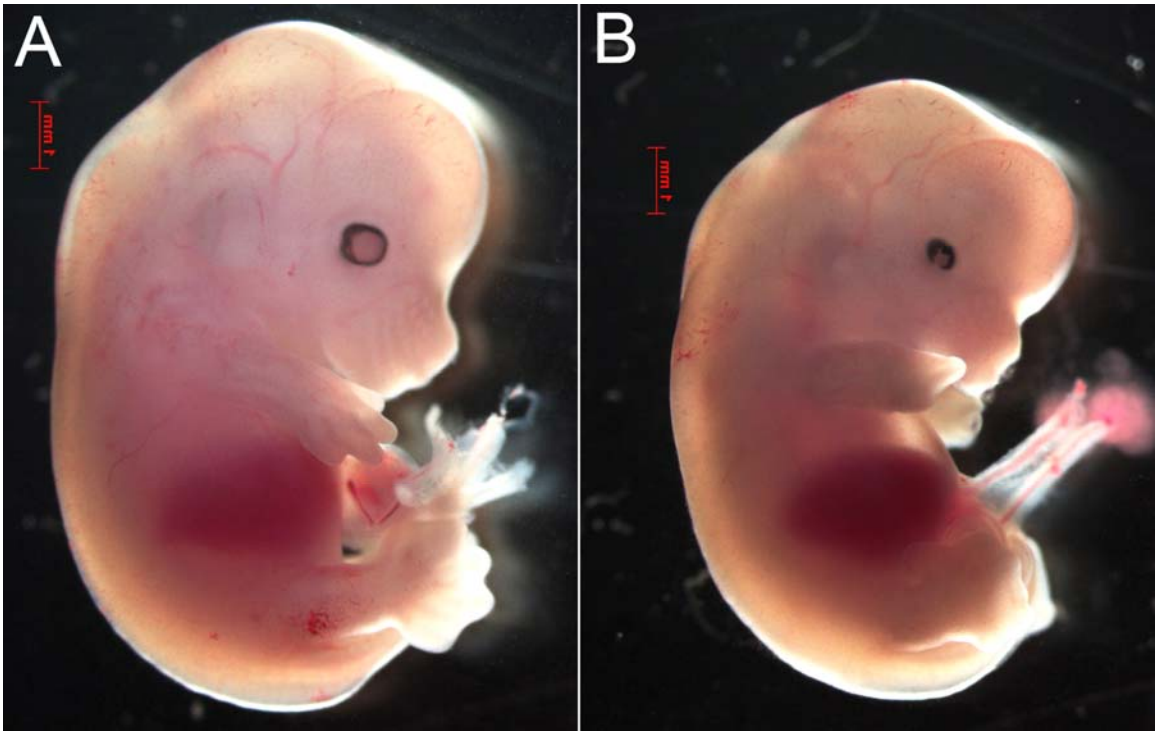


**Figure 22. Isoproterenol rescued trigenic embryos.** Isoproterenol pump was inserted under the skin of pregnant females at E8.5, females were then switched to doxycycline containing food at E9.5, and embryos were harvested at E14.5. **(A)** Control embryos. **(B)** Trigenic embryos. Trigenic embryos were alive when harvested at E14.5, even though they still had hypoplastic jaws and abnormal developed limbs.

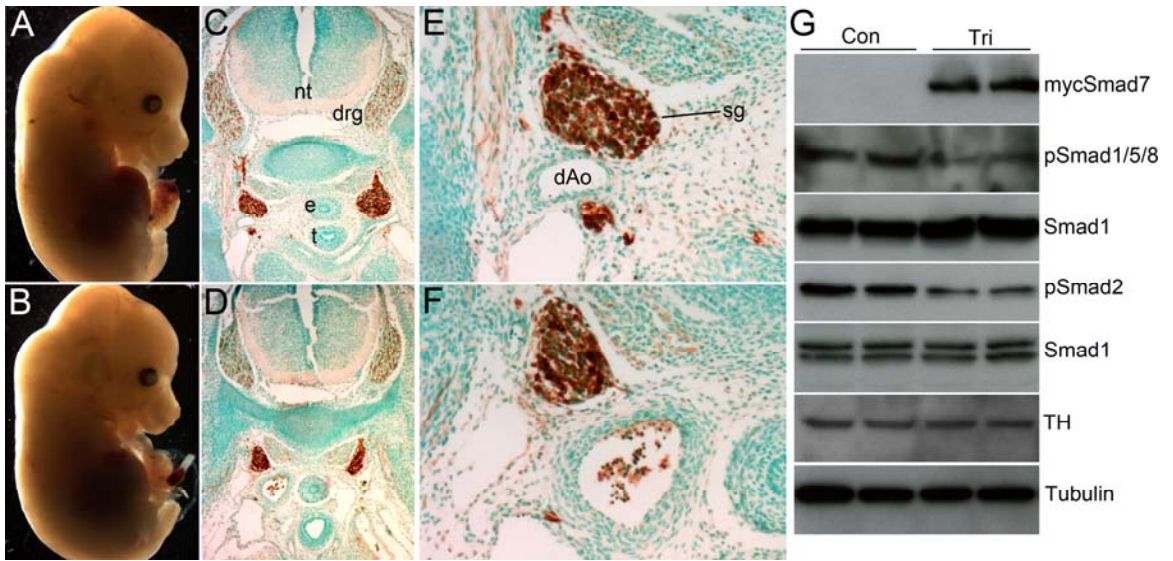


**Figure 23. Overexpression of Smad7 in post-differentiated sympathetic ganglia did not result in mid-gestational lethality.** Embryos were fed doxycycline food from E12.5 and harvested at E14.5. **(A, B)** Trigenic embryos (B, n=8) were alive and grossly normal compared to controls (A). **(C-F)** TH immunohistochemistry assay on crossed sectioned embryos showed normal and abundant staining on sympathetic ganglia adjacent to the dorsal aorta in both control (C, E) and trigenic embryos (D, F). The size and shape of the sympathetic ganglia also appeared normal in trigenic embryos (D, F). **(G)** Western blotting showed that overexpression of mycSmad7 still suppressed both BMP and TGF $\beta$  signaling, demonstrated by decreased pSmad1/5/8 and pSmad2 levels, respectively, but the TH expression levels in trigenic embryos were comparable to those in control embryos. Abbreviations: dAo, dorsal aorta; drg, dorsal root ganglia; e, esophagus; nt, neural tube; sg, sympathetical ganglia; t, trachea.



## Chapter VI: Discussion

### A. The purpose of creating the inducible trigenic mouse system

Neural crest cells (NCC) are a transient population of cells formed during early vertebrate embryonic development. NCC are multipotent cells. After neurulation, they delaminate and migrate along defined pathways to contribute to the formation of a wide variety target tissues, including neurons and glia of the peripheral nervous system, melanocytes, smooth muscle cells and most craniofacial cartilages and bones [12, 14, 63]. NCC also contribute crucial cell populations to several thoracic tissues, including the developing aortic arch arteries (AAA) and OFT of the heart [13, 20, 64-65].

TGF $\beta$  superfamily signaling has been shown playing critical roles in NCC development. Systemic or conditional knock out of the components of TGF $\beta$  superfamily signaling resulted in various NCC development defects [28-41]. However, normal NCC development is determined by expressing genes at both the right time and right place. Systemic knock out mouse models can not address where and when gene expression is important. Using mouse models based on Cre/loxp recombination can partially address this issue in that this method can target gene knock out or expression in certain confined cell types or tissues at a specific time point. In my thesis project, I built a triple transgenic (trigenic) system to address the issue of expressing genes at both the right time and right place. This system uses not only Cre/loxp recombination but also doxycycline

induction elements. By using this system, where a gene is expressed is determined by the *Cre* mouse line used, and when that gene is expressed is controlled by when I apply the inducer, doxycycline, to the system. The inclusion of doxycycline induction elements adds a further temporal control for gene expression, allowing me to induce gene expression at different time points instead of only one time point that is determined by *Cre* expression in mouse model systems based on only *Cre/loxP* recombination. To study NCC development, I used *Wnt1-Cre* and *Peri-Cre* transgenic mice. *Wnt1-Cre* has been shown to express before NCC migrate out of neural tube and so it marks all NCC lineages [14, 20]. *Peri-Cre* marks the peripheral nervous system, and the endocardial cushions of the OFT, which are a subpopulation of post-migratory NCC when they are undergoing differentiation (Conway lab).

### **B. The reasons of using *Smad7* to study NCC development**

There were two major reasons why I chose to overexpress *Smad7* in my transgenic system. First of all, *Smad7* negatively regulates TGF $\beta$  superfamily signaling *in vitro* [4-8]. Since TGF $\beta$  superfamily signaling is known to play important roles in NCC development, we are using *Smad7* as a tool to negatively regulate TGF $\beta$  superfamily signaling. Second, we also want to know the possible roles of endogenous *Smad7* in NCC development. Endogenous *Smad7* mRNA is transiently activated pre-implantation, then is re-expressed widely post-gastrulation [100]. In E10 and E12.5 embryos, *Smad7* mRNA is widespread outside the developing central nervous system, including the NCC-derived

mandibular and medial nasal processes, developing pharyngeal arches, OFT cushions of the heart, adrenal primordium and trigeminal ganglion [55, 100]. Transgenic reporter and Cre/loxP lineage mapping using a partial *Smad7* promoter have also confirmed the robust expression of *Smad7* mRNA within the craniofacial, pharyngeal arch and cardiovascular system [75, 101].

### **C. The common results from *Wnt1-Cre* and *Peri-Cre* trigenic mouse models**

Our data provide compelling genetic evidence demonstrating that forced expression of *Smad7* within NCC is detrimental to development of NCC and their derivatives. Moreover, we showed that levels of both TGF $\beta$  and BMP phosphorylated R-Smads were reduced in the NCC lineages expressing myc-*Smad7*. Since TGF $\beta$  superfamily signaling is known to increase production of phosphorylated forms of R-Smad proteins, our data provide good evidence that TGF $\beta$  signaling *in vivo* is impaired by myc-*Smad7* induction in NCC. In addition, we showed that the hypoplastic or missing tissues observed in both *Wnt1-Cre* and *Peri-Cre* trigenic mouse models were caused by elevated apoptosis in *Smad7* overexpressing cells and their neighboring cells, indicating *Smad7* mediated TGF $\beta$  superfamily signaling or *Smad7* itself or both were probably important for NCC differentiation, differentiated cell maintenance and survival.

### **D. The differences between *Wnt1-Cre* and *Peri-Cre* trigenic mouse models**

Since *Wnt1-Cre* marks all NCC lineages and *Peri-Cre* marks only a subpopulation of post-migratory NCC, we expected overexpression of *Smad7* in

*Wnt1-Cre* lineages would have more severe phenotypes than that in *Peri-Cre* lineages. However, we observed embryonic lethality at E12.5 in *Peri-Cre/R26<sup>rtTA-EGFP</sup>/tetO-Smad7* trigenic mouse model, much earlier than that observed in *Wnt1-Cre/R26<sup>rtTA-EGFP</sup>/tetO-Smad7* trigenic mouse. One probable explanation is the *Wnt1-Cre* expression pattern. *Wnt1-Cre* lineage tracing by crossing with *Rosa26* reporter [85] mice show *Wnt-Cre* mediated *lacZ* gene expression starts in the rostral hindbrain around the four somite (E8.0) stage and extends anteriorly to the midbrain, forebrain, and posteriorly to the caudal hindbrain, cardiac and trunk levels by eight somite (E8.5) stage [39]. However, once NCC have formed, they migrate out of the neural tube at all axis levels simultaneously. So it could be that some NCC have already migrated out of the neural tube before *Wnt1-Cre* expresses at certain axis levels. Indeed, when diphtheria toxin A fragment (DTA), a fatal toxin that kills cells autonomously, was expressed in *Wnt1-Cre* lineages, *Wnt1-Cre;DTA* embryos survive to birth and developed normal adrenal glands (unpublished data, Conway lab), even though the medullar portion of the adrenal gland is derived from NCC. Another possible explanation could be from the difference those two Cre mouse lines express at developmental stages. *Wnt1-Cre* expresses before NCC migrate out the neural tube, and *Peri-Cre* expresses in post-migratory NCC when they are undergoing differentiation. So it could be that TGF $\beta$  superfamily signaling or Smad7 itself or both play a more important role in the NCC differentiation stage than they do in the stages before NCC migration. The third explanation could be as simple as these two Cre mouse lines drive gene expression in some common but not completely overlapping cell

populations, thus we observed different results in the two trigenic Smad7 overexpression mouse models.

### **E. Smad7 and its role in apoptosis**

Like other Smads, Smad7 shuttles between the nucleus and the cytoplasm [129-131]. In resting cells, Smad7 is localized in the nucleus. In response to TGF $\beta$  stimulation Smad7 is exported to the cytoplasm [129] to negatively regulate TGF $\beta$  superfamily signaling.

Although Smad7 was originally identified as an inhibitory Smad for TGF $\beta$  superfamily signaling, there are several reports suggesting that Smad7 may have other cellular functions and can cooperate with TGF $\beta$  to show some other activities. It has been shown to interact with histone deacetylase 1 [132] to modulate gene expression. Smad7 can also regulate gene transcription by modulating its phosphorylation status [133]. Over-expression of Smad7 has recently been demonstrated to cause activation of the JNK pathway and apoptosis in MvLu1 (epithelial cells), MDCK (epithelial cells) and COS7 cells (African Green Monkey SV40-transferred kidney fibroblast cell line), suggesting roles of the Smad7 in regulation of the MAP kinase pathways [134].

My thesis project supports the idea that Smad7 plays other roles other than just suppresses TGF $\beta$  superfamily signaling via Smad. In both mouse models, we observed elevated apoptosis in Smad7 overexpressing tissues. Since

pSmad1/5/8 and pSmad2 levels were both downregulated in these two mouse models, we speculated that increased apoptosis in various tissues was caused by suppression of TGF $\beta$  superfamily signaling. In the *Peri* trigenic model, we also showed that phospho-p38 levels were upregulated in tissues with elevated apoptosis. TGF $\beta$  superfamily signaling can mediate cell undergo apoptosis via p38 pathway. What makes this observation interesting is that Smad7 may play a role as a mediator in this process. Indeed, Smad7 was reported to be involved in TGF $\beta$ -induced apoptosis of prostate cancer cells by activating p38 via TGF $\beta$ -activated kinase 1 (TAK1) and MAPK kinase (MKK3) [125]. Besides, Smad7 is reported to promote apoptosis in keratinocyte cell lines [135]. In yet another report, over-expression of Smad7 by adenoviral infection induced DNA fragmentation and significant increases in cell death in rat mesangial cells [124]. However, in other reports, Smad7 has been showed to inhibit apoptosis induced by TGF $\beta$  in B cells [136] and Hep3B cells [137]. So it seems that Smad7's ability to pro- or anti-apoptosis is dependent on different cell types, and it might function as a TGF $\beta$  superfamily signaling mediator or by other mechanisms. Therefore, the role Smad7 plays in cells or tissues largely depend on the balance between different signals the cells or tissues get, which is important for determining cell fate, survival or death.

In my thesis, I was able to use the doxycycline inducible trigenic mouse model to study TGF $\beta$  superfamily roles in a really defined time window, so that I was able to observe different yet interesting phenotypes that people who are using

systemic or conditional knock out methods are unable to see. I think that my method for conditional myc-Smad7 expression are useful for elucidating further TGF $\beta$  superfamily roles in other organs and tissues and addressing the biological significance of the concerted action between growth and transcription factors in regulating normal development and disease.

### **F. Future studies**

Despite being the foremost congenital heart defect (CHD) found in patients, isolated VSD in mice mutants are usually found in association with altered myocardial growth, OFT/AAA abnormalities and/or valvular defects [138]. VSD pathogenesis is complex and multifactorial: it may result from defects in the NCC, cardiomyocyte, endothelial, endocardial cushion, epicardial and/or cardiac fibroblast lineages because each of the above defects can alter left-right ventricular morphogenesis, chamber formation and septal positioning. In chapter II, we were able to obtain isolated VSD mouse model by feeding trigenic embryos after the cardiac NCC have colonized the OFT even though we do not know what are the mechanism underlying this defect. Future studies focusing on dissecting the molecular mechanism of this mouse model will prove useful to address the role of the NCC lineage in these CHDs.

Another interesting discovery of my thesis is that I found increased apoptosis in trigenic embryo pharyngeal arches, not in the OFT cushions even though both tissues have cells contributed by Peri-Cre lineages. One explanation could be

that TGF $\beta$  superfamily signaling ligands or receptors are differentially expressed at these two organ systems. In the future, we want to check the expression patterns of a list of genes by *in situ hybridization*, including TGF $\beta$  superfamily signaling ligands and their receptors. Another explanation could be that the downstream target genes respond differently to suppression of TGF $\beta$  superfamily signaling. To test this possibility, we are going to microdissect the tissues from the heart and pharyngeal arches, and extract total RNA out of those tissues, then perform microarray assay to find out the differential expressed genes between the heart and pharyngeal arches. The results come from this future study can not only explain why there is differential apoptosis between trigenic embryo pharyngeal arches and the OFT cushions, but also give us hints of why requirement for TGF $\beta$  superfamily signaling in these two tissues is different.



## References

1. Kingsley, D.M., *The TGF-beta superfamily: new members, new receptors, and new genetic tests of function in different organisms*. Genes Dev, 1994. **8**(2): p. 133-46.
2. Massague, J., *TGFbeta in Cancer*. Cell, 2008. **134**(2): p. 215-30.
3. Hata, A., et al., *Smad6 inhibits BMP/Smad1 signaling by specifically competing with the Smad4 tumor suppressor*. Genes Dev, 1998. **12**(2): p. 186-97.
4. Ishisaki, A., et al., *Differential inhibition of Smad6 and Smad7 on bone morphogenetic protein- and activin-mediated growth arrest and apoptosis in B cells*. J Biol Chem, 1999. **274**(19): p. 13637-42.
5. Casellas, R. and A.H. Brivanlou, *Xenopus Smad7 inhibits both the activin and BMP pathways and acts as a neural inducer*. Dev Biol, 1998. **198**(1): p. 1-12.
6. Hayashi, H., et al., *The MAD-related protein Smad7 associates with the TGFbeta receptor and functions as an antagonist of TGFbeta signaling*. Cell, 1997. **89**(7): p. 1165-73.
7. Nakao, A., et al., *Identification of Smad7, a TGFbeta-inducible antagonist of TGF-beta signalling*. Nature, 1997. **389**(6651): p. 631-5.
8. Saika, S., et al., *Effect of Smad7 gene overexpression on transforming growth factor beta-induced retinal pigment fibrosis in a proliferative vitreoretinopathy mouse model*. Arch Ophthalmol, 2007. **125**(5): p. 647-54.
9. He, W., et al., *Overexpression of Smad7 results in severe pathological alterations in multiple epithelial tissues*. Embo J, 2002. **21**(11): p. 2580-90.
10. Kuang, C., et al., *In vivo disruption of TGF-beta signaling by Smad7 leads to premalignant ductal lesions in the pancreas*. Proc Natl Acad Sci U S A, 2006. **103**(6): p. 1858-63.
11. Trainor, P.A., *Specification of neural crest cell formation and migration in mouse embryos*. Semin Cell Dev Biol, 2005. **16**(6): p. 683-93.
12. Le Douarin, N.M.a.K., C. , *The Neural Crest*. New York: Cambridge University Press, 1999.
13. Kirby, M.L. and K.L. Waldo, *Neural crest and cardiovascular patterning*. Circ Res, 1995. **77**(2): p. 211-5.
14. Chai, Y., et al., *Fate of the mammalian cranial neural crest during tooth and mandibular morphogenesis*. Development, 2000. **127**(8): p. 1671-9.
15. Kanzler, B., et al., *BMP signaling is essential for development of skeletogenic and neurogenic cranial neural crest*. Development, 2000. **127**(5): p. 1095-104.
16. Osumi-Yamashita, N., et al., *The contribution of both forebrain and midbrain crest cells to the mesenchyme in the frontonasal mass of mouse embryos*. Dev Biol, 1994. **164**(2): p. 409-19.

17. Creuzet, S., G. Couly, and N.M. Le Douarin, *Patterning the neural crest derivatives during development of the vertebrate head: insights from avian studies*. J Anat, 2005. **207**(5): p. 447-59.
18. Graham, A., J. Begbie, and I. McGonnell, *Significance of the cranial neural crest*. Dev Dyn, 2004. **229**(1): p. 5-13.
19. Helms, J.A., D. Cordero, and M.D. Tapadia, *New insights into craniofacial morphogenesis*. Development, 2005. **132**(5): p. 851-61.
20. Jiang, X., et al., *Fate of the mammalian cardiac neural crest*. Development, 2000. **127**(8): p. 1607-16.
21. Morikawa, Y., et al., *BMP signaling regulates sympathetic nervous system development through Smad4-dependent and -independent pathways*. Development, 2009. **136**(21): p. 3575-84.
22. Markwald, R.R., T.P. Fitzharris, and F.J. Manasek, *Structural development of endocardial cushions*. Am J Anat, 1977. **148**(1): p. 85-119.
23. Mjaatvedt, C.H., R.C. Lepera, and R.R. Markwald, *Myocardial specificity for initiating endothelial-mesenchymal cell transition in embryonic chick heart correlates with a particulate distribution of fibronectin*. Dev Biol, 1987. **119**(1): p. 59-67.
24. Sugi, Y., et al., *Bone morphogenetic protein-2 can mediate myocardial regulation of atrioventricular cushion mesenchymal cell formation in mice*. Dev Biol, 2004. **269**(2): p. 505-18.
25. Waldo, K., et al., *Cardiac neural crest cells provide new insight into septation of the cardiac outflow tract: aortic sac to ventricular septal closure*. Dev Biol, 1998. **196**(2): p. 129-44.
26. Yutzey, K.E. and M.L. Kirby, *Wherefore heart thou? Embryonic origins of cardiogenic mesoderm*. Dev Dyn, 2002. **223**(3): p. 307-20.
27. Loffredo, C.A., *Epidemiology of cardiovascular malformations: prevalence and risk factors*. Am J Med Genet, 2000. **97**(4): p. 319-25.
28. Reissmann, E., et al., *Involvement of bone morphogenetic protein-4 and bone morphogenetic protein-7 in the differentiation of the adrenergic phenotype in developing sympathetic neurons*. Development, 1996. **122**(7): p. 2079-88.
29. Schneider, C., et al., *Bone morphogenetic proteins are required in vivo for the generation of sympathetic neurons*. Neuron, 1999. **24**(4): p. 861-70.
30. Wurdak, H., et al., *Inactivation of TGFbeta signaling in neural crest stem cells leads to multiple defects reminiscent of DiGeorge syndrome*. Genes Dev, 2005. **19**(5): p. 530-5.
31. Dunker, N. and K. Kriegelstein, *Tgfbeta2 -/- Tgfbeta3 -/- double knockout mice display severe midline fusion defects and early embryonic lethality*. Anat Embryol (Berl), 2002. **206**(1-2): p. 73-83.
32. Ito, Y., et al., *Conditional inactivation of Tgfbr2 in cranial neural crest causes cleft palate and calvaria defects*. Development, 2003. **130**(21): p. 5269-80.
33. Ittner, L.M., et al., *Compound developmental eye disorders following inactivation of TGFbeta signaling in neural-crest stem cells*. J Biol, 2005. **4**(3): p. 11.

34. Choudhary, B., et al., *Cardiovascular malformations with normal smooth muscle differentiation in neural crest-specific type II TGFbeta receptor (Tgfbr2) mutant mice*. Dev Biol, 2006. **289**(2): p. 420-9.
35. Dudas, M., et al., *Epithelial and ectomesenchymal role of the type I TGF-beta receptor ALK5 during facial morphogenesis and palatal fusion*. Dev Biol, 2006. **296**(2): p. 298-314.
36. Wang, J., et al., *Defective ALK5 signaling in the neural crest leads to increased postmigratory neural crest cell apoptosis and severe outflow tract defects*. BMC Dev Biol, 2006. **6**: p. 51.
37. Dudas, M., et al., *Craniofacial defects in mice lacking BMP type I receptor Alk2 in neural crest cells*. Mech Dev, 2004. **121**(2): p. 173-82.
38. Kaartinen, V., et al., *Cardiac outflow tract defects in mice lacking ALK2 in neural crest cells*. Development, 2004. **131**(14): p. 3481-90.
39. Stottmann, R.W., et al., *BMP receptor IA is required in mammalian neural crest cells for development of the cardiac outflow tract and ventricular myocardium*. Development, 2004. **131**(9): p. 2205-18.
40. Jia, Q., et al., *Smad signaling in the neural crest regulates cardiac outflow tract remodeling through cell autonomous and non-cell autonomous effects*. Dev Biol, 2007. **311**(1): p. 172-84.
41. Ko, S.O., et al., *Smad4 is required to regulate the fate of cranial neural crest cells*. Dev Biol, 2007. **312**(1): p. 435-47.
42. Tang, S., et al., *Trigenic neural crest-restricted Smad7 over-expression results in congenital craniofacial and cardiovascular defects*. Dev Biol, 2010.
43. Akhurst, R.J., et al., *TGF beta in murine morphogenetic processes: the early embryo and cardiogenesis*. Development, 1990. **108**(4): p. 645-56.
44. Millan, F.A., et al., *Embryonic gene expression patterns of TGF beta 1, beta 2 and beta 3 suggest different developmental functions in vivo*. Development, 1991. **111**(1): p. 131-43.
45. Jones, C.M., K.M. Lyons, and B.L. Hogan, *Involvement of Bone Morphogenetic Protein-4 (BMP-4) and Vgr-1 in morphogenesis and neurogenesis in the mouse*. Development, 1991. **111**(2): p. 531-42.
46. Abdelwahid, E., et al., *Overlapping and differential localization of Bmp-2, Bmp-4, Msx-2 and apoptosis in the endocardial cushion and adjacent tissues of the developing mouse heart*. Cell Tissue Res, 2001. **305**(1): p. 67-78.
47. Kim, R.Y., E.J. Robertson, and M.J. Solloway, *Bmp6 and Bmp7 are required for cushion formation and septation in the developing mouse heart*. Dev Biol, 2001. **235**(2): p. 449-66.
48. Solloway, M.J. and E.J. Robertson, *Early embryonic lethality in Bmp5;Bmp7 double mutant mice suggests functional redundancy within the 60A subgroup*. Development, 1999. **126**(8): p. 1753-68.
49. Dickson, M.C., et al., *Defective haematopoiesis and vasculogenesis in transforming growth factor-beta 1 knock out mice*. Development, 1995. **121**(6): p. 1845-54.

50. Koo, S.H., et al., *The transforming growth factor-beta 3 knock-out mouse: an animal model for cleft palate*. *Plast Reconstr Surg*, 2001. **108**(4): p. 938-48; discussion 949-51.
51. Winnier, G., et al., *Bone morphogenetic protein-4 is required for mesoderm formation and patterning in the mouse*. *Genes Dev*, 1995. **9**(17): p. 2105-16.
52. Jena, N., et al., *BMP7 null mutation in mice: developmental defects in skeleton, kidney, and eye*. *Exp Cell Res*, 1997. **230**(1): p. 28-37.
53. Kingsley, D.M., et al., *The mouse short ear skeletal morphogenesis locus is associated with defects in a bone morphogenetic member of the TGF beta superfamily*. *Cell*, 1992. **71**(3): p. 399-410.
54. Solloway, M.J., et al., *Mice lacking Bmp6 function*. *Dev Genet*, 1998. **22**(4): p. 321-39.
55. Luukko, K., A. Ylikorkala, and T.P. Makela, *Developmentally regulated expression of Smad3, Smad4, Smad6, and Smad7 involved in TGF-beta signaling*. *Mech Dev*, 2001. **101**(1-2): p. 209-12.
56. Galvin, K.M., et al., *A role for smad6 in development and homeostasis of the cardiovascular system*. *Nat Genet*, 2000. **24**(2): p. 171-4.
57. Snider, P., et al., *Periostin is required for maturation and extracellular matrix stabilization of noncardiomyocyte lineages of the heart*. *Circ Res*, 2008. **102**(7): p. 752-60.
58. Li, R., et al., *Deletion of exon I of SMAD7 in mice results in altered B cell responses*. *J Immunol*, 2006. **176**(11): p. 6777-84.
59. Chen, Q., et al., *Smad7 is required for the development and function of heart*. *J Biol Chem*, 2008.
60. Armstrong, E.J. and J. Bischoff, *Heart valve development: endothelial cell signaling and differentiation*. *Circ Res*, 2004. **95**(5): p. 459-70.
61. Olson, E.N., *A decade of discoveries in cardiac biology*. *Nat Med*, 2004. **10**(5): p. 467-74.
62. Serbedzija, G.N., M. Bronner-Fraser, and S.E. Fraser, *Vital dye analysis of cranial neural crest cell migration in the mouse embryo*. *Development*, 1992. **116**(2): p. 297-307.
63. Nichols, D.H., *Neural crest formation in the head of the mouse embryo as observed using a new histological technique*. *J Embryol Exp Morphol*, 1981. **64**: p. 105-20.
64. Snider, P., et al., *Cardiovascular development and the colonizing cardiac neural crest lineage*. *ScientificWorldJournal*, 2007. **7**: p. 1090-113.
65. Gittenberger-de Groot, A.C., et al., *Basics of cardiac development for the understanding of congenital heart malformations*. *Pediatr Res*, 2005. **57**(2): p. 169-76.
66. Itoh, S. and P. ten Dijke, *Negative regulation of TGF-beta receptor/Smad signal transduction*. *Curr Opin Cell Biol*, 2007. **19**(2): p. 176-84.
67. Massague, J., J. Seoane, and D. Wotton, *Smad transcription factors*. *Genes Dev*, 2005. **19**(23): p. 2783-810.
68. Moustakas, A. and C.H. Heldin, *The regulation of TGFbeta signal transduction*. *Development*, 2009. **136**(22): p. 3699-714.

69. Aybar, M.J. and R. Mayor, *Early induction of neural crest cells: lessons learned from frog, fish and chick*. *Curr Opin Genet Dev*, 2002. **12**(4): p. 452-8.
70. Christiansen, J.H., E.G. Coles, and D.G. Wilkinson, *Molecular control of neural crest formation, migration and differentiation*. *Curr Opin Cell Biol*, 2000. **12**(6): p. 719-24.
71. Knecht, A.K. and M. Bronner-Fraser, *Induction of the neural crest: a multigene process*. *Nat Rev Genet*, 2002. **3**(6): p. 453-61.
72. Buchmann-Moller, S., et al., *Multiple lineage-specific roles of Smad4 during neural crest development*. *Dev Biol*, 2009. **330**(2): p. 329-38.
73. Nie, X., et al., *Disruption of Smad4 in neural crest cells leads to mid-gestation death with pharyngeal arch, craniofacial and cardiac defects*. *Dev Biol*, 2008. **316**(2): p. 417-30.
74. Belteki, G., et al., *Conditional and inducible transgene expression in mice through the combinatorial use of Cre-mediated recombination and tetracycline induction*. *Nucleic Acids Res*, 2005. **33**(5): p. e51.
75. Snider, P., et al., *Generation of Smad7(-Cre) recombinase mice: A useful tool for the study of epithelial-mesenchymal transformation within the embryonic heart*. *Genesis*, 2009. **47**(7): p. 469-75.
76. Snider, P., et al., *Generation and characterization of Csrp1 enhancer-driven tissue-restricted Cre-recombinase mice*. *Genesis*, 2008. **46**(3): p. 167-76.
77. Rios, H., et al., *periostin null mice exhibit dwarfism, incisor enamel defects, and an early-onset periodontal disease-like phenotype*. *Mol Cell Biol*, 2005. **25**(24): p. 11131-44.
78. Zhou, H.M., et al., *Lineage-specific responses to reduced embryonic Pax3 expression levels*. *Dev Biol*, 2008. **315**(2): p. 369-82.
79. Conway, S.J., D.J. Henderson, and A.J. Copp, *Pax3 is required for cardiac neural crest migration in the mouse: evidence from the splotch (Sp2H) mutant*. *Development*, 1997. **124**(2): p. 505-14.
80. Conway, S.J., et al., *Decreased neural crest stem cell expansion is responsible for the conotruncal heart defects within the splotch (Sp(2H))/Pax3 mouse mutant*. *Cardiovasc Res*, 2000. **47**(2): p. 314-28.
81. Brault, V., et al., *Inactivation of the beta-catenin gene by Wnt1-Cre-mediated deletion results in dramatic brain malformation and failure of craniofacial development*. *Development*, 2001. **128**(8): p. 1253-64.
82. Zambrowicz, B.P., et al., *Disruption of overlapping transcripts in the ROSA beta geo 26 gene trap strain leads to widespread expression of beta-galactosidase in mouse embryos and hematopoietic cells*. *Proc Natl Acad Sci U S A*, 1997. **94**(8): p. 3789-94.
83. Perl, A.K., J.W. Tichelaar, and J.A. Whitsett, *Conditional gene expression in the respiratory epithelium of the mouse*. *Transgenic Res*, 2002. **11**(1): p. 21-9.
84. Han, G., et al., *Smad7-Induced beta-Catenin Degradation Alters Epidermal Appendage Development*. *Dev Cell*, 2006. **11**(3): p. 301-12.

85. Soriano, P., *Generalized lacZ expression with the ROSA26 Cre reporter strain*. Nat Genet, 1999. **21**(1): p. 70-1.
86. Dietrich, P., et al., *Congenital hydrocephalus associated with abnormal subcommissural organ in mice lacking huntingtin in Wnt1 cell lineages*. Hum Mol Genet, 2009. **18**(1): p. 142-50.
87. Wang, Y.Q., et al., *Restricted expression of type-II TGF beta receptor in murine embryonic development suggests a central role in tissue modeling and CNS patterning*. Mech Dev, 1995. **52**(2-3): p. 275-89.
88. Anderson, R.M., et al., *Endogenous bone morphogenetic protein antagonists regulate mammalian neural crest generation and survival*. Dev Dyn, 2006. **235**(9): p. 2507-20.
89. Snider, P. and S.J. Conway, *Developmental biology: the power of blood*. Nature, 2007. **450**(7167): p. 180-1.
90. Stalmans, I., et al., *VEGF: a modifier of the del22q11 (DiGeorge) syndrome?* Nat Med, 2003. **9**(2): p. 173-82.
91. Epstein, J.A., et al., *Migration of cardiac neural crest cells in Splotch embryos*. Development, 2000. **127**(9): p. 1869-78.
92. Brewer, S., et al., *Requirement for AP-2alpha in cardiac outflow tract morphogenesis*. Mech Dev, 2002. **110**(1-2): p. 139-49.
93. Frank, D.U., et al., *An Fgf8 mouse mutant phenocopies human 22q11 deletion syndrome*. Development, 2002. **129**(19): p. 4591-603.
94. Poelmann, R.E., et al., *Apoptosis in cardiac development*. Cell Tissue Res, 2000. **301**(1): p. 43-52.
95. Arnold, N.B., et al., *Thioredoxin is downstream of Smad7 in a pathway that promotes growth and suppresses cisplatin-induced apoptosis in pancreatic cancer*. Cancer Res, 2004. **64**(10): p. 3599-606.
96. Boulay, J.L., et al., *SMAD7 is a prognostic marker in patients with colorectal cancer*. Int J Cancer, 2003. **104**(4): p. 446-9.
97. Asano, Y., et al., *Impaired Smad7-Smurf-mediated negative regulation of TGF-beta signaling in scleroderma fibroblasts*. J Clin Invest, 2004. **113**(2): p. 253-64.
98. Monteleone, G., et al., *Blocking Smad7 restores TGF-beta1 signaling in chronic inflammatory bowel disease*. J Clin Invest, 2001. **108**(4): p. 601-9.
99. Chen, Q., et al., *Smad7 is required for the development and function of the heart*. J Biol Chem, 2009. **284**(1): p. 292-300.
100. Zwijsen, A., et al., *Expression of the inhibitory Smad7 in early mouse development and upregulation during embryonic vasculogenesis*. Dev Dyn, 2000. **218**(4): p. 663-70.
101. Liu, X., et al., *A 4.3 kb Smad7 promoter is able to specify gene expression during mouse development*. Biochim Biophys Acta, 2007. **1769**(2): p. 149-52.
102. Dorsky, R.I., R.T. Moon, and D.W. Raible, *Environmental signals and cell fate specification in premigratory neural crest*. Bioessays, 2000. **22**(8): p. 708-16.
103. Garcia-Castro, M.I., C. Marcelle, and M. Bronner-Fraser, *Ectodermal Wnt function as a neural crest inducer*. Science, 2002. **297**(5582): p. 848-51.

104. Lee, H.Y., et al., *Instructive role of Wnt/beta-catenin in sensory fate specification in neural crest stem cells*. Science, 2004. **303**(5660): p. 1020-3.
105. Shah, N.M., A.K. Groves, and D.J. Anderson, *Alternative neural crest cell fates are instructively promoted by TGFbeta superfamily members*. Cell, 1996. **85**(3): p. 331-43.
106. Smart, N.G., et al., *Conditional expression of Smad7 in pancreatic beta cells disrupts TGF-beta signaling and induces reversible diabetes mellitus*. PLoS Biol, 2006. **4**(2): p. e39.
107. Chadwick, K., et al., *Smad7 alters cell fate decisions of human hematopoietic repopulating cells*. Blood, 2005. **105**(5): p. 1905-15.
108. Moon, A.M., et al., *Crkl deficiency disrupts Fgf8 signaling in a mouse model of 22q11 deletion syndromes*. Dev Cell, 2006. **10**(1): p. 71-80.
109. Nakamura, T., et al., *Noonan syndrome is associated with enhanced pERK activity, the repression of which can prevent craniofacial malformations*. Proc Natl Acad Sci U S A, 2009. **106**(36): p. 15436-41.
110. Kobrynski, L.J. and K.E. Sullivan, *Velocardiofacial syndrome, DiGeorge syndrome: the chromosome 22q11.2 deletion syndromes*. Lancet, 2007. **370**(9596): p. 1443-52.
111. Rope, A.F., et al., *DiGeorge anomaly in the absence of chromosome 22q11.2 deletion*. J Pediatr, 2009. **155**(4): p. 560-5.
112. Shaikh, T.H., et al., *Low copy repeats mediate distal chromosome 22q11.2 deletions: sequence analysis predicts breakpoint mechanisms*. Genome Res, 2007. **17**(4): p. 482-91.
113. Randall, V., et al., *Great vessel development requires biallelic expression of Chd7 and Tbx1 in pharyngeal ectoderm in mice*. J Clin Invest, 2009. **119**(11): p. 3301-10.
114. Kato, Y., et al., *A component of the ARC/Mediator complex required for TGF beta/Nodal signalling*. Nature, 2002. **418**(6898): p. 641-6.
115. Fulcoli, F.G., et al., *Tbx1 regulates the BMP-Smad1 pathway in a transcription independent manner*. PLoS One, 2009. **4**(6): p. e6049.
116. Noden, D.M. and P.A. Trainor, *Relations and interactions between cranial mesoderm and neural crest populations*. J Anat, 2005. **207**(5): p. 575-601.
117. Hutson, M.R. and M.L. Kirby, *Model systems for the study of heart development and disease. Cardiac neural crest and conotruncal malformations*. Semin Cell Dev Biol, 2007. **18**(1): p. 101-10.
118. Kirby, M.L., et al., *Abnormal patterning of the aortic arch arteries does not evoke cardiac malformations*. Dev Dyn, 1997. **208**(1): p. 34-47.
119. Luo, Y., et al., *N-cadherin is required for neural crest remodeling of the cardiac outflow tract*. Dev Biol, 2006. **299**(2): p. 517-28.
120. Carmona-Fontaine, C., et al., *Contact inhibition of locomotion in vivo controls neural crest directional migration*. Nature, 2008. **456**(7224): p. 957-61.
121. Xu, X., et al., *Connexin 43-mediated modulation of polarized cell movement and the directional migration of cardiac neural crest cells*. Development, 2006. **133**(18): p. 3629-39.

122. Lindsley, A., et al., *Identification and characterization of a novel Schwann and outflow tract endocardial cushion lineage-restricted periostin enhancer*. *Dev Biol*, 2007. **307**(2): p. 340-55.
123. Ludwig, A., et al., *Sox10-rtTA mouse line for tetracycline-inducible expression of transgenes in neural crest cells and oligodendrocytes*. *Genesis*, 2004. **40**(3): p. 171-5.
124. Okado, T., et al., *Smad7 mediates transforming growth factor-beta-induced apoptosis in mesangial cells*. *Kidney Int*, 2002. **62**(4): p. 1178-86.
125. Edlund, S., et al., *Transforming growth factor-beta1 (TGF-beta)-induced apoptosis of prostate cancer cells involves Smad7-dependent activation of p38 by TGF-beta-activated kinase 1 and mitogen-activated protein kinase kinase 3*. *Mol Biol Cell*, 2003. **14**(2): p. 529-44.
126. Waldo, K.L., D. Kumiski, and M.L. Kirby, *Cardiac neural crest is essential for the persistence rather than the formation of an arch artery*. *Dev Dyn*, 1996. **205**(3): p. 281-92.
127. Willette, R.N., et al., *BMP-2 gene expression and effects on human vascular smooth muscle cells*. *J Vasc Res*, 1999. **36**(2): p. 120-5.
128. Etchevers, H.C., et al., *The cephalic neural crest provides pericytes and smooth muscle cells to all blood vessels of the face and forebrain*. *Development*, 2001. **128**(7): p. 1059-68.
129. Itoh, S., et al., *Transforming growth factor beta1 induces nuclear export of inhibitory Smad7*. *J Biol Chem*, 1998. **273**(44): p. 29195-201.
130. Kavsak, P., et al., *Smad7 binds to Smurf2 to form an E3 ubiquitin ligase that targets the TGF beta receptor for degradation*. *Mol Cell*, 2000. **6**(6): p. 1365-75.
131. Hanyu, A., et al., *The N domain of Smad7 is essential for specific inhibition of transforming growth factor-beta signaling*. *J Cell Biol*, 2001. **155**(6): p. 1017-27.
132. Bai, S. and X. Cao, *A nuclear antagonistic mechanism of inhibitory Smads in transforming growth factor-beta signaling*. *J Biol Chem*, 2002. **277**(6): p. 4176-82.
133. Pulaski, L., et al., *Phosphorylation of Smad7 at Ser-249 does not interfere with its inhibitory role in transforming growth factor-beta-dependent signaling but affects Smad7-dependent transcriptional activation*. *J Biol Chem*, 2001. **276**(17): p. 14344-9.
134. Mazars, A., et al., *Evidence for a role of the JNK cascade in Smad7-mediated apoptosis*. *J Biol Chem*, 2001. **276**(39): p. 36797-803.
135. Landstrom, M., et al., *Smad7 mediates apoptosis induced by transforming growth factor beta in prostatic carcinoma cells*. *Curr Biol*, 2000. **10**(9): p. 535-8.
136. Patil, S., et al., *Smad7 is induced by CD40 and protects WEHI 231 B-lymphocytes from transforming growth factor-beta -induced growth inhibition and apoptosis*. *J Biol Chem*, 2000. **275**(49): p. 38363-70.
137. Yamamura, Y., et al., *Critical role of Smads and AP-1 complex in transforming growth factor-beta -dependent apoptosis*. *J Biol Chem*, 2000. **275**(46): p. 36295-302.



138. Conway, S.J., et al., *What cardiovascular defect does my prenatal mouse mutant have, and why?* *Genesis*, 2003. **35**(1): p. 1-21.

## Curriculum Vitae

### Sunyong Tang

#### Education

1995-1999

Wuhan University, Wuhan, China

B.S.: Biology

1999-2002

Chinese Academy of Sciences, Beijing, China

M.S.: Genetics

2003-2010

Indiana University, Indianapolis, IN

Ph.D.: Biochemistry

Minor: Life Sciences

#### Honors, Awards and Fellowships

2002 *Liu-Yongling* scholarship, Chinese Academy of Sciences

2008 Indiana University Education Enhancement Grant Award, Indiana University

2008-2010 American Heart Association Fellowship

#### Research and Training Experience

1999-2002 Institute of Genetics, Chinese Academy of Sciences, Beijing, China

M.S. student, Institute of Genetics

Wenbin Li, Ph.D. (2000-2002)

2003-2010 Indiana University School of Medicine, Indianapolis, IN

Ph.D. Student, Department of Biochemistry and Molecular Biology

Matthew Grow, Ph.D. (2004-2006)

Simon J Conway, Ph.D. (2006-2010)

#### Professional Experience

2002-2003 Shanghai CAS Microarray Co., LTD, Shanghai, China

Technology Consultant

#### Posters and oral presentations

- **Sunyong Tang.** Blocking TGF $\beta$  signaling in endocardial cushions by over-expression of Smad7 will affect normal heart valve morphogenesis. Riley heart research center retreat, 2006
- **Sunyong Tang** and Simon Conway. Examination of the roles of Smad7 during cardiac valve development and remodeling. International Society for Heart Research Meeting, Cincinnati, OH, 2008

- **Sunyong Tang**, Paige Snider and Simon J. Conway. Over-expression of Smad7 in neural crest cells leads to craniofacial and cardiac defects. Weinstein Cardiovascular Development Conference, San Francisco, CA, 2009
- **Sunyong Tang**. Smad7 trigenic. Riley heart research center retreat, 2009

#### Peer Reviewed Publications

- **Sunyong Tang**, Hengyao Niu, Liming Zhang, Yongru Sun and Wenbin Li. The current state in research of chemically inducible systems of plant genetic engineering. *Journal of Chinese Biotechnology Vol22:77-83, 2002*
- **Sunyong Tang**, Bolan Yu, Hengyao Niu, Liming Zhang, Yongru Sun and Wenbin Li. Construction of a tapetum-specific and tetracycline-inducible system. *Journal of Integrative Plant Biology (ACTA BOTANICA SINICA) 45(1):64-67, 2003*
- Paige Snider, **Sunyong Tang**, Goldie Lin, Jian Wang, and Simon J. Conway. Generation of Smad7-Cre recombinase mice: a useful tool for the study of epithelial-mesenchymal transformation within the embryonic heart. *Genesis 47:469-475, 2009*
- **Sunyong Tang**, Paige Snider, Antony B. Firulli, and Simon J. Conway. Trigenic neural crest-restricted Smad7 over-expression results in congenital craniofacial and cardiovascular defects. *Developmental Biology* in press 2010
- **Sunyong Tang**, Paige Snider, and Simon J. Conway. Regulation of TGF $\beta$  superfamily signaling is critical during sympathetic ganglia and craniofacial neural crest differentiation but is dispensable post-differentiation. Manuscript in preparation for submission to *Development*, 2010